NBSIR 73-199

Experimental and Analytical Studies of Floor Covering Flammability with a Model Corridor

Wells Denyes

Research Associate
Man-Made Fiber Producers Association, Inc.
Washington, D. C. 20036

and

James Quintiere

Institute for Applied Technology
National Bureau of Standards
Washington, D. C. 20234

May 1973

Final Report

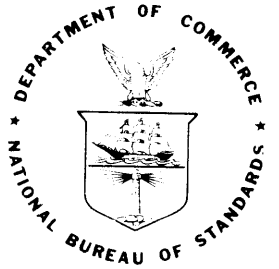

U. S. DEPARTMENT OF COMMERCE
NATIONAL BUREAU OF STANDARDS

NBSIR 73-199

EXPERIMENTAL AND ANALYTICAL STUDIES OF FLOOR COVERING FLAMMABILITY WITH A MODEL CORRIDOR

Wells Denyes

Research Associate
Man-Made Fiber Producers Association, Inc.
Washington, D. C. 20036

and

James Quintiere

Institute for Applied Technology
National Bureau of Standards
Washington, D. C. 20234

May 1973

Final Report

U. S. DEPARTMENT OF COMMERCE, Frederick B. Dent, Secretary
NATIONAL BUREAU OF STANDARDS, Richard W. Roberts, Director

PREFACE

This report describes one of several concepts examined at the National Bureau of Standards for a floor covering flammability test which could be related to performance in real fire conditions. We believe that this work provides substantial support for the critical energy concept as a measure of hazard potential for floor coverings. A test method based on this concept but substituting a radiant panel as the energy flux source is now being investigated in detail at NBS.

J. E. Clark
Chief, Fire Technology Division
June 1973

CONTENTS

		Page
1.	INTRODUCTION	1
2.	OBJECTIVE	2
3.	EQUIPMENT AND INSTRUMENTATION	2
4.	EXPERIMENTAL RESULTS	4
	4.1 General Description of Phenomenon	4
	4.2 Bimodal Distribution of Results	7
	4.3 Effect of Variables	11
	4.3.1 Ceiling Height	11
	4.3.2 Model Width	17
	4.3.3 Heat Input	17
	4.3.4 Air Velocity	21
	4.3.5 Underlay	21
	4.3.6 Other Variables	27
5.	FLOOR COVERING TESTS	27
6.	QUANTITATIVE EVALUATION OF CONTRIBUTING FACTORS	39
	6.1 Ignition Flame	39
	6.2 Air Flow	47
	6.3 Energy Release Rate from Floor Covering	53
	6.4 Radiant Preheating	63
	6.5 Heat Balance Analysis	72
7.	OVERALL ANALYSIS AND SCALING RELATIONSHIPS	77
8.	CONCLUSIONS	83
9.	SUGGESTED TEST METHOD	88
APPENDIX A.	REVIEW OF LITERATURE ON CORRIDOR AND DUCT FIRES	90
APPENDIX B.	RADIANT PREHEATING CALCULATIONS	94
APPENDIX C.	ANALYSIS OF A LINE SOURCE PLUME IN A CROSSWIND	98
REFERENCES		103

ILLUSTRATIONS

		Page
3-1	Model corridor apparatus	3
4-1	Factors influencing flame spread	6
4-2	Distribution of results	8
4-3	Typical flame spread characteristics	9
4-4	Some flame spread results for N-2/U	10
4-5a	Flame spread curves	12
4-5b	Flame spread curves	13
4-6	Ceiling temperature profiles at various ceiling heights (500 BTU/min)	15
4-7	Ceiling temperature profiles at various ceiling heights (1000 BTU/min)	16
4-8	Effect of model width on flame spread	18
4-9	Effect of heat input on ceiling temperature	19
4-10	Effect of flame spread on ceiling temperature	22
4-11	Effect of air velocity on ceiling temperature	23
4-12	Effect of air flow on flame spread	25
4-13	Effect of under-lay on flame spread	26
6-1	Burner flame plume 30 seconds after ignition V_∞= 100 fpm, $\dot{E}_B$= 500 BTU/min	40
6-2	Burner plume characteristics	41
6-3	Thermal-flow field of burner flame plume	42
6-4	Example of flame spread for melting carpet pile fibers	43
6-5	Example of flame spread for charring carpet pile fibers	44
6-6	Initial flame spread velocity for A-4 and N-5	45
6-7	Initial flame spread velocity for W-1, A-2, and P-2	46
6-8	Nylon carpet flame displaying three-dimensionel flow pattern	49
6-9	Vertical gas temperature profiles	50
6-10	Effect of air flow on flame spread	51
6-11	Flame propagation map	52
6-12	Energy release characteristics of carpets based on the NBS rate calorimeter	54
6-13	Energy release--comparison of NBS rate calorimeter and oxygen bomb	55
6-14	Carpet incident heat flux as a function of flame position	65
6-15	Calculated incident radiant heat flux	66
6-16	Flame spread as a function of calculated incident radiation	67
6-17	Carpet preheating characteristics	69
6-18	Flame spread--radiation analysis	70
6-19	Calculated radiant flux at flame front	71

6-20	Theoretical flame spread with radiant heating . . .	73
6-21	Sensor locations for energy balance analysis. . . .	76
6-22	Some results of an overall energy balance	78
7-1	Simplified preheating model	79
7-2	Partial scaling applied to model corridor flame spread for nylon carpet N-5/U.	85
7-3	Partial scaling applied to model corridor flame spread for acrylic carpet A-4/U.	86
A-1	Model mine fire characteristics	91
A-2	Estimated energy release rate from fires of various occupancies.	91
C-1	Plume coordinate system	98
C-2	Plume measured results for β' vs. Fr.	102

NOMENCLATURE

a	=	plume thickness
A	=	area
B	=	mass transfer number
c_p	=	specific heat at constant pressure
E	=	energy release by combustion
F_{12}	=	geometric shape factor, floor to ceiling
F_{1s}	=	geometric shape factor, floor to surroundings
Fr	=	Froude number, defined by Eq. 6-2
g	=	gravitational force per unit mass, or convective mass transfer coefficient
h	=	convective heat transfer coefficient
H	=	height
ΔH_f	=	heat of reaction per unit mass of fuel at reference temperature T_∞
i	=	enthalpy per unit mass
Δi_{vap}	=	energy required to vaporize fuel per unit mass of fuel
k	=	thermal conductivity
L	=	length
$\dot{m}$	=	rate of mass flow
m	=	mass
P	=	perimeter
$\dot{q}$	=	heat transfer rate
r	=	mass of oxidant per unit mass of fuel
s	=	plume coordinate
t	=	time
T	=	temperature

u = plume velocity

v_{ent} = entrainment velocity

V = velocity

W = width

x,y = horizontal and vertical coordinates

Y_o = mass fraction of oxidant

α = thermal diffusivity, entrainment constant, parameter defined by (6-9)

β = entrainment constant

γ = thermal inertia, $k\rho c$

ρ = density

$\Delta\rho$ = density difference

δ = thickness

θ = angle

Θ = dimensionless temperature

τ = dimensionless time

Subscripts

b - refers to burning carpet

B - refers to gas burner

c - refers to carpet

f - refers to final state

F - refers to flame

g - refers to gas

i - refers to initial state

L - refers to heat loss

r - refers to radiation

s - refers to surface

∞ - refers to ambient condition

Superscripts

$( )'$ - indicates per unit length

$( )''$ - indicates per unit area

$\overline{( )}$ - indicates average

EXPERIMENTAL AND ANALYTICAL STUDIES OF FLOOR COVERING FLAMMABILITY WITH A MODEL CORRIDOR

Wells Denyes
and
James Quintiere

ABSTRACT

An experimental model corridor facility was designed, constructed, and instrumented. The facility examines flame spread over floor covering materials in a small scale corridor under a forced air flow condition. A gas burner flame serves as the ignition source.

A study was made of the factors influencing flame spread in the model corridor. These factors included energy release rate of the ignition source, air velocity, and model corridor geometry. Twenty-six carpet materials and 5 other floor covering materials were studied in the model corridor, and 369 flame spread runs were conducted.

It was found that flame spread behavior in the model corridor involves either a rapidly accelerating flame front which propagates the full 8 foot length of the test section ("flameover"), or involves a decelerating flame front which results in extinction a short distance from the ignition source. Radiant heating of the floor material due to hot products of combustion heating the ceiling is a significant factor in causing flameover. Carpet assembly was found to affect flame spread more significantly than pile fiber type.

The data have been analyzed to determine quantitatively the effects of the factors influencing flame spread. Scaling relationships have been presented to attempt to extrapolate the model corridor results to full scale corridor fires.

Finally a procedure has been suggested for using the facility in a floor covering flammability test method. The procedure is based on determining the minimum energy input rate to cause flameover.

Key words: Flame spread; floor covering materials; model corridor; scaling laws; test method.

1. INTRODUCTION

Historically, carpets and rugs have not been considered to be particularly hazardous materials in either residential or commercial use. Meaningful statistics are difficult to obtain because there are so few cases in which the involvement of carpets and rugs in fires is clearly defined. However, during the past 15 years a revolution has taken place in both the manufacture and use of carpets. The simultaneous introduction of the tufting process and development of high performance, man-made fibers has made quality carpet available at low cost with the result that carpet usage has expanded exponentially. With billions of square yards of carpets in use, two inevitable consequences began to emerge: 1) some carpet constructions that could be relatively easily ignited appeared on the market and 2) vast exposure greatly increased the probability that carpets could be involved in major fires. With expanding usage of carpets in institutional and public buildings, some local, state, and federal authorities established arbitrary flammability standards.

On April 16, 1970, the Department of Commerce promulgated the first national standard to control the flammability of carpets, DOC FF 1-70[1]. It became effective one year later. This standard was developed by the National Bureau of Standards in cooperation with the carpet and rug industry. It is designed to eliminate from commerce those carpets that can be easily ignited by small ignition sources such as cigarettes, matches, glowing embers from fireplaces, or minor electrical short circuits. This standard was supported by both government and industry for the following reasons: 1) a national flammability standard is in the public interest, and 2) the proposed standard is appropriate on the basis of simplicity, reproducibility, and effectiveness in screening out easily ignitable materials.

During this same time there was a growing effort to develop a more rigorous standard for carpets used in institutional buildings. National attention was focused on this effort on January 9, 1970, when a fire took the lives of 31 elderly patients in a nursing home in Marietta, Ohio. Carpet has been claimed to be at least partially responsible for the spread of fire. This tragedy precipitated further activity to set additional flammability standards for carpets used in institutional and commercial buildings.

The most widely adopted method has been the ASTM E 84-68 Tunnel Test [2]. Although this method has been widely used to classify the surface burning characteristics of building materials, it has not been shown to be relevant when used for floor covering materials. Among other methods under consideration are the E 84 Tunnel using floor mounting of the samples, U. L. Subject 992 Floor Covering Chamber Test [3], ASTM E 162-67 Radiant Panel Test [4], and the Armstrong Flooring Radiant Panel [5]. At this time none of these methods has been shown to be repeatable and reproducible, and a reliable measure of the hazard contribution of floor coverings to building fires.

Experts in the fire field often say that the problem of flame spread in buildings may not be solved until adequate detection and suppression systems are developed and incorporated into buildings codes. Many groups are urging that fully automatic sprinkler systems be required in public buildings. Until this has been accomplished there remains the need to define the nature of hazard presented by carpet and other floor covering material in building fires and to develop a test method to measure hazard potential. Recognizing this need, the National Bureau of Standards and other organizations initiated programs to study the burning characteristics of these materials in full scale environments. The results of these programs should make it possible to develop a test method that relates to actual hazard.

2. OBJECTIVE

With this need for a floor covering flammability test method directed specifically towards carpets to be used in corridors and exitways of institutional buildings, a Research Associate Program was begun at the National Bureau of Standards in July 1971. This program was carried out under the sponsorship of Man-Made Fiber Producers Association, Inc. and with the cooperation of the Carpet and Rug Institute. The objective of this program was to develop a laboratory scale test procedure which would provide a high degree of confidence in prediction of the flammability and flame propagation characteristics of carpeting in full-scale real-life situations.

3. EQUIPMENT AND INSTRUMENTATION

A model corridor facility was designed and constructed in Building 65 of the National Bureau of Standards in Washington, D. C. The facility was designed with a test or burning section eight feet in length, four feet in width and four feet in height. A moveable wall and ceiling were used so that the cross-sectional dimension could be varied. Construction material for this section was 3/8 inch thick asbestos board. A curb was installed on each side of the test section which served to hold the test material in place and to inhibit edge burning effects.

The air handling system was designed so that air velocity could be varied from 50 to 300 feet per minute. The system is capable of providing a uniform, stable air flow with little change in velocity even during a fire test.

Heat input to the system is provided by a diffusion flame gas burner which is mounted in the center of the upstream end of the test section. The burner flame impinges on the floor mounted test sample. Heat input can be varied up to 2000 BTU per minute. A schematic diagram of the model corridor facility is shown in figure 3.1.

A 20-channel data acquisition system was assembled so that temperatures and energy fluxes could be automatically monitored throughout the program. Outputs from thermocouples, radiometers and total heat flux meters were scanned by the system. A computer program was used to convert

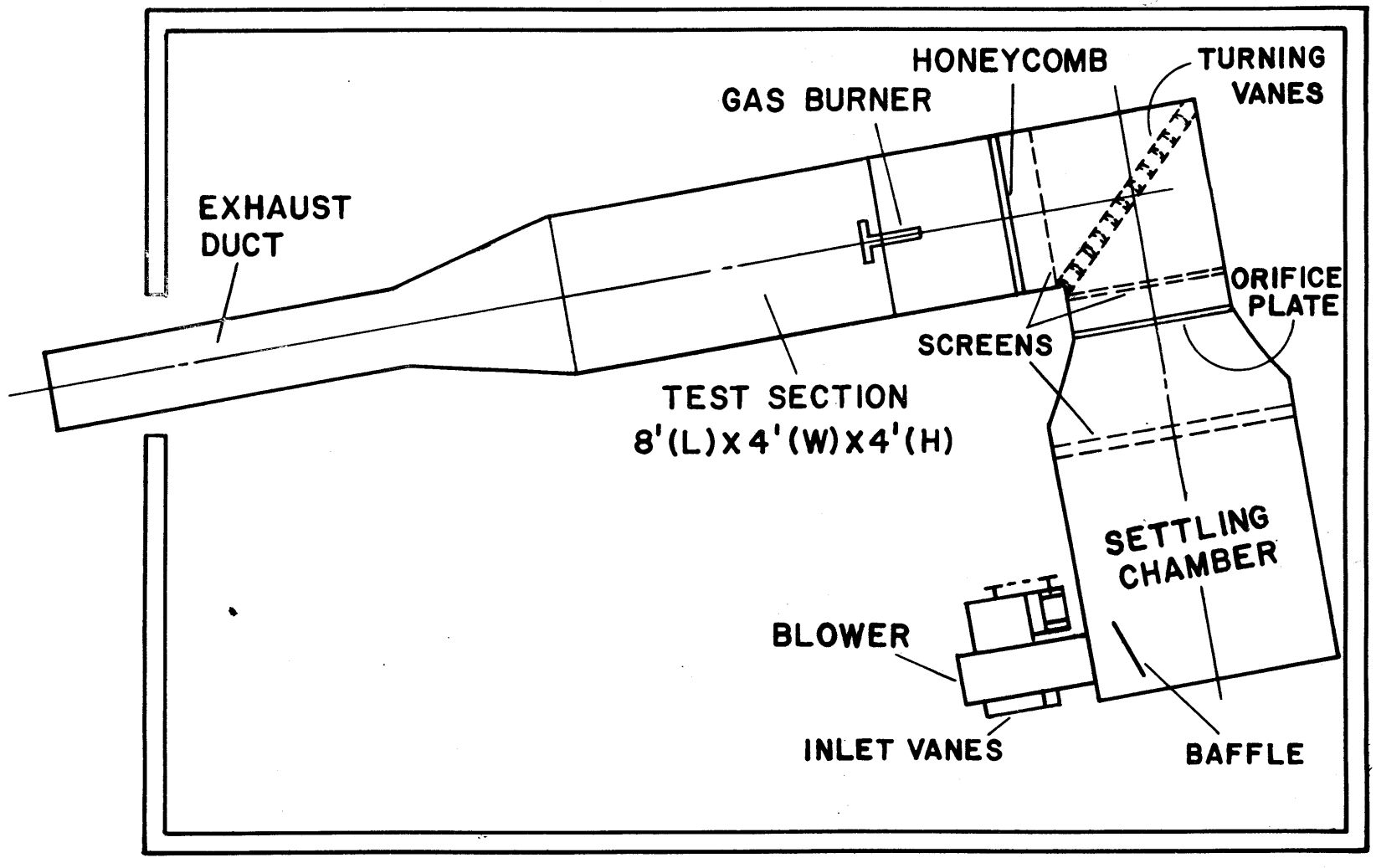

Figure 3-1. Model corridor apparatus.

the paper tape output from the system into time dependent printouts. Locations of sensors were changed from time to time throughout the program so that the greatest amount of information would be available.

The test procedure used in most of the experiments is to run with the gas burner "on", impinging on the carpet surface, for 12 minutes. An additional 12 minutes with the burner "off" follows. During the entire 24 minutes the position of the flame front is observed and recorded. This procedure is similar to that used in the U.L. Subject 992 Floor Covering Chamber Test and investigation of many of the variables was motivated by this test.

A detailed description of the construction, instrumentation and operation of the model corridor facility is contained in the report, "A Model Corridor for the Study of the Flammability of Floor Coverings", by Denyes and Raines [6].

4. EXPERIMENTAL RESULTS

4.1 General Description of Phenomenon

The phenomenon that is being investigated here can be described as unsteady flame spread over a porous composite material in a hydrodynamic entrance region of a duct with a wind blown diffusion flame as an ignition source. Using the facility described, a flooring material is ignited by the gas burner under the influence of a relatively steady laminar air flow in the duct and flame propagation is observed and examined. Propagation usually takes the form of a uniform flame spread velocity while under the influence of the burner flame. This is then generally followed by a decrease in flame spread velocity which is subsequently followed by either extinguishment or more rapid flame spread. The initial conditions, namely air flow, duct cross-sectional dimensions, and burner gas flow, along with the nature of the floor covering assembly establish whether the fire will be propagating or non-propagating. The term "flameover" has been employed to describe the outcome of a rapidly propagating accelerating fire which runs the full length of the test section.

From a practical viewpoint, the nature of the test has at least a qualitative semblance of real life. The burner diffusion flame simulates a real fire, such as a fully developed room fire exposure through an open doorway to a corridor with a floor covering. The test duct geometry simulates a corridor with a unidirectional forced flow air ventilation pattern. Hence the system is composed in such a manner to reflect a realistic hazard configuration which has the potential for resultant rapid flame spread. Although the physical set-up is a rational reflection of a real life configuration, that alone does not suffice for its acceptance as a quantitative representation of full scale reality. Some questions and issues remain for consideration. Two subtle points to consider are the nature of air flow in a "typical" building corridor, and the fact that the primary ignition burner has a prescribed fuel output as opposed to the natural time dependent burning rate of a real

fire. Ultimately all of these issues will have to be addressed before one can establish by design a correlation between a laboratory flammability test and the corresponding real life hazard.

Returning now to the phenomenon under investigation in this study, the factors influencing flame spread are portrayed schematically in figure 4-1. In order for the flame to propagate, heat transfer at the leading edge of the flame front must be sufficient to raise the energy level of the floor covering material so that volatilization can occur and a combustible gas mixture can form. In the case of those materials that pass the Pill Test this forward heat transfer is not sufficient to propagate a fire. However, in the model corridor the forward heat transfer is augmented by the burner plume and feedback from heated surroundings. Also air flow, V_∞, affects the inclination of the burner flame plume and the inclination of the leading edge of the floor flame. This air is entrained and mixed in the combustion zone and this mixing process basically determines the extent of the combustion zone.

At the initiation of a model corridor test the floor flame moves under the direct influence of the burner flame plume. Radiant and convective energy is transferred from the burner flame plume which promotes a steadily spreading floor flame. Once the floor flame emerges from the direct influence of the burner, it tends to decrease in velocity. In this region continued flame spread is strongly dependent on energy transfer from the surroundings. The rising plume impinges on the ceiling and results in a heated ceiling downstream of the flame front. The gas temperature in the duct downstream of the flame tends to be stratified, and radiation tends to be the dominant heat transfer mode to the floor covering material beyond several inches from the floor flame. As flame spread becomes rapid and the flame zone grows, the level of gas temperatures across the duct increases and convective heating of the floor material can then become significant. Flame spread V_F, and burning rate, $\dot{m}_b$, both can be simply related as:

$$[V_F, \dot{m}_b] \propto \frac{[\text{net heat transfer rate to fuel}]}{[\text{energy required to vaporize fuel}]}$$

Burning rate depends on heat feedback to the burning material and heat losses from the fuel bed. An increasing burning rate promotes higher plume and ceiling temperatures. This in turn leads to increasing radiant flux levels to the floor (preheating) raising the "effective" floor temperature, T_o. Heat transfer, $\dot{Q}_F$, just ahead of the flame front raises the fuel to its "vaporization" temperature, T_{vap}, to sustain flame spread. The additional energy required to vaporize the fuel has been reduced from its initial value due to preheating. The entire process is transient, leading to an accelerating propagation rate or extinguishment. Before continuing with a more detailed analysis of the components of this model corridor study, some comments on past related work will be made. A review of the literature on fire propagation in

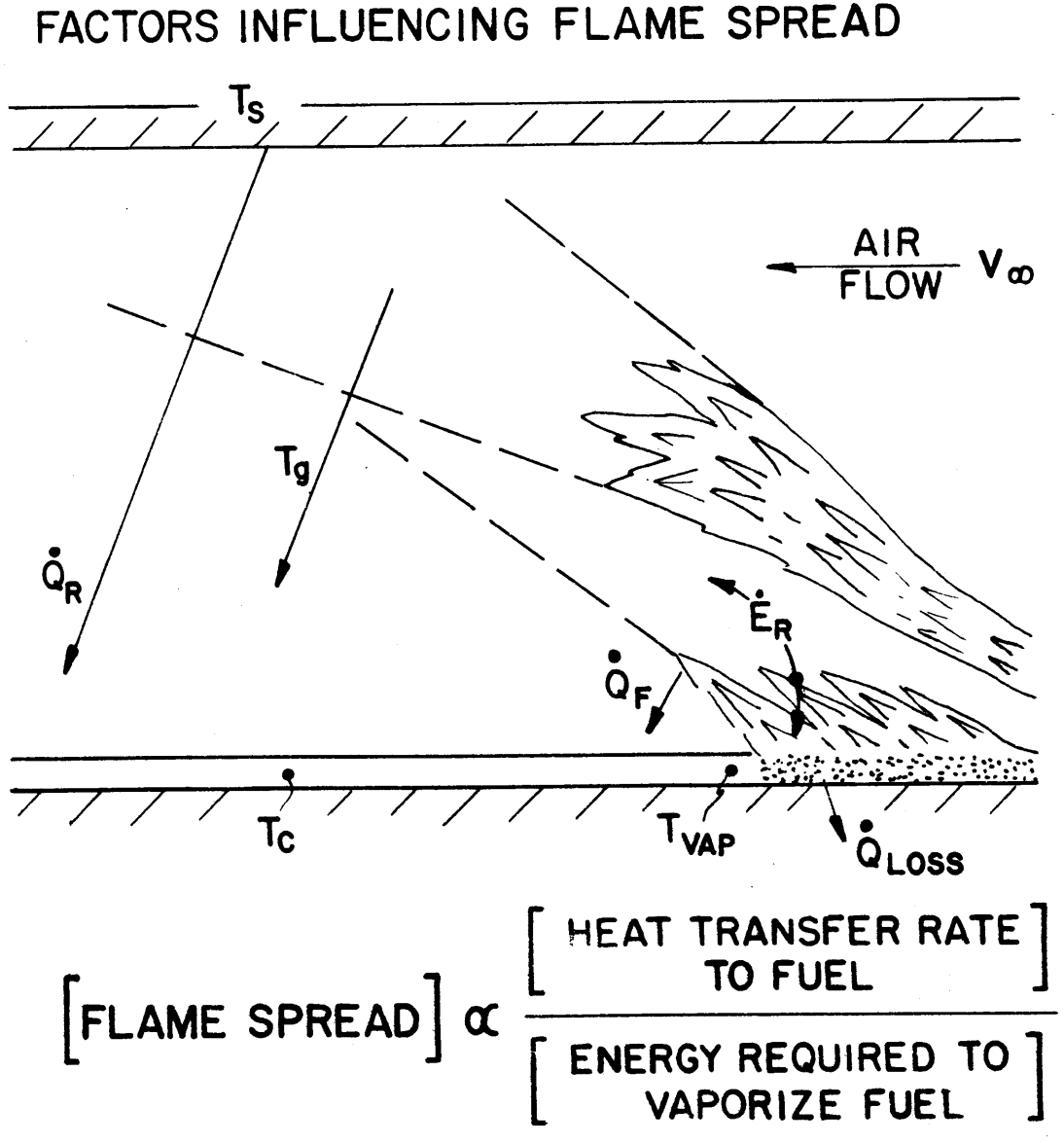

Figure 4-1. Factors influencing flame spread.

model mine tunnels and building corridors [7-15] is presented in Appendix A. Several conclusions can be drawn from these studies:

1. Sustained flame propagation depends on the energy release of the ignition source.

2. Steady-state fuel-rich flame propagation depends on the velocity of forced air flow into the duct.

3. Flame spread is more likely to occur in ducts and corridors which have combustible wall and ceiling linings than combustible floor materials.

4. No single flammability test has been demonstrated to express the true hazard of floor materials in building corridors.

4.2 Bimodal Distribution of Results

Results of this work and review of past experimentation both suggest that duct fires are bimodal in nature. Depending on initial conditions the fire will be either propagating or non-propagating. If a propagating fire develops, it will have the potential of rapid acceleration and involvement of the total duct length. Results of the experimental program in the model corridor confirm this bimodal distribution.

A total of 369 floor covering tests have been made in the model corridor. The results of these tests, illustrated graphically in figure 4-2, show this bimodal distribution. Over 90% of the tests resulted in either flame spread of 4 feet or less or flame spread the entire 8 foot length. Figure 4-3 illustrates the flame spread modes observed in the majority of tests. In the ignition zone a linear flame spread rate occurs which is dependent on the heat input from the burner and on the material being tested. Just beyond influence of the burner, in the flame spread zone, the burn rate normally decreases. It is within this zone that heat flux conditions develop that will result in either an accelerating rate of flame spread leading to flameover or a decelerating flame spread. In many cases the decelerating flame front will extinguish.

Although more than 90% of the tests demonstrate one of the two described flame spread modes, an explanation is needed for the apparent anomalies--those that result in flame spread distances greater than four feet but less than eight feet. In most cases it was found that the initial parameters were just below the critical conditions that would result in flameover. For example, as illustrated in figure 4-4, carpet assembly N-2/U* in a model 24 in. x 11 in. using 100 feet/minute air flow and 600 BTU/min heat input burned at a fairly uniform rate for the entire 24 minute test time. When initial conditions were increased in severity (750 BTU/minute) flameover occurred. When initial conditions

*Notation defined in table 5-1 and Section 5, page 29.

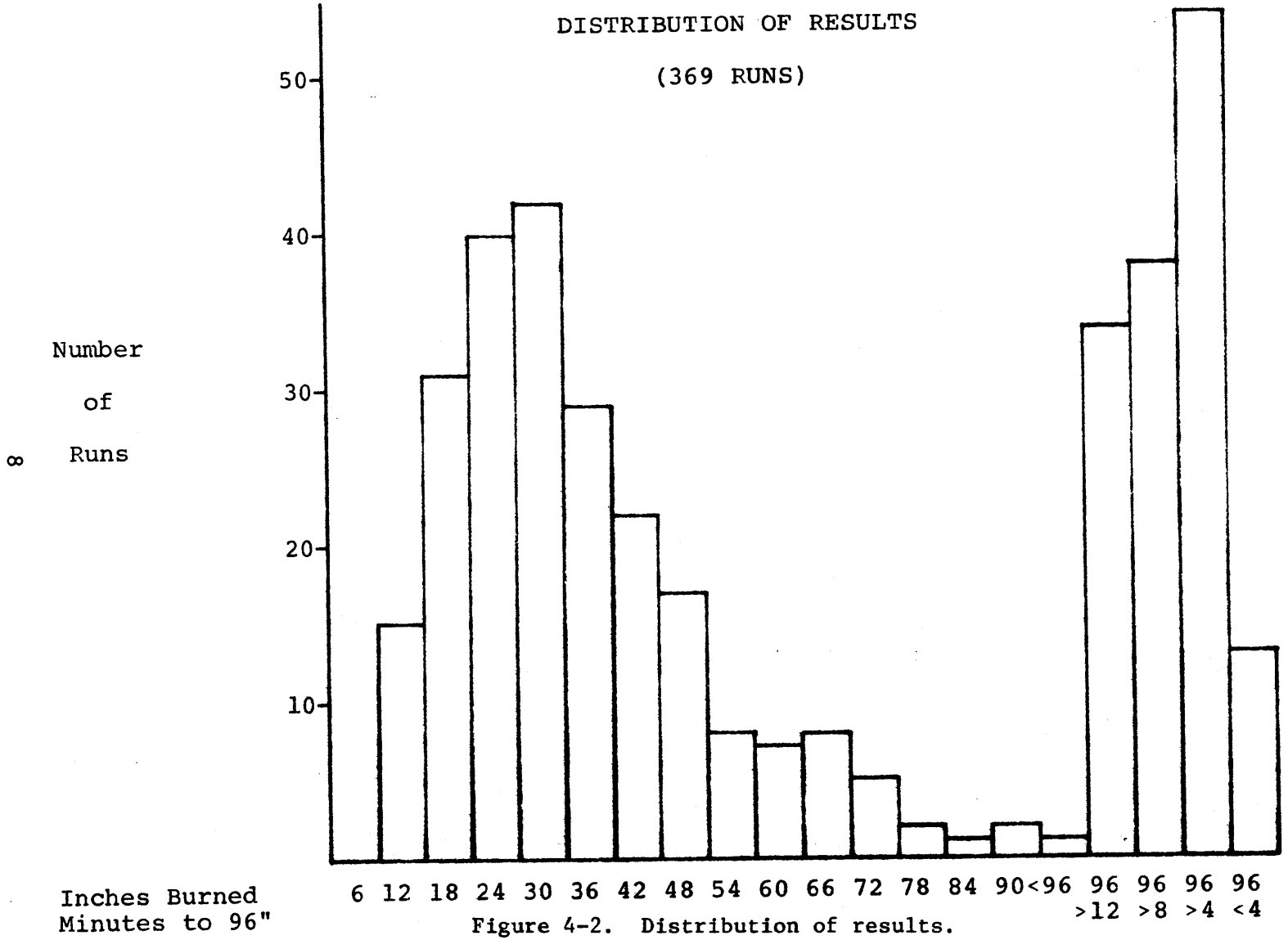

Figure 4-2. Distribution of results.

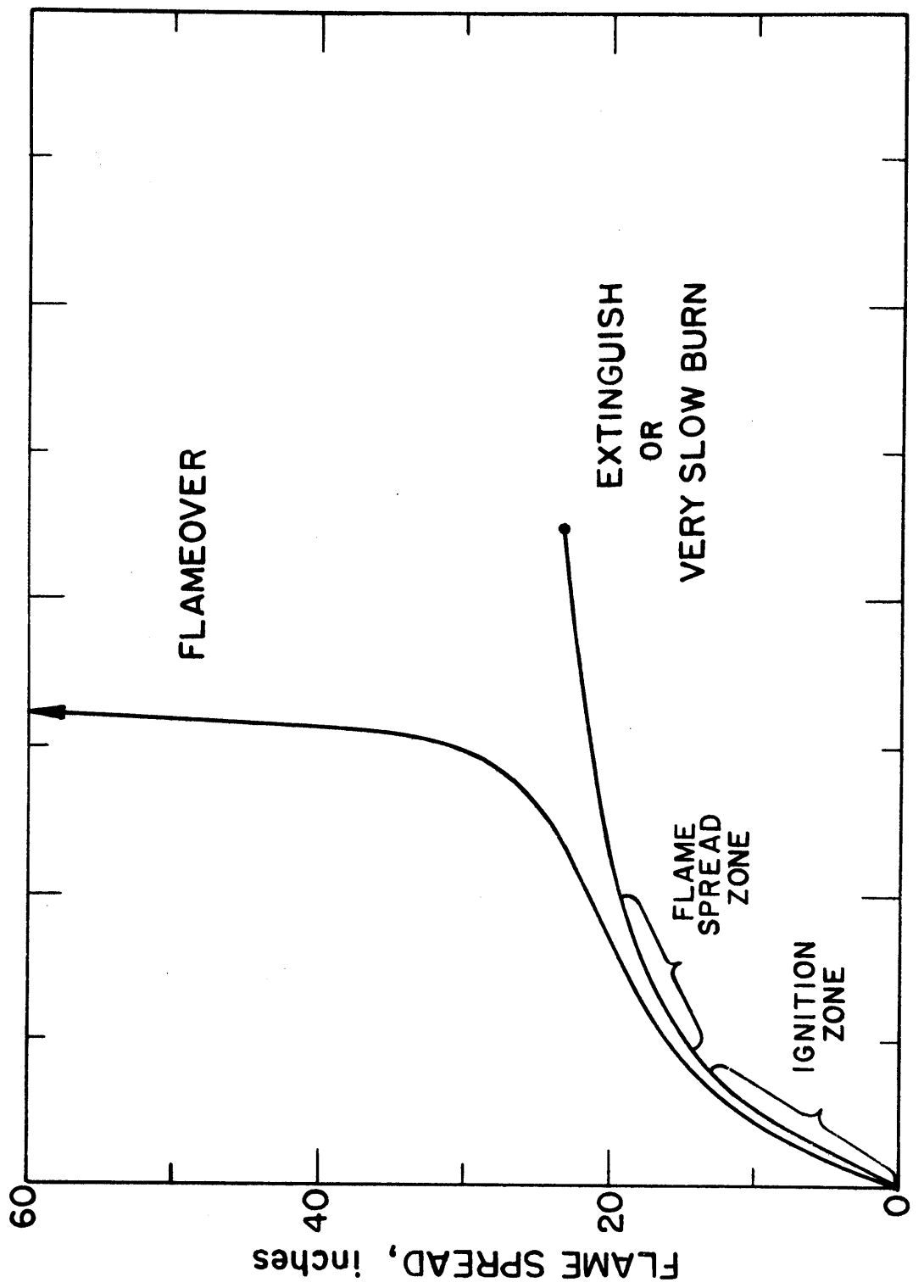

Figure 4-3. Typical flame spread characteristics.

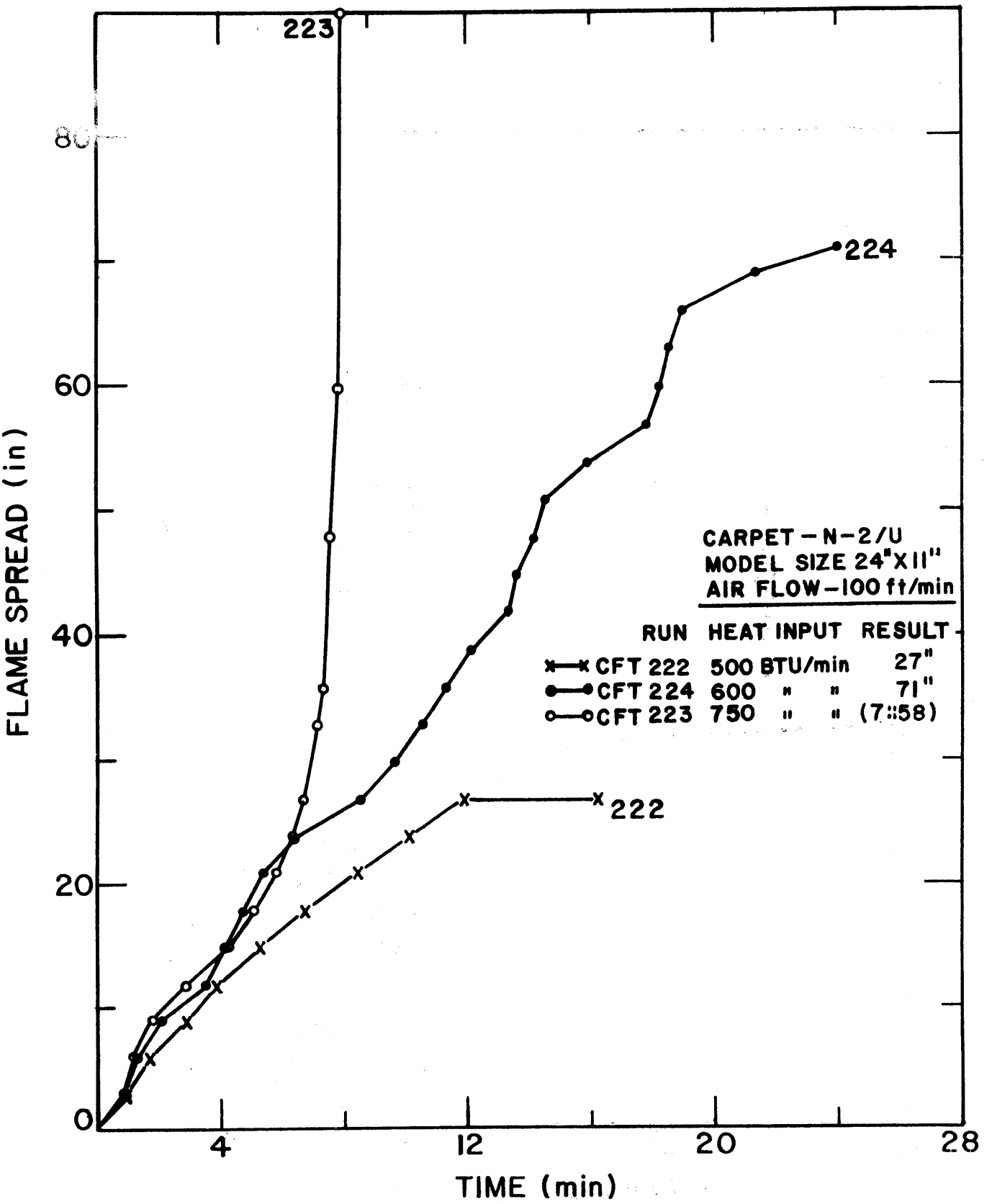

Figure 4-4. Some flame spread results for N-2/U.

were decreased in severity (500 BTU/minute) a decelerating flame developed and the carpet flame extinguished.

Figures 4-5a and 4-5b show flame spread curves for many of the materials tested. Most illustrate the bimodal characteristics described. Additional flame spread rate curves are referred to in other sections of the report.

These results suggest that the flammability performance of floor covering materials in a duct or model corridor should be dependent on whether or not conditions develop that lead to total involvement of the sample. They suggest that a hazard index that is either distance or time dependent may not be appropriate. Therefore, the effect of variables and testing procedures that will be discussed are based on the question, "Does flameover occur?"

4.3 Effect of Variables

An initial experiment was carried out using one carpet (A-2) to get a preliminary indication of the effects on flame spread of model dimensions, air velocity, heat input and the use of an underlay. The results of this 2^4 factorial experiment are shown in table 4-1. Analysis showed that the effects of model dimensions, heat input and underlay were all significant at the 95% confidence level. The effect of air velocity appeared uncertain.

It was in this and other early experiments that the bimodal distribution of results was first detected. With this fact and an understanding of the factors influencing flame spread, it became possible to determine the effect of the selected variables. Radiant preheating of the carpet assembly ahead of the flame front is dependent on ceiling temperature. Therefore, ceiling temperature will be used as the primary indicator for impending flameover. To establish a fixed reference, blank runs were used to illustrate the effect of variables on ceiling temperature distribution.

4.3.1 Ceiling Height

To determine the effect of varying ceiling height, blank runs (no carpet) were made and ceiling temperatures recorded after a steady state had been reached (about five minutes). Examples of these data are shown in figures 4-6 and 4-7. As was anticipated, ceiling temperatures increased as ceiling height was reduced. This indicates that as ceiling height is lowered, the chance of flameover occurring is greater. This is confirmed by substantial data that will be discussed later in this report.

During the testing to determine this relationship it was found that with low ceilings (i.e. 11"), very high ceiling temperatures occurred locally in the region 12 to 18 inches from the burner. It was observed that the luminous burner flame plume tended to approach the ceiling in this region. With higher ceiling a much more uniform temperature

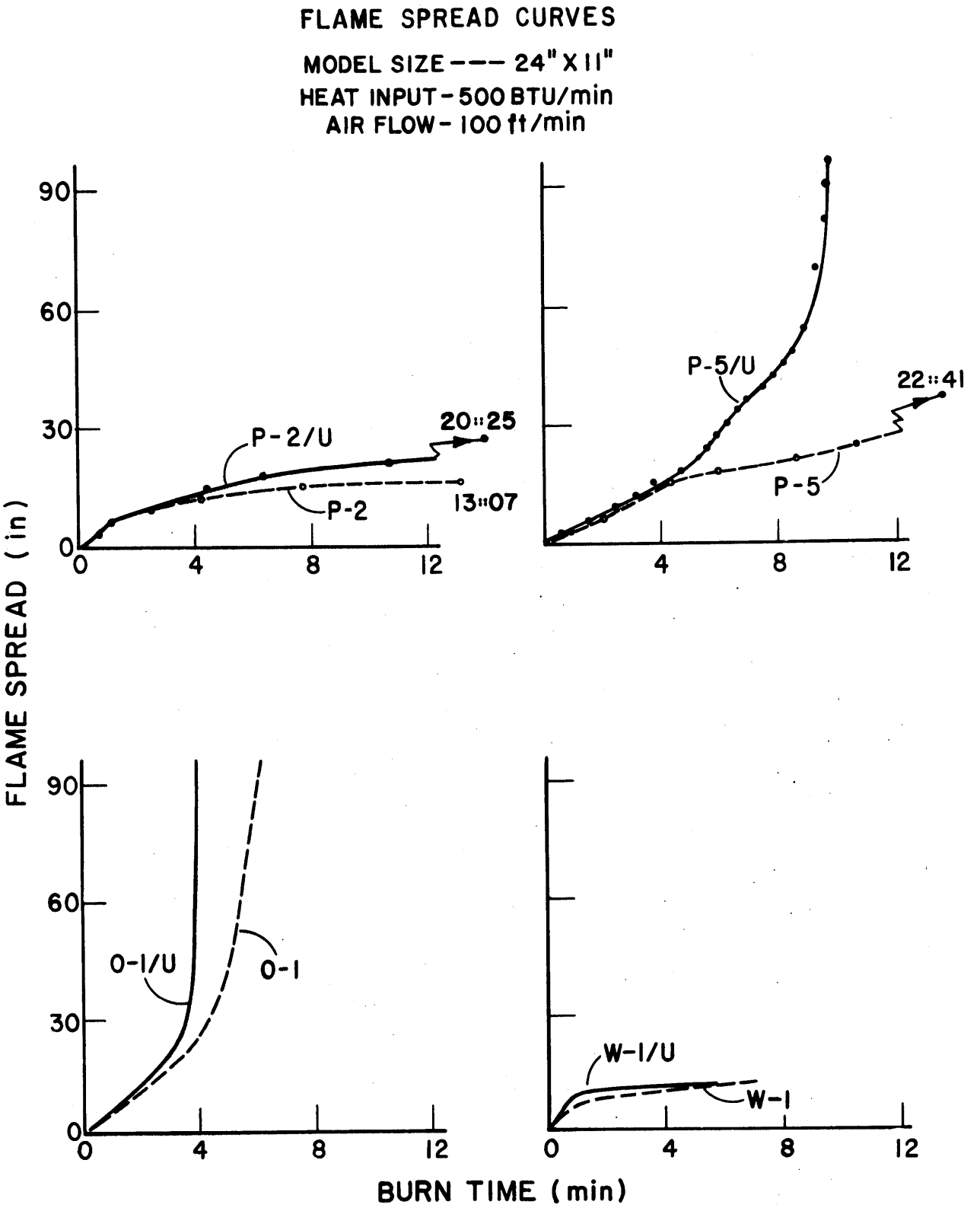

Figure 4-5a. Flame spread curves.

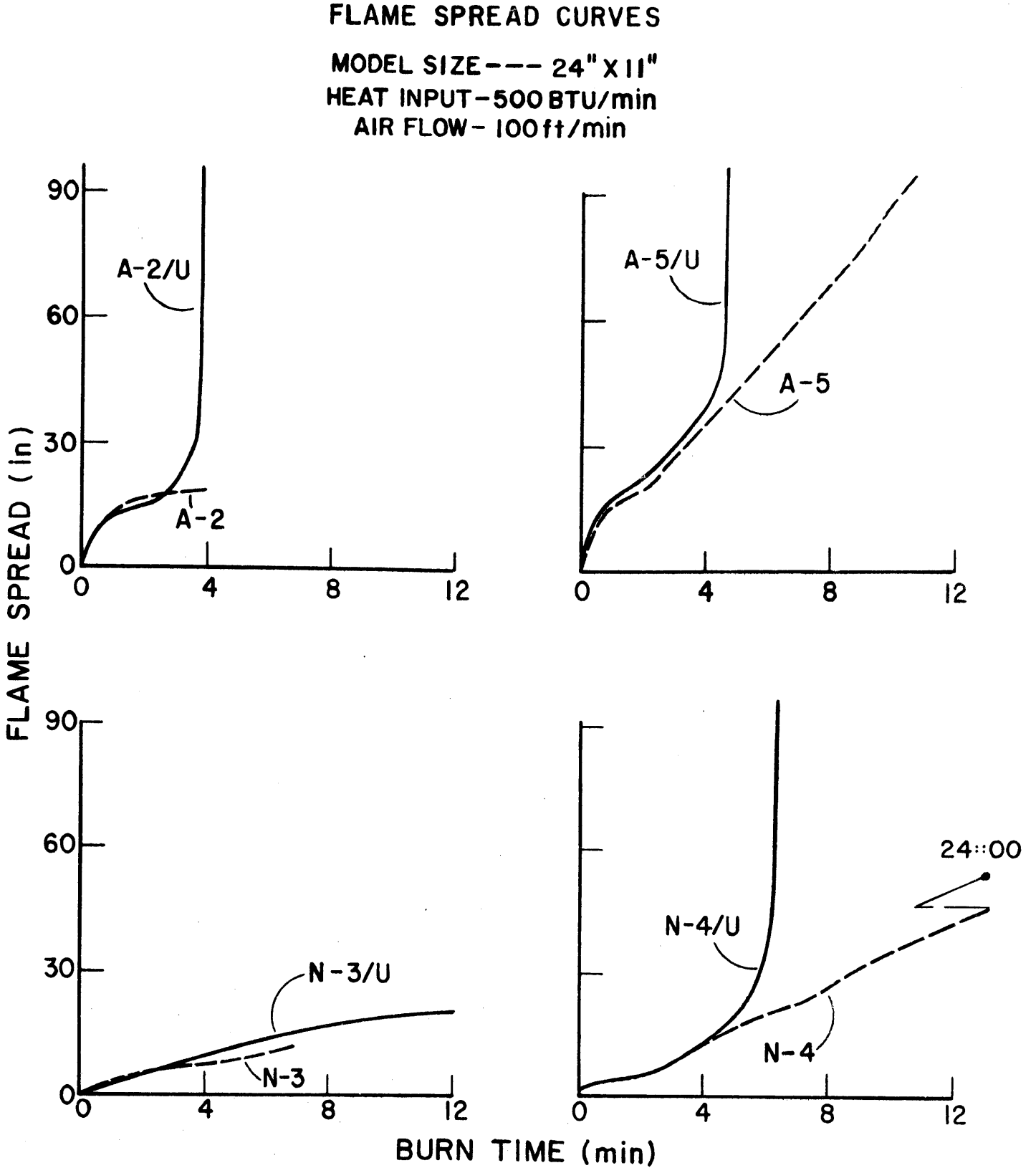

Figure 4-5b. Flame spread curves.

TABLE 4-1

EFFECT OF SELECTED VARIABLES ON FLAME SPREAD

CARPET - A-2
(Acrylic)

Test CFT No.	Dimension (W' x H')	Air (Ft/min)	Gas (BTU/min)	Underlay	Results*
3	4 x 4	100	500	Yes	15"
4	"	"	"	No	10"
2	"	"	1000	Yes	26"
1	"	"	"	No	21"
7	"	200	500	Yes	18"
6	"	"	"	No	11"
8	"	"	1000	Yes	29"
5	"	"	"	No	18"
12	2 x 1	100	500	Yes	(3::40)
21	"	"	"	No	19"
**	"	"	1000	Yes	--
10	"	"	"	No	38"
26	"	200	500	Yes	57"
25	"	"	"	No	10"
29	"	"	1000	Yes	(2::51)
24	"	"	"	No	61"

*Results reported in inches burned if flameover did not occur or in time (min::sec) to flameover.

**Experiment not run.

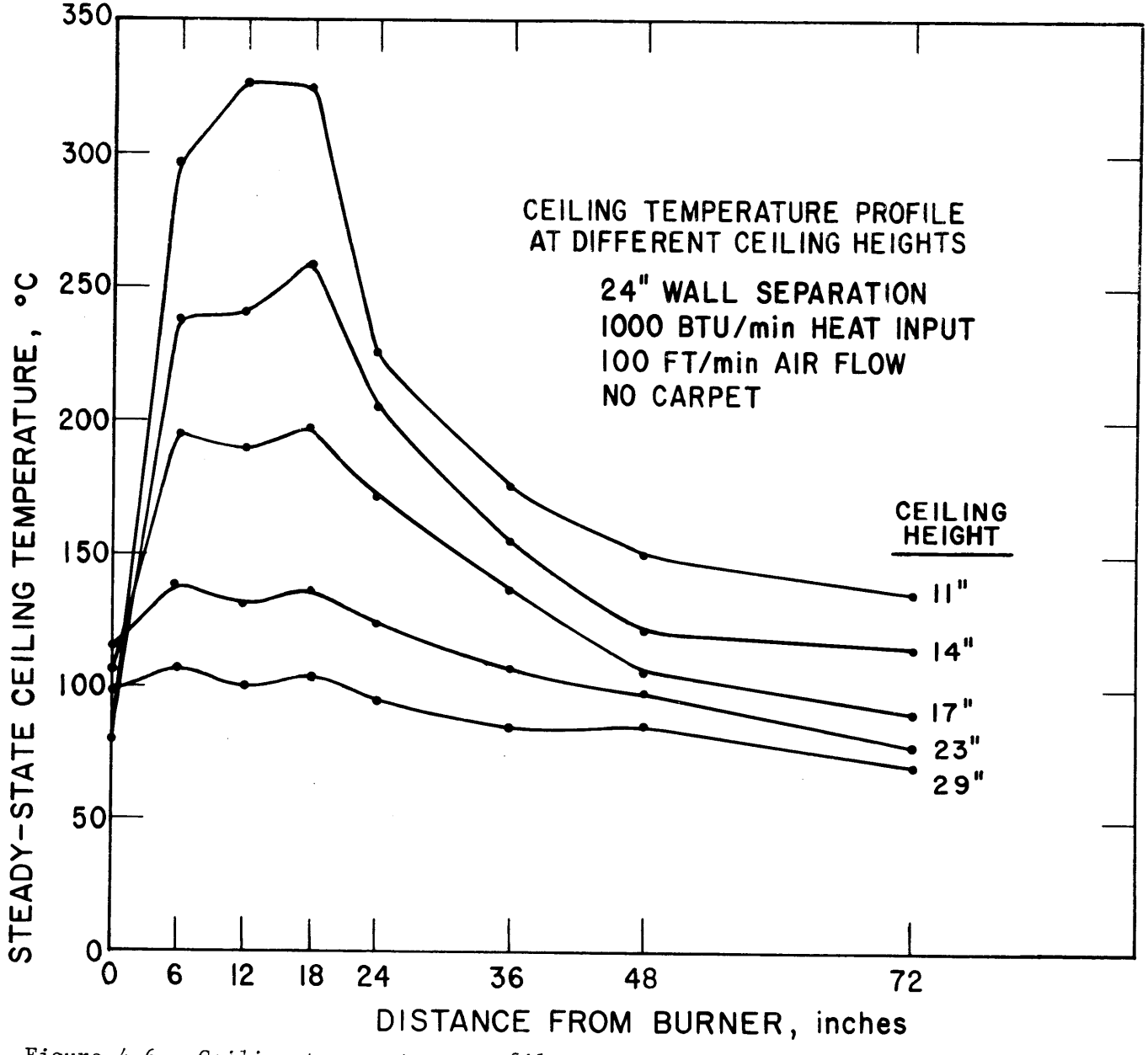

Figure 4-6. Ceiling temperature profiles at various ceiling heights (500 BTU/min).

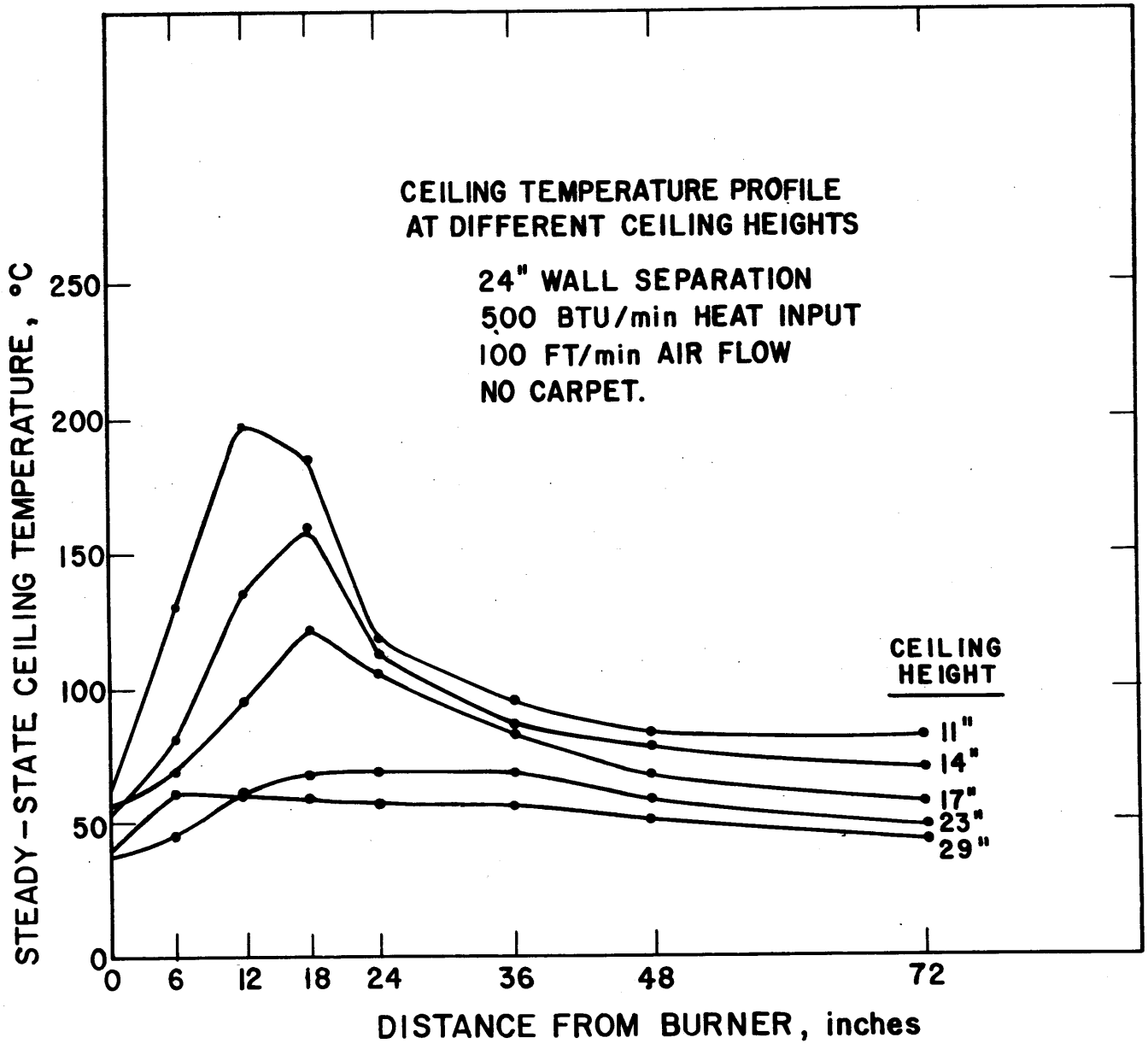

Figure 4-7. Ceiling temperature profiles at various ceiling heights (1000 BTU/min).

profile occurred. This may suggest a lower limit to ceiling height to achieve more realistic scaled conditions.

4.3.2 Model Width

The width of the test section was also found to influence flame spread behavior. Pairs of runs were made in which the only parameter varied was model width. In every case flame spread was greater in the narrower width and in several cases, as illustrated in figure 4-8, flameover occurred in the narrower width model. In this figure it is noted that flame spread rate is very similar during the first 2 1/2 minutes, but during this time the ceiling temperature had become higher in the narrower (24") model. At this time the flame front began to accelerate, ceiling temperature rose further and flameover occurred at 3::36. In the wider (48") model an accelerating flame front did not develop and the carpet flame extinguished at 4::57 at a distance of 45".

It should be noted that throughout the experimental program the same gas burner was used. This means that burner width was not scaled with model width. Had this been done, model width might have had a somewhat different influence on flame spread characteristics.

4.3.3 Heat Input

Heat input from the burner was varied over a wide range during the program. As expected, increasing heat inputs caused higher ceiling temperatures as illustrated in figure 4-9.

Tables 4-2 and 4-3 illustrate the effect of both ceiling height and heat input. In each experiment the carpet assembly, wall separation, and air velocity remained constant. As the test conditions were increased in severity (conditions causing higher ceiling temperatures) by either increasing the heat input or lowering the ceiling height the distance burned increased gradually up to the point at which flameover occurred. If test conditions are further increased in severity, time to flameover decreases.

The total heat released in the system consists of two factors; heat input from the burner and heat released by the carpet or floor covering system. It was found that, with any one carpet assembly, as gas supplied to the burner increased the area of carpet burned in the ignition zone increased. No other factor influenced the area of carpet burned in the ignition zone. This suggests that the two sources of energy vary directly, so if the controlled energy supply (heat input from burner) is varied the uncontrolled energy supply (heat released from carpet during the early stage of a test) will vary directly. It must be recognized, however, that different floor coverings do have different energy release rates which is a part of the reason for their different flammability behavior.

Having established that the two energy sources vary directly, it was necessary to determine the relative magnitude of the two. Experimental runs were made to compare ceiling temperatures both with and without a

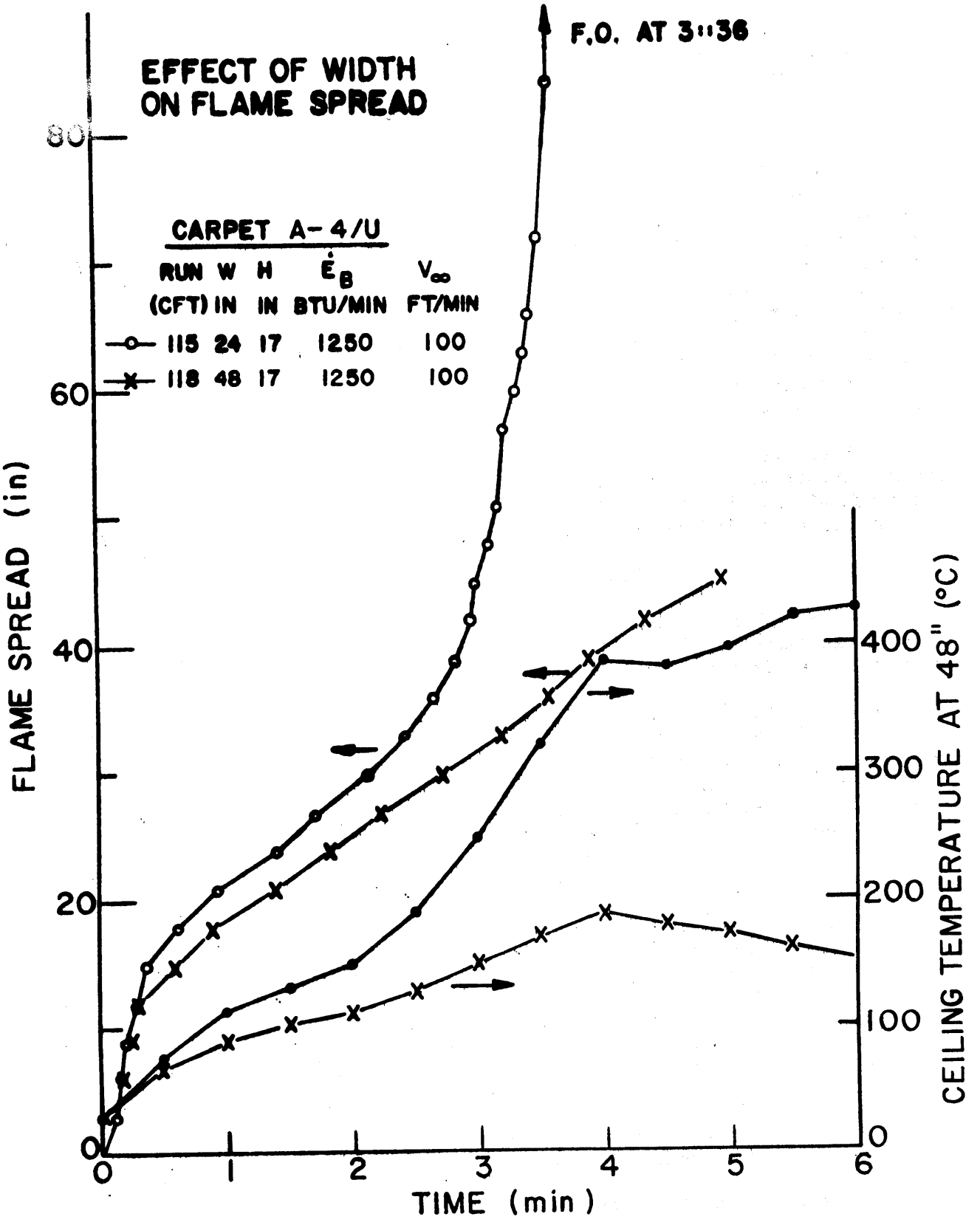

Figure 4-8. Effect of model width on flame spread.

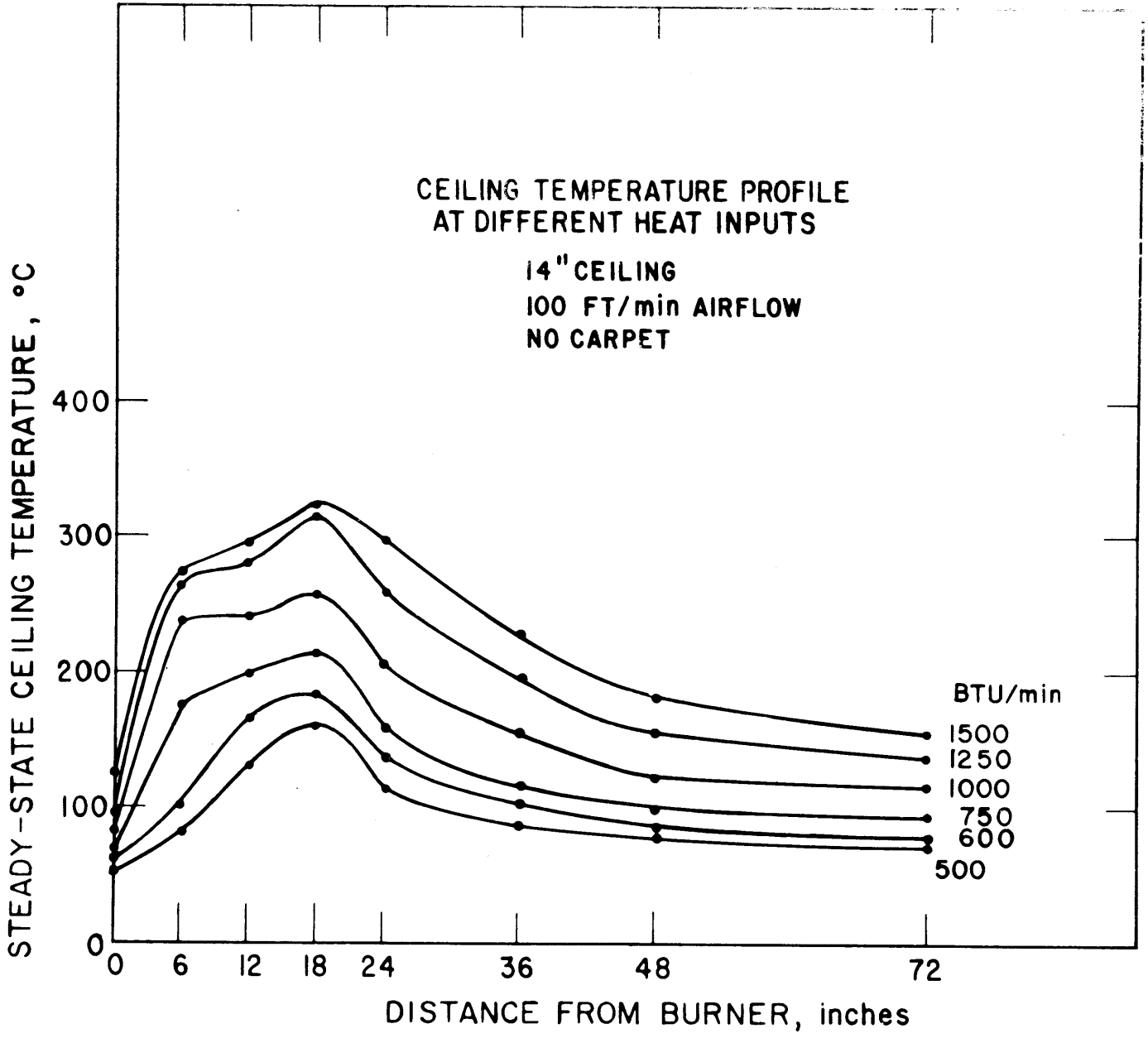

Figure 4-9. Effect of heat input on ceiling temperature.

TABLE 4-2

EFFECT OF CEILING HEIGHT AND HEAT INPUT
ON THE EXTENT OF BURN OR TIME OF FLAMEOVER - CARPET A-4/U

Air - 100 Ft/min Model Width - 24"

		CEILING HEIGHT			
		11"	14"	17"	23"
HEAT INPUT (BTU/MIN)	400	21"			
	450	22"			
	500	(5::39)	19"	16"	17"
	600		22"		
	750		(5::24)		
	1000		(4::58)	73"	32"
	1250			(3::36)	
	1500			(2::40)	60"
	2000				70"

TABLE 4-3

EFFECT OF CEILING HEIGHT AND HEAT INPUT
ON THE EXTENT OF BURN OR TIME OF FLAMEOVER - CARPET N-5/U

Air - 100 Ft/min Model Width - 24"

		CEILING HEIGHT			
		11"	14"	17"	23"
HEAT INPUT (BTU/MIN)	300	23"			
	400	(17::08)	13"		
	500	(11::02)	(19::03)	28"	25"
	600	(9::40)		19"	
	750	(6::32)		90"	
	1000			(7::24)	
	1250				38"
	1500				38"
	1750				44"
	2000				65"

burning carpet. An example of these data is shown in figure 4-10. At two minutes, the ceiling temperature 24" from the burner for the one with carpet was about 170°C (140°C above the ambient). At the same time the ceiling temperature for the blank run was 100°C (70°C above ambient). This indicates that the energy contribution from the carpet is quite comparable to that from the gas fuel source. Once an accelerating flame front develops the heat release from the carpet assembly becomes dominant.

4.3.4 Air Velocity

The effect of air velocity on flame spread was investigated in a similar manner. Ceiling temperature profiles, as illustrated in figure 4-11, show that as air velocity increases ceiling temperatures decrease. This change in ceiling temperature, however, is quite small at velocities of about 100 feet per minute and lower. Table 4-4 and figure 4-12 show the results of one experiment carried out to determine the effect of air velocity. Using the same carpet assembly (N-5/U) and model size (24" x 11") runs were made with different heat inputs over a range of air velocities. In each series a critical air velocity range was found in which the chance of flameover occurring was greatest. As velocity is increased above this range, the flame spread was less severe. At low velocities (below 75 to 100 feet per minute) severity of flame spread was less. This suggests as indicated earlier, that the mechanism of flame spread may be different at low velocity air flows.

4.3.5 Underlay

Throughout the program the use of an underlay was found to significantly influence flame spread characteristics. When an underlay is used the chance of flameover occurring becomes greater, meaning that flameover will occur with less severe conditions of heat input or model dimensions. Two explanations for this difference existed; the underlay contributed additional fuel or the underlay provided thermal insulation from the floor. To determine which of these two factors is dominant, an experiment, illustrated in figure 4-13, was carried out. Using a model size of 24" x 11", 500 BTU/min heat input and 100 ft/min air flow, a carpet assembly (A-4/U) was selected with which flameover had occurred at 5::39.

In the first experimental run a fiberglass batting (from which all organic binder was pre-burned) was substituted for the standard rubberized hair-jute pad. This was done to simulate an underlay with good insulating properties but one that would contribute no fuel. Flameover occurred at 4::30. The slightly shorter time to flameover may have resulted because the more porous structure of the fiberglass batting provided an oxygen supply directly to the flame front.

The second experimental run was made using a thin sheet of aluminum foil between the carpet and the standard rubberized hair-jute pad. The purpose of the foil was to prevent any air supply or combustion products released by the heated underlay from contributing to the fuel. In this run, flameover occurred at 7::04. It is reasoned that the slightly longer time to flameover may have resulted because of the heat sink

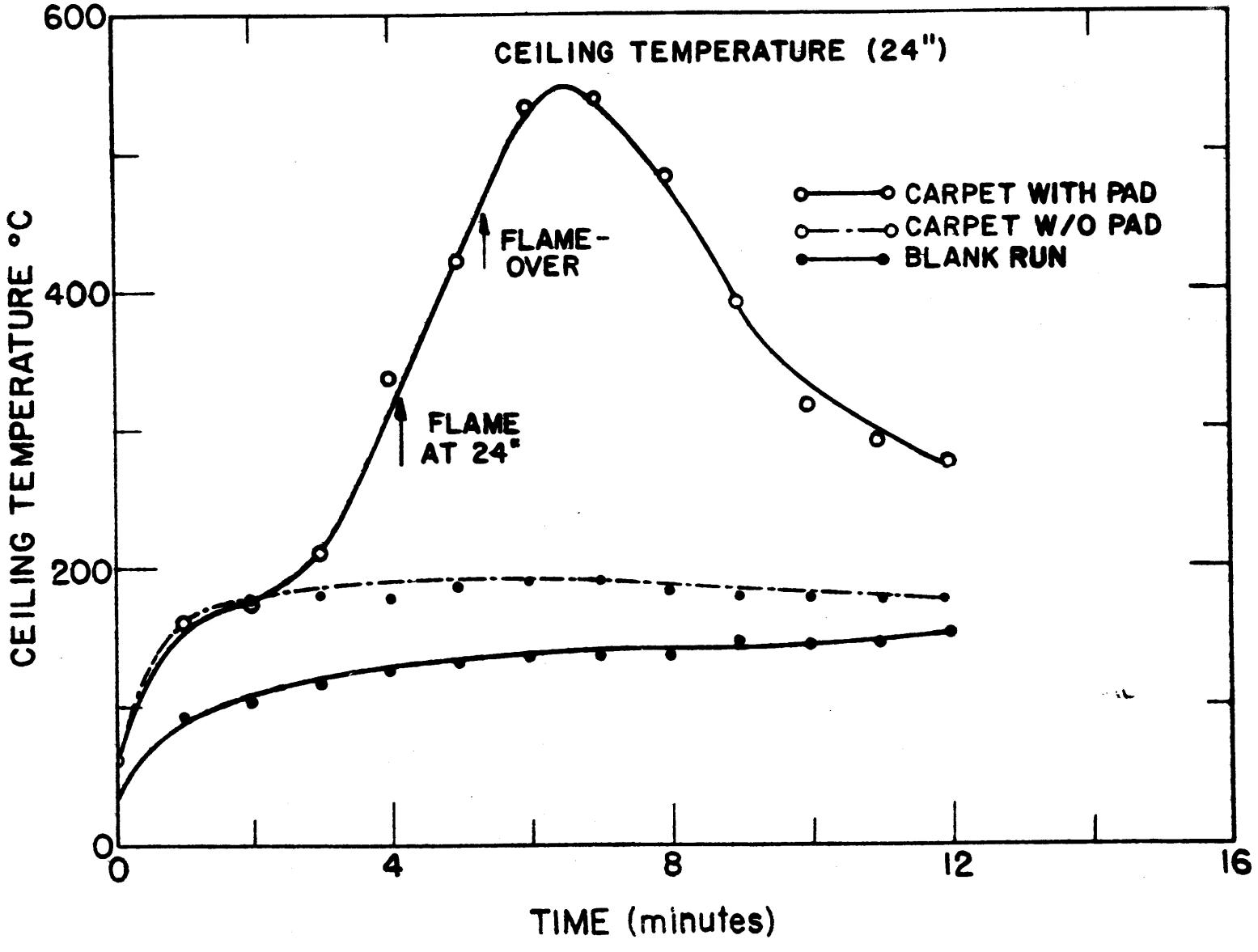

Figure 4-10. Effect of flame spread on ceiling temperature.

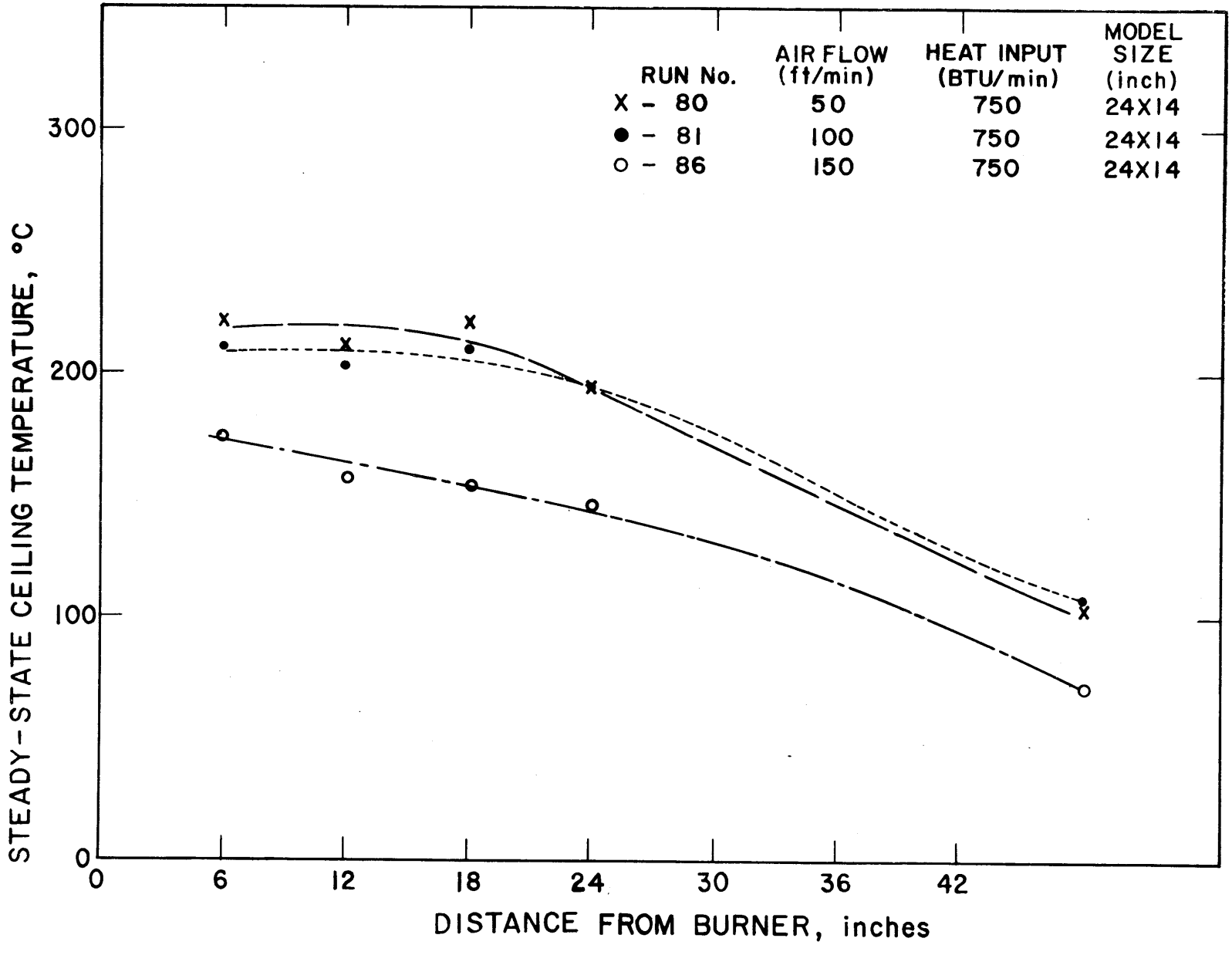

Figure 4-11. Effect of air velocity on ceiling temperature.

TABLE 4-4

EFFECT OF AIR VELOCITY
ON THE EXTENT OF FLAME SPREAD AND FLAMEOVER TIME

CARPET - N-5/U

MODEL SIZE - 24" x 11"

		HEAT, INPUT (BTU/min)				
		400	500	600	750	1,000
AIR VELOCITY (ft/min)	50	19"	(18::00)	(10::05)		
	75	37"	(9::15)	(8::06)	(6::53)	(4::48)
	100	(17::08)	(12::21)	(9::40)	(6::32)	(9::06)
	125	20"	87"	(17::18)	(18::41)	(8::10)
	150		21"	21"	30"	(9::40)
	200				30"	82"
	300				37"	61"

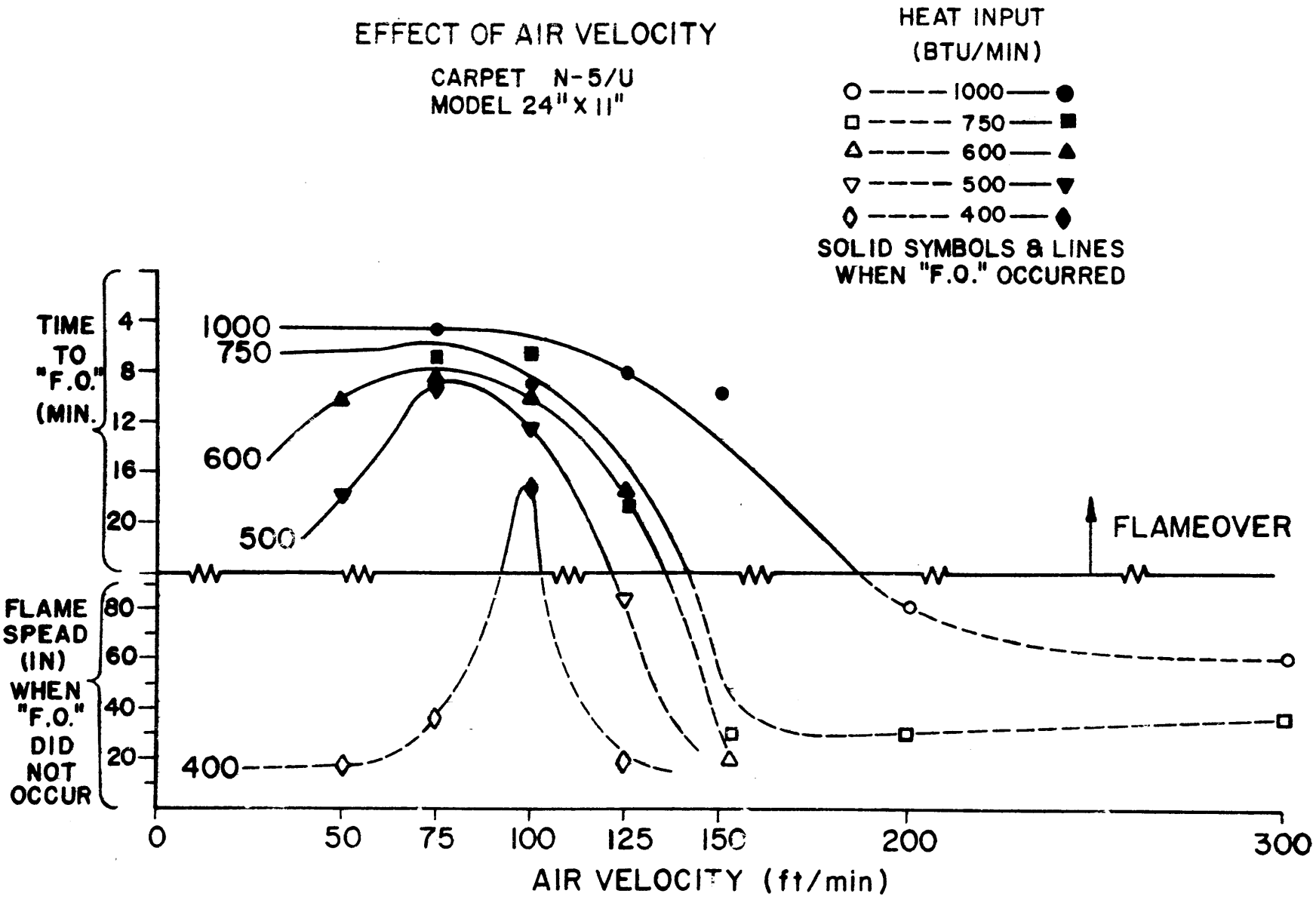

Figure 4-12 Effect of air flow on flame spread.

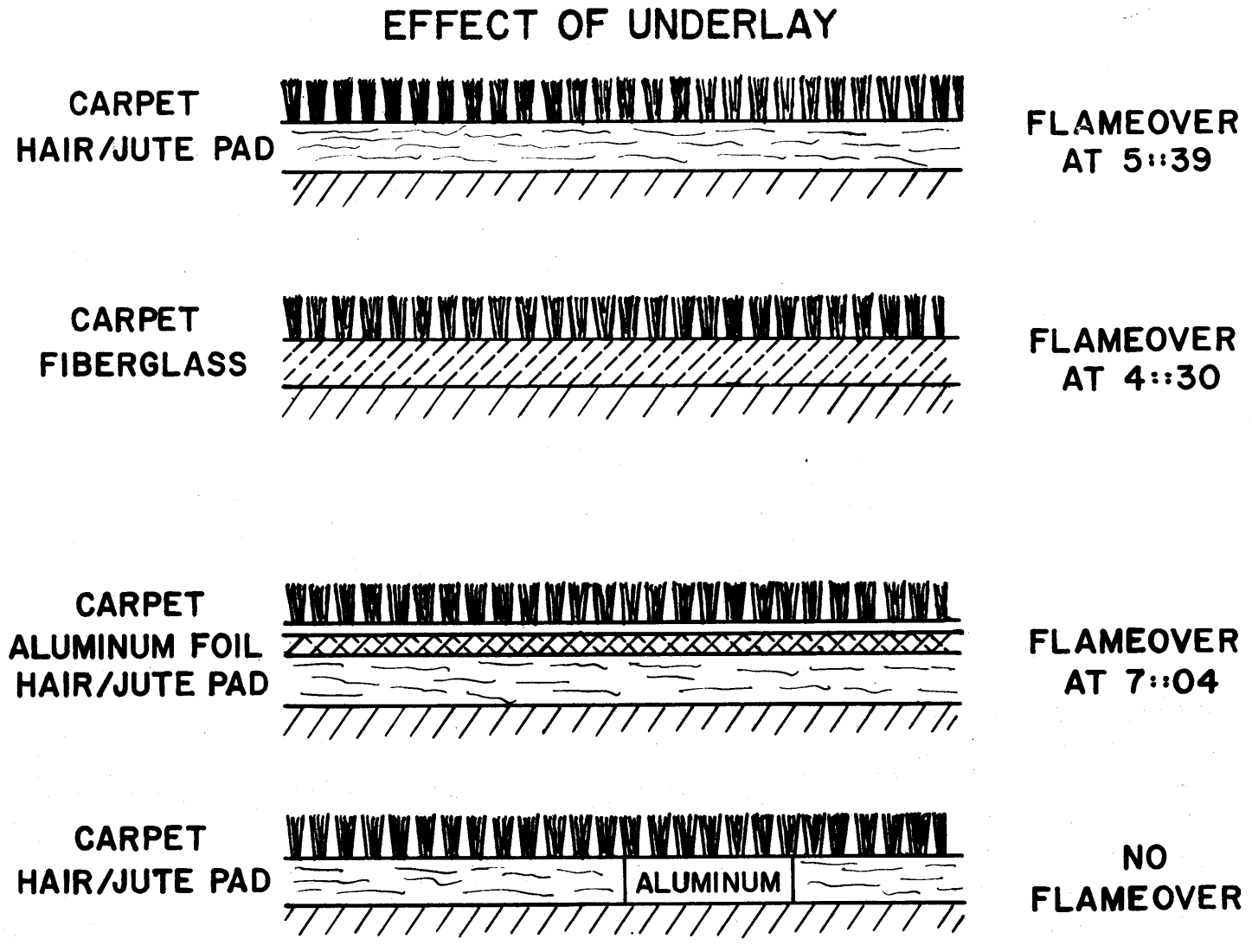

Figure 4-13. Effect of under-lay on flame spread.

property of even a thin foil, or blockage of flow by the foil.

In the final run in this experiment, a 1/2 inch thick aluminum plate was substituted for a section of the rubberized hair-jute pad. It was 12 inches in length, was positioned 24 inches from the burner and covered the full width of the test section (24"). This position was selected because in the previous runs it was at this distance from the burner that the rapidly accelerating flame front had developed which led to flameover. In this run a rapidly accelerating flame did develop just before the flame front reached the aluminum plate. When it reached the plate it quickly decelerated and the sample extinguished a few inches beyond the aluminum plate.

Additional experiments were carried out to reaffirm these results. Carpet assemblies and test conditions were set that would lead to flameover. Just before flameover occurred the tests were stopped and the carpet assemblies extinguished. It was found, both by visual observations and weight loss measurements, that the underlay had not contributed significantly to the fuel.

These results show clearly that the dominant influence of an underlay is the thermal insulation it provides. This thermal insulation causes a greater heat release rate from the carpet and results in higher ceiling temperatures (as seen in figure 4-9), thereby creating a greater chance of flameover.

4.3.6 Other Variables

During the experimental work it was noticed that some of the carpets tended to buckle. This buckling occurred locally in the area just ahead of the moving flame front. It appeared to happen more frequently with carpets having thermoplastic backing materials. When buckling occurs the rate of burning is accelerated leading to higher gas and ceiling temperatures and greater chance of flameover. Several carpets which had been found to buckle were bonded to the floor of the test section and rerun. In every case, as illustrated in table 4-5, flame spread was reduced. A bonded installation of carpeting would minimize buckling and also would provide greater contact to the floor so that, depending on the flooring material, there could be a greater heat loss to the floor.

Several other factors were found to influence results in the model corridor. Changes in temperature of the intake air influenced flame spread. Also the initial condition of the construction material in the test section, probably mositure content, affected results. With careful control of test conditions, good repeatability of results was obtained. These factors are described more thoroughly in reference [6].

5. FLOOR COVERING TESTS

The final phase of the experimental program was to determine how a facility such as the model corridor might be used to realistically separate or rank floor covering materials for flame spread characteristics.

TABLE 4-5

EFFECT OF BONDING CARPET TO FLOOR ON FLAME SPREAD
Results in time to flameover (min::sec) or distance burned (in.)

RUN NO. CFT	CARPET	BONDING	TYPE OF ADHESIVE	MODEL SIZE (in.)	HEAT INPUT (BTU/min)	AIR FLOW (fpm)	RESULT	OBSERVATION*
208	0-5	Yes	Insulating	24x11	500	100	17"	(1)
200	0-5	No	None	24x11	500	100	(9::56)	(3)
209	0-4	Yes	Insulating	24x11	1000	100	41"	(1)
207	0-4	No	None	24x11	1000	100	(9::15)	(3)
153	0-1	Yes	Insulating	24x11	500	100	25"	(1)
158	0-1	Yes	Latex	24x11	500	100	(16::20)	(2)
53	0-1	No	None	24x11	500	100	(6::12)	(3)

* (1) No buckling
(2) Slight buckling
(3) Severe buckling

For this purpose, 26 different carpets were provided by The Carpet and Rug Institute. Included were carpets using each of the major types of pile fiber (nylon, acrylic, polyester, polypropylene and wool) and both institutional and domestic styles. The underlay used throughout the program was a 55 oz/yd^2 rubberized hair-jute pad. A designation, /U, is used to identify carpet assemblies with this underlay. A designation, /F, denotes carpets having an integral foam pad. Four resilient floor coverings were provided by Armstrong Cork Co. Red oak flooring was included in some of the testing. Complete identification of all of the materials is appended in table 5-1.

The findings of the program made it apparent that a method to separate or rank carpets should be based on a "Go : No-Go" decision; that is, either flameover develops and the sample burns the entire distance, or a decelerating flame develops and the sample does not burn the entire length of the test section within a specified time. Therefore, to determine if floor covering materials could be ranked over a wide range it was necessary to vary one or more of the test parameters. Two parameters that seemed practical to vary in an experimental facility were "ceiling height" and "heat input" from the burner. Both approaches were investigated.

A series of carpet assemblies was tested to determine the minimum ceiling height under which each would resist flameover. Ceiling heights of 11", 14", 17" and 23" were used while all other test conditions were held constant (24" wall separation, 500 BTU/min heat input and 100 ft/min air flow). Results of these runs are shown in table 5-2. It was found that many of the carpet assemblies did not flameover at the lowest ceiling height (11") while others did flameover even with the highest ceiling (23"). Results show that it is possible to separate or rank carpet assemblies for flame spread characteristics using this "critical ceiling height" method.

All of the floor covering materials included in the program were tested to determine the maximum heat input each could resist without flameover occurring. In this experiment a model dimension of 24" x 11" and an air velocity of 100 ft/min were used. Heat inputs selected were from 300 to 1250 BTU/min. Table 5-3 lists all of the runs made to determine the "critical heat" value for each material. The results are summarized in table 5-4. Several conclusions can be drawn from these data. Using a facility of this type in the manner described it is possible to rank floor covering materials for flammability over a wide range without encountering a biomodal distribution often associated with other test methods. It is noted that within the group having the lowest heat resistance there is a predominance of carpets having an underlay, either separate pad or attached foam. Conversely, in the materials having the greatest heat resistance there is a predominance of materials without an underlay.

Having established that floor covering materials can be ranked for flammability as described, other model dimensions were investigated. A test facility to be used to measure flammability of carpets in corridors

TABLE 5-1
CARPET IDENTIFICATION

Code	Number	Fiber	Type	Backing	Weight (oz/yd^2) Pile	Weight (oz/yd^2) Total	Pile Height
N-1	NBS-9	BCF Nylon	Level Loop	PP/Foam	20	89	1/8"
N-2	NBS-19	Nylon	Shag	Jute/Jute	24	64	1-1/8"
N-3	300-101	BCF Nylon	Level Loop	Jute/Jute	25	69	1/4"
N-4	300-102	Nylon	Shag	Jute/Jute	28	75	7/8"
N-5	300-103	BCF Nylon	Multi-level Loop	Jute/Jute	16	64	1/8-5/16"
N-6	300-104	BCF Nylon	Woven Cut/Loop	Jute & Cotton	30	69	3/16"
N-7	300-105	BCF Nylon	Level Loop	PP/Foam	15	57	1/8"
A-1	NBS-1	100% Acrylic	Woven Level Loop	Jute & Cotton	38	55	1/4"
A-2	NBS-3	100% Acrylic	Random Shear	PP/Jute	32	69	1/16-5/16"
A-3	300-201	100% Acrylic	Level Loop	PP/PP	36	65	1/8"
A-4	300-202	100% Acrylic	Random Shear	Jute/Jute	36	80	1/8-3/8"
A-5	300-203	100% Acrylic	Plush	PP/Jute	30	66	3/8"
A-6	300-601	70/30 Acrylic/PVC	Level Loop	PP/Jute	35	92	1/4"
P-1	300-401	Polyester	Level Loop	PP/Jute	38	70	1/4"
P-2	300-402	Polyester	Random Shear	Jute/Jute	32	73	1/4-3/8"
P-4	300-404	Polyester	Shag-Plush	Jute/Jute	45	97	1"
P-5	3964-3	Polyester	Tip Shear	Jute/Jute	34	80	1/2"
P-6	3964-1	Polyester	Level Loop	PP/Jute	42	85	1/2"
P-7	3964-2	70/30 Polyester/Modacrylic	Level Loop	PP/Jute	42	85	1/2"
O-1	NBS-11	BCF Olefin	Level Loop	PP/Jute	13	55	1/8"
O-2	300-501	Olefin	Needlefelt	PP Scrim	25	29	3/16"
O-3	300-502	BCF Olefin	Level Loop	PP/Foam	28	94	3/16"
O-4	300-503	BCF Olefin (FR)	Level Loop	PP/PP	20	60	3/16"
O-5	300-504	BCF Olefin	Level Loop	PP/PP	20	60	3/16"
W-1	NBS-10	Wool	Woven Level Loop	Jute & Cotton	38	76	7/32"
W-2	300-301	Wool	Woven Saxony	Jute & Cotton	40	76	9/16"

OTHER FLOOR COVERINGS

R-1	Vinyl Sheet.010" Vinyl Surface	.035" Vinyl Foam	.030" Inorganic Felt Back
R-2	Vinyl Sheet.035" Vinyl Surface	Glass Strands & PVC Film	.100"PVC Foam Back
R-3	Linoleum .050" Linoleum	.040" Cellulosic Film Back	
R-4	Vinyl Sheet.050" Vinyl Surface	.040" Inorganic Felt Back	
RO	Red Oak Flooring	3/4" x 2-1/4" Tongue & Groove	
U-1	Rubberized	Hair-Jute Pad	55 oz/yd^2

TABLE 5-2

"CEILING HEIGHT" TESTS

Distance Burned or Flameover Time as Influenced by Ceiling Height

CARPETS	CEILING HEIGHT				Minimum Ceiling Hgt Without "Flameover"
	23"	17"	14"	11"	
N-1/F		18"	20"	39"	≤11"
N-3	12"		14"	13"	≤11"
N-3/U			19"	21"	≤11"
N-4	30"			54"	≤11"
N-4/U	22::47			6::24	>23"
N-5	13"			18"	≤11"
N-5/U	25"	28"	19::03	12::21	17"
N-6/U			25"	12::50	14"
N-7/F			32"	8::43	14"
A-1				23"	≤11"
A-1/U		26"	13::28	11::13	17"
A-2	14"			19"	≤11"
A-2/U	20"	25"	37"	3::40	14"
A-3	16"			20"	≤11"
A-3/U	42"	8::32		3::57	23"
A-4	11"			18"	≤11"
A-4/U	17"	16"	19"	5::39	14"
A-5	30"	10::43		10::50	23"
A-5/U	11::47			4::39	>23"
P-1/U	41"	41"	39"	6::17	14"
P-4			25"	15::41	14"
P-4/U	49"	16::08		6::18	23"
P-6/U	53"	20::49		9::01	23"
O-1	48"	49"	13::11	6::12	17"
O-1/U	11::03			4::03	>23"
O-2		27"	37"	9::44	14"
O-3/F	52"	9::04		5::25	23"
W-1			9"	13"	≤11"
W-1/U			12"	9"	≤11"

Test Conditions:
Model Width - 24"
Heat Input - 500 BTU/min.
Air Velocity- 100 Ft./min.

TABLE 5-3
"CRITICAL HEAT" SERIES
Influence of Gas Energy Input Rate on Flamespread

CARPET	HEAT INPUT - BTU/MIN							MAXIMUM HEAT INPUT WITHOUT FLAMEOVER
	300	400	500	600	750	1000	1250	600 BTU/min
N-1F			39"	30"	6::44			
			18"		21"	52"	9::20	1000
N-2/U			27"	71"	7::58			600
N-3			13"		20"	32"	8::55	1000
N-3/U			21"		45"	6::14		750
N-4			54"	14::46				500
N-4/U	14::12		6::24					<300
N-5			18"		23"	7::17		750
N-5/U	23"	17::08	12::21	9:40	6;:32	9::06		300
N-6			17"		27"	9::34		750
N-6/U		35"	12::50					400
N-7/F	22"	27"	8::43					400
A-1			23"		33"	3::29		750
A-1/U	36"	16::18	11::13					300
A-2			19"		48"	2::38		750
A-2/U		21"	3::40					400
A-3			20"	28"	4::50	3::15		600
A-3/U	5::53	4::40	3::57					<300
A-4			18"		31"	2::25	2::01	750
A-4/U		21"	5::39					400
A-5	27"	9::40	10::50					300
A-5/U	11::48		4::39					<300
A-6			11"			22"	31"	1250
A-6/U			22"			47"	4::43	1000
P-1			43"	9::46				500
P-1/U	12::45	7::32	6::17					<300
P-2			16"			37"	5::10	1000
P-2/U			27"	18::50	8::00			500
P-4		39"	15::41					400
P-4/U	9::45		6::18					<300
P-5			38"	38"	47"	4::50		750
P-5/U	14:39	16:04	9::44					<300
P-6			38"	10::52	7::58			500
P-6/U	20::20		9::01					<300
P-7			15"			31"	7::00	1000
P-7/U			12"		59"	8::25		750
O-1	30"	20::56	6::12					300
O-1/U	9::36		4::03					<300
O-2	66"	8::36	9::44					300
O-3/F	8::44		5::25					<300
O-4			30"	35"	29"	9::15		750
O-5	21"	21"	9::56					400
W-1			13"				44"	1250
W-1/U			9"		33"	5::00		750
W-2			14"				33"	1250
W-2/U			13"			29"	29"	1250
R-1			9"				27"	1250
R-2			14"			36"	3::10	1000
R-3			34"	16::16	5::24			500
R-4			8"				19"	1250
R-0			15"				31"	1250

TEST CONDITIONS: Model Size 24" x 11"

TABLE 5-4

CRITICAL HEAT

MAXIMUM HEAT INPUT WITHOUT FLAMEOVER

BTU/MINUTE							
<300	300	400	500	600	750	1000	≥ 1,50
N-4/U	N-5/U	N-6/U	N-4	N-1/F	N-3/U	N-2	A-6
A-3/U	A-1/U	N-7/F	P-1	N-2/U	N-5	N-3	W-1
A-5/U	A-5	A-2/U	P-2/U	A-3	N-6	A-6/U	W-
P-1/U	A-4/U	A-4/U	P-6		A-1	P-2	W-
P-4/U	O-2	P-4	R-3		A-2	P-7	R-1
P-5/U		O-5			A-4	R-2	R-2
P-6/U					P-5		R-
O-1/U					P-7/U		
O-3/F					O-4		
					W-1/U		

should be designed with a shape factor (height to width ratio) more nearly like real corridors. Additionally the data suggests that very low ceilings in a test facility may not correlate as well with real corridors. For these reasons tests were conducted on many of the floor covering materials in the model corridor using cross-sectional dimensions of both 18" x 18", and 16" x 16". Data obtained in the 16" x 16" model corridor are shown on table 5-5. These data again indicate that floor covering materials can be ranked for flammability over a wide range of heat inputs. Good correlation was found between results in this 16" x 16" model corridor and the "ceiling height" and the "critical heat" rankings.

Using the critical heat ranking established for the 26 carpets, table 5-4, a correlation study was made to determine if any factor of carpet construction consistently influenced flammability. It should be realized before commenting on this analysis, that the carpets in the program were not chosen to permit this type of analysis. Data indicate that the wool carpets, based on only two samples, tended to rank high for heat resistance. Polypropylene tended to rank low. The other fiber types (nylon, acrylic, and polyester) showed no trend. Carpets with these three fibers covered a wide range of heat resistance. Tufted carpets having a polypropylene primary or secondary backing tended to have lower heat resistance than those made with jute primary and secondary. Foam backed carpets performed less satisfactorily than those without an integral pad, which is consistent with results discussed earlier regarding the influence of an underlay. No correlation was found between heat resistance and carpet style, pile or total weight, pile height, or pile density. Results suggest that carpet flammability performance is not associated with any single characteristic of the carpet but is dependent on the total carpet structure.

To determine if flammability rankings for floor covering materials obtained using the model corridor correlate with other test methods, results were obtained and are shown on table 5-6. The samples are ordered on this table by "critical heat" values (Column A) as obtained in the experimental program. Within each level of critical heat the materials are not ordered. Good correlation is found between "critical heat" and "critical ceiling height" (Column B) values. This indicates that either method as described earlier, can be used to measure the resistance of a carpet assembly or floor covering material to the conditions leading to flameover.

Each of the floor covering materials was tested using a model size of 24" x 11", 500 BTU/min heat input and 100 ft/min air velocity. These results are shown in Column C of table 5-6. Results are shown in time (minutes::seconds) to flameover or flame spread distance (inches) if flameover did not occur. Obviously, those materials with a "critical heat" resistance of 500 BTU/min or higher did not flameover in this test. Within this group there is an indication of agreement between distance burned in this standard test and "critical heat" value, however, correlation is poor.

TABLE 5-5

Test in 16" x 16" Model Corridor

Critical Heat**	Sample No.	16" x 16" Model 500*	600*	750*	1000*
750	N-3/U		20"		
600	N-1/F		27"		
500	N-4		36"	39"	
	P-1		34"		
	P-2/U		29"	87"	
400	N-6/U		11::14	8::08	
	N-7/F		17::48	7::48	
	A-2/U		34"	49"	
	A-4/U		17"	27"	34"
	P-4		61"	13::53	
300	N-5/U		29"	29"	8::31
	A-1/U		47"		
	A-5		28"	45"	7::25
	O-1		61"	11::31	
	O-2		5::30		
<300	N-4/U	68"	9::54		
	A-3/U	47"	5::13		
	P-1/U		7::14		
	P-5/U		6::45		
	O-1/U	9::51	5::14		
	O-3/F		4::59		

*Heat Input, BTU/min.
**Rank established in "Critical Heat" Series Table 5-3

TABLE 5-6

COMPARISON OF TEST METHODS

"Critical Heat" BTU/min	Sample No.	MMFPA Tests "Critical Ceiling"	MMFPA Tests Standard Test	U.L. Chamber	E-84 Tunnel	Radiant Panels Armstrong	Radiant Panels E-162
1250	A-6	11"	11"				
	W-1	11"	13"		50	39	64
	W-2	11"	14"				
	W-2/U	11"	13"				
	R-1	11"	9"			43	
	R-4	11"	8"		45	44	
	RO	11"	15"	1.0	100		100
1000	N-2	11"	18"		179	65	210
	N-3	11"	13"			52	140
	A-6/U	11"	22"				
	P-2	11"	16"				
	P-7	11"	15"				
	R-2	11"	14"			66	
750	N-3/U	11"	21"			69	185
	N-5	11"	18"	1.1		69	241
	N-6	11"	17"				
	A-1	11"	23"	.9	43	85	145
	A-2	11"	19"	1.2	50	227	404
	A-4	11"	18"	1.3		131	262
	P-5	11"	38"				
	P-7/U	11"	12"				
	O-4	11"	30"		70		
	W-1/U	11"	9"			46	119
600	N-1/F	11"	39"	1.1	237	86	284
	N-2/U	11"	27"			90	289
	A-3	11"	20"			131	225
500	N-4	11"	54"	1.9		79	173
	P-1	11"	43"				
	P-2/U	11"	27"				
	P-6	11"	38"		200		
	R-3	11"	34"			98	
400	N-6/U	14"	(12::50)				
	N-7/F	14"	(8::43)				
	A-2/U	14"	(3::40)	2.3	279	453	445
	A-4/U	14"	(5::39)	1.7			291
	P-4	14"	(15::41)				
	O-5		(9::56)		220		
300	N-5/U	17"	(12::21)			96	332
	A-1/U	17"	(11::13)	2.6	298	131	150
	A-5	23"	(10::50)			385	309
	O-1	17"	(6::12)	2.1	71	116	616
	O-2	14"	(9::44)				
<300	N-4/U	>23"	(6::24)	11.8		135	253
	A-3/U	23"	(3::57)			179	265
	A-5/U	>23"	(4::39)			533	400
	P-1/U	14"	(6::17)				
	P-4/U	23"	(6::18)				
	P-5/U		(14::39)				
	P-6/U	23"	(20::20)				
	O-1/U	>23"	(4::03)	24.0		358	764
	O-3/F	23"	(5::25)				

Those materials having "critical heat" values of 400 BTU/min or less did, as expected, flameover in this standard test. There is no correlation between time to flameover and the "critical heat" value for a material. It can also be noted on tables 5-2 and 5-3 that often a material with good flame spread resistance (high "critical heat") reaches flameover in a short time with a large ignition source, whereas a material with poorer resistance may flameover in a longer time under much lower ignition energy release rate. In general it was observed that materials that char and burn (acrylics and wool) tend to flameover in short time, whereas the thermoplastic materials tend to flameover in longer times. This further confirms that a time dependent index may not be a good measure of flammability, especially, if the real hazard is concerned with the potential for flame spread rather than the speed of flame spread.

A number of the materials used in the program were tested by the Underwriters' Laboratory Subject 992 Floor Covering Test Method. Results are recorded in Column D of table 5-6. These results were obtained using one of the existing chambers. There is some question regarding control of air flow in these units. This raises the possibility that the indexes may be lower than would occur with more positive air flow control. Since the index obtained is dependent on distance burned or time to burn the full distance (flameover), some lack of correlation with "critical heat" values would be expected. Results of ASTM E 84-68 Tunnel Test were obtained for some of the materials and are shown in Column E. Correlation between these results and "critical heat" values is not good.

Results of two radiant panel test methods were obtained on many of the materials used in the program and are shown on table 5-6. The methods used were the Armstrong Flooring Radiant Panel and ASTM E 162-67 Radiant Panel Test. The numerical index in the former test was based on flame spread rate or distance burned. The latter test index relates to spread rate and energy release. Some correlation of results is indicated but several anomalies exist in both methods. It appears that in these radiant panel test methods the controlling source of energy causing flame spread is the radiant panel, whereas in the model corridor, U. L. Chamber and E 84 Tunnel the fuel contributed by the specimen being tested is a significant factor.

The model corridor was designed as an experimental facility, not a test apparatus, and therefore a statistical plan for determining repeatability and reproducibility was not developed. In the course of the experimental program, however, many runs were replicated and are available as a measure of repeatability. These data are shown on table 5-7. Another measure of experimental reliability is available. In many of the experiments the severity of the heating conditions was gradually increased from run to run (reducing ceiling height or increasing heat input). As this is done, the distance burned increases slightly up to flameover. If severity of heating conditions is further increased, time to flameover is shortened. These results are shown on tables 5-2 and 5-3. These consistent trends imply repeatability of results within

TABLE 5-7

REPEATABILITY DATA

Carpet	Test Conditions*	Run. No.	Result**
N-5/U	24x11, 500, 100	41	8::50
		47	7::04
		64	10::07
A-4/U	24x11, 500, 100	49	5::28
		68	4::25
		107	5::24
		129	6::50
W-1/U	24x11, 500, 100	51	8"
		139	10"
A-4/U	24x14, 750, 100	82	5::40
		126	5::08
A-3/U	24x17, 500, 100	92	5::06
		96	11::57
O-4	24x11, 500, 100	201	31"
		202	29"
N-5/U	24x11, 750, 150	301	29"
		329	31"

* Test Conditions are:
Model Size (W"xH"), Heat Input (BTU/min), Air Flow (Ft/min).
**Results shown in inches burned or time (min::sec) to Flameover.

the tolerance levels indicated.

6. QUANTITATIVE EVALUATION OF CONTRIBUTING FACTORS

In this section a closer examination of the factors which influence flame propagation in the model corridor will be presented. A qualitative description of the phenomenon of flame propagation has been presented. Here the focus will be on the components and mechanisms. An effort was made to quantify the effects of these factors. This was accomplished from measurements, analysis, and modelling. At this point, no attempt has been made to generalize these results. The factors influencing flame propagation which will be discussed include: (1) the ignition flame characteristics, (2) the thermal aerodynamics of the flow, (3) the energy release rate by the carpet in the ignition zone, (4) radiant preheating and (5) the results of an overall energy balance on the model corridor.

6.1 Ignition Flame

The hardware associated with the burner has been described elsewhere [6]. Here the concern is with the resultant diffusion flame characteristics. The general description of the flame is yellow to orange in color, visibly turbulent a short distance from the burner ports, and tends to expand an inch or two from its initial 6 inch "line" width at the ports. A photograph looking into the burner flame prior to carpet ignition in a test is shown in figure 6-1. A series of runs were conducted without combustible floor covering to examine some details of the burner flame. These characteristics are shown in figure 6-2 and span the normal range of operating conditions for the tests. Some judgment had to be used in defining the boundary of the luminous flame zone since it is quasi-steady and irregular. The general flame shape is shown in the figure. It is significant that flame length, L_B, increased as air flow, V_∞, decreased. This reflects increased mixing with increasing air flow. Flame angle was virtually constant over the range of these parameters; however, later test results (not shown) indicate below an air flow of 40 fpm the plume inclination will begin to increase towards the vertical. In fact for all ranges of gas flow used, the burner plume would be essentially vertical at zero forced air flow. By placing a radiometer upstream of the flame, heat flux was measured, and later forward flame radiant flux was calculated by modeling the flame as a sheet with a projected surface area of H_B x 8 inches. (Note that since most of the flame radiation would be attributed to emission from carbon particles the sapphire window is adequate since soot has an absorption coefficient inversely related to wave length [16] and sapphire is transparent to 5μ.) Figure 6-3 is a schematic side view of the burner flame. The temperatures were recorded by bare type K thermocouple (approximately 20 mils) inserted into the flow stream and the flame. The trajectory paths that were sketched are based on observations made using titanium tetrachloride induced smoke tracings. Finally it should be emphasized that in all the work burner gas flow rate was used to calculate burner energy release rate, $\dot{E}_B$. Although more than sufficient air is available for complete combustion all the energy released is not necessarily

Figure 6-1. Burner flame plume 30 seconds after ignition.
V_∞= 100 fpm, $\dot{E}_B$ = 500 BTU/min.

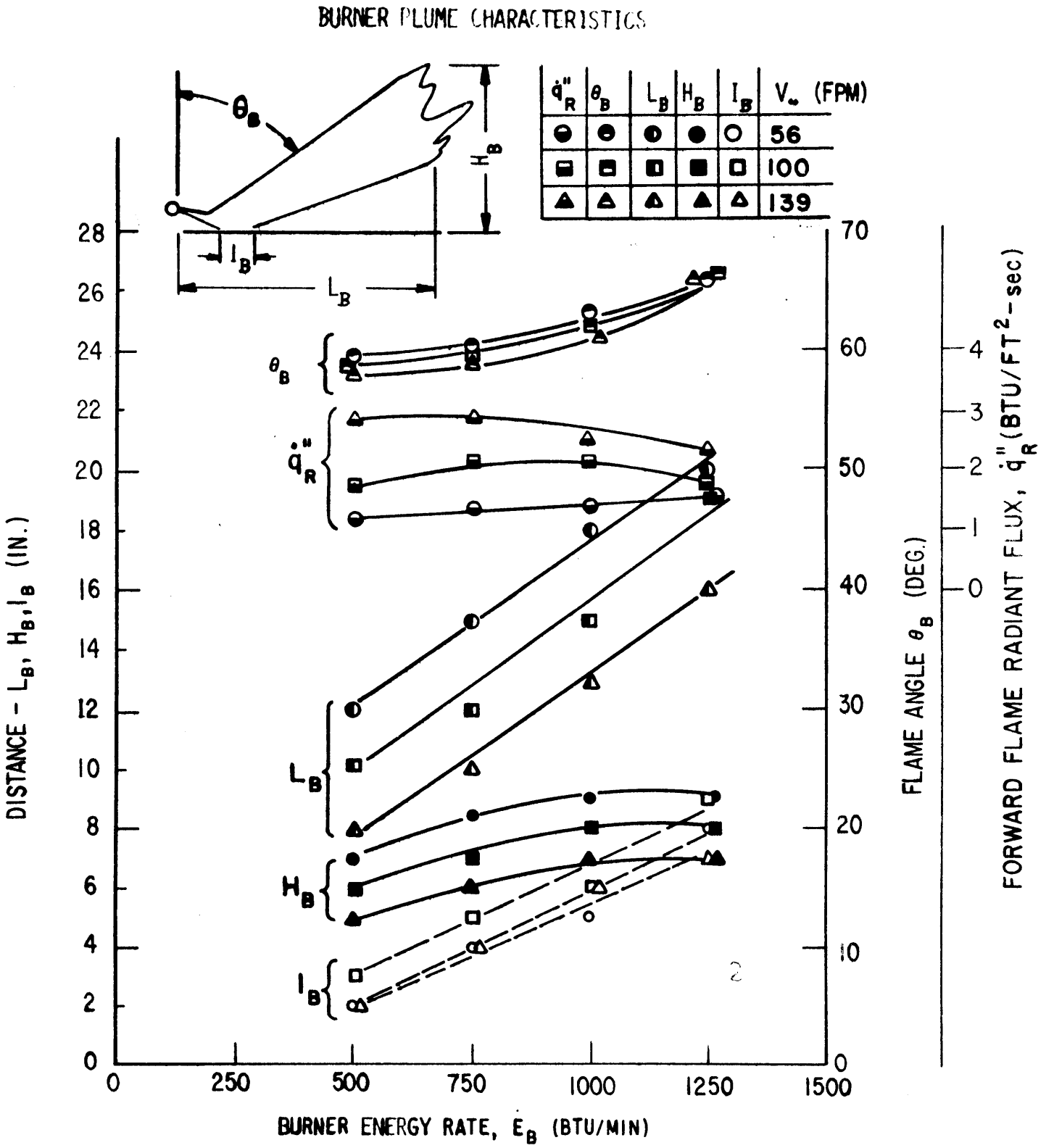

Figure 6-2. Burner plume characteristics.

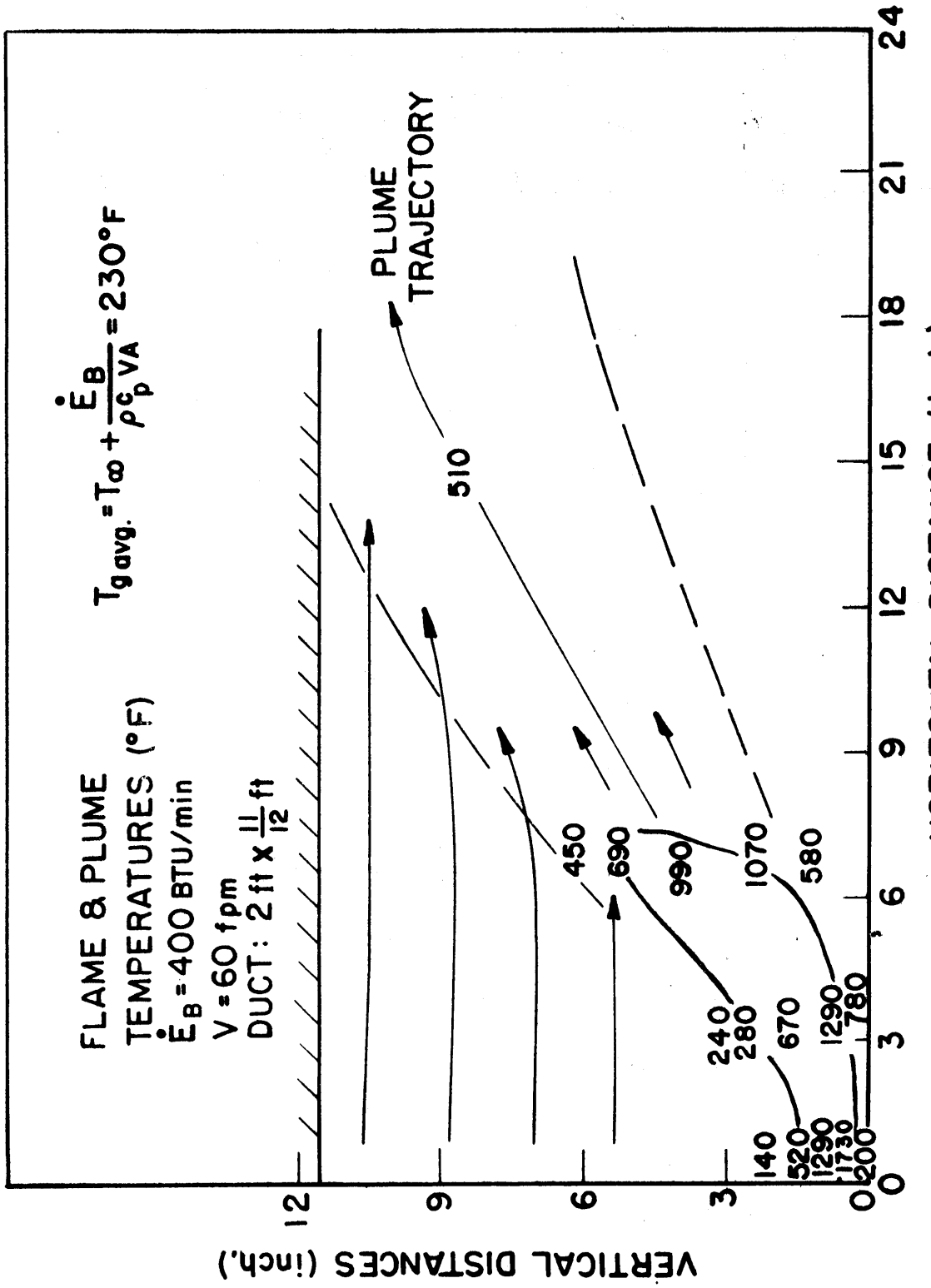

Figure 6-3. Thermal-flow field of burner flame plume.

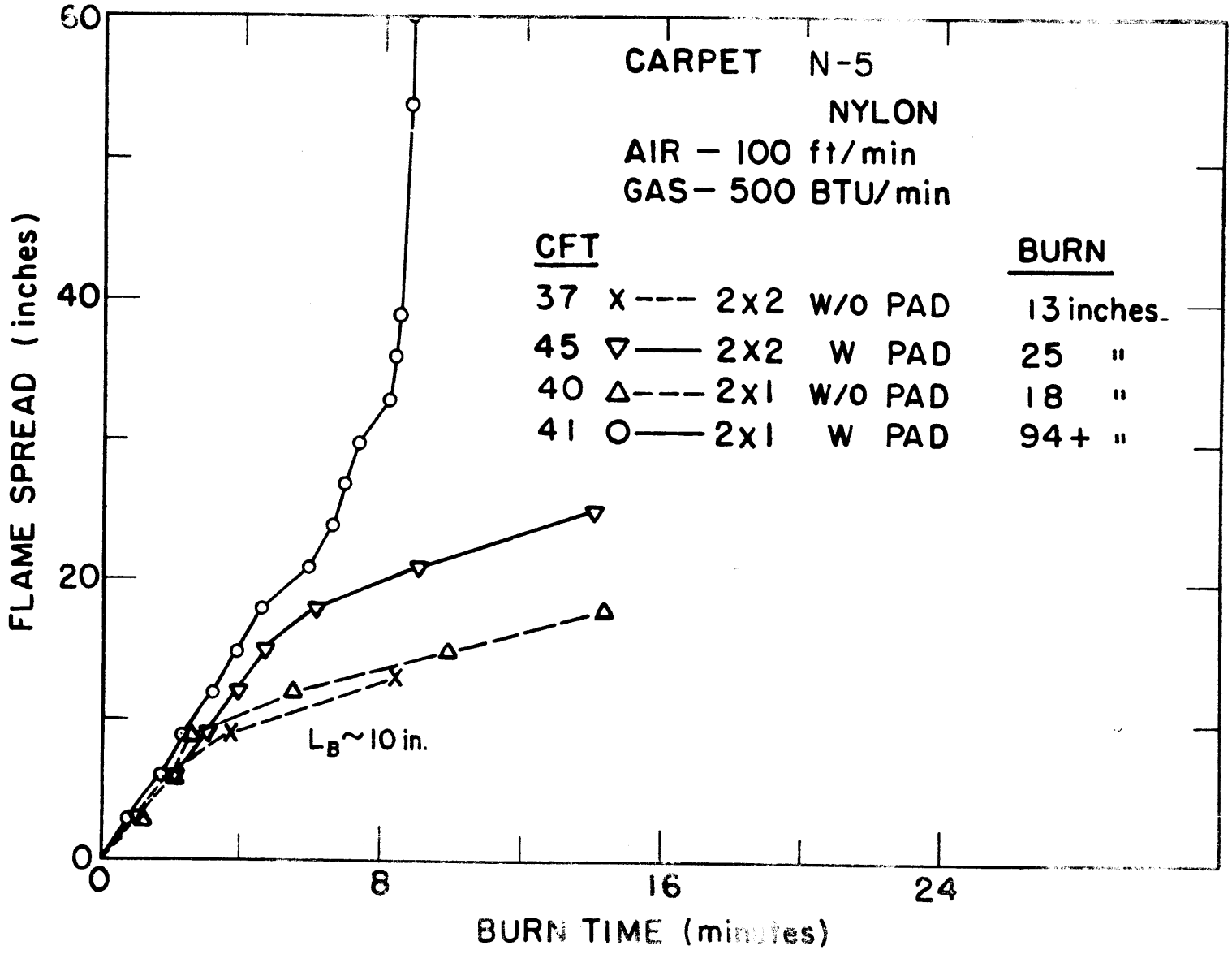

Figure [illegible]. Example of flame spread for melting carpet pile fibers.

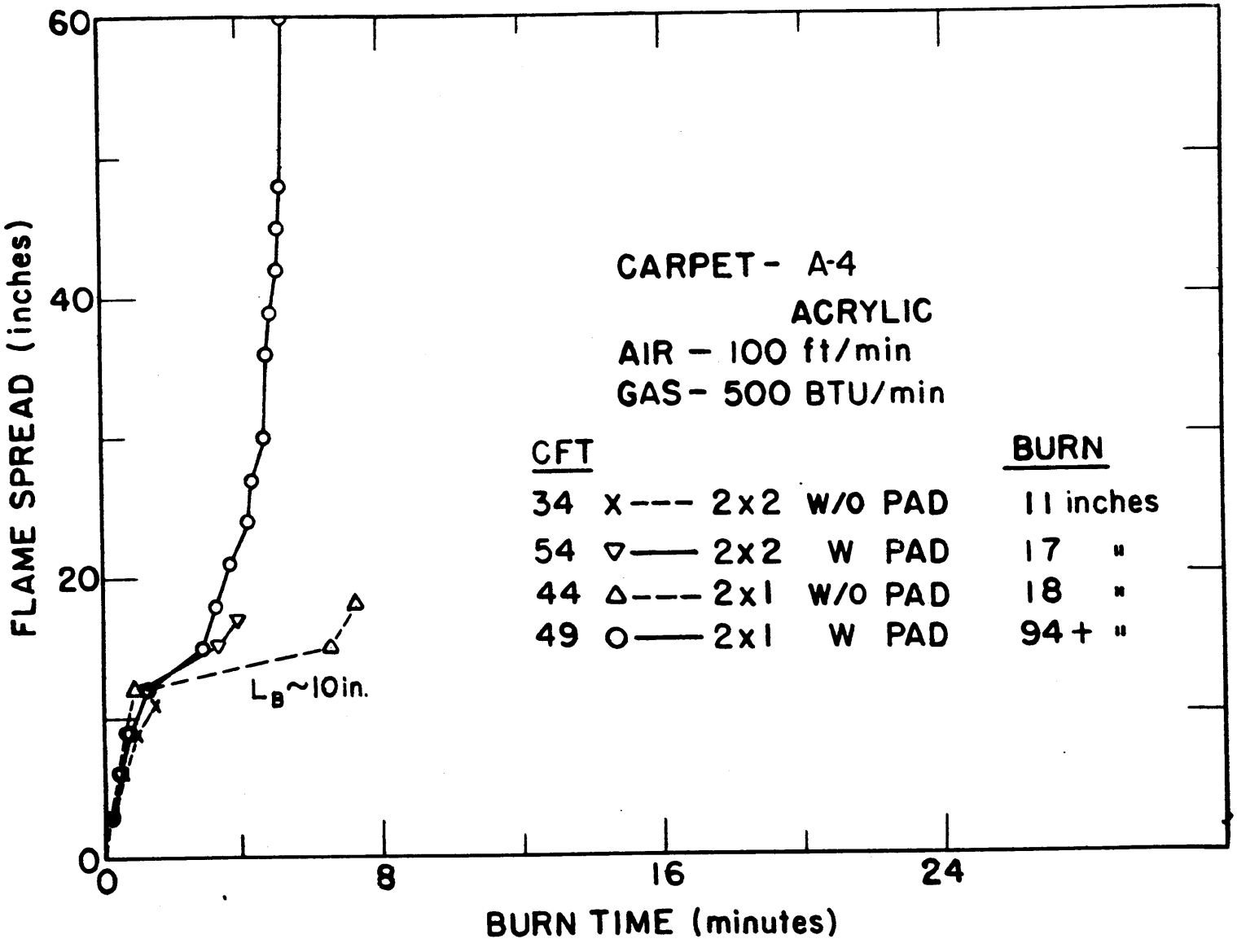

Figure 6-5. Example of flame spread for charring carpet pile fibers.

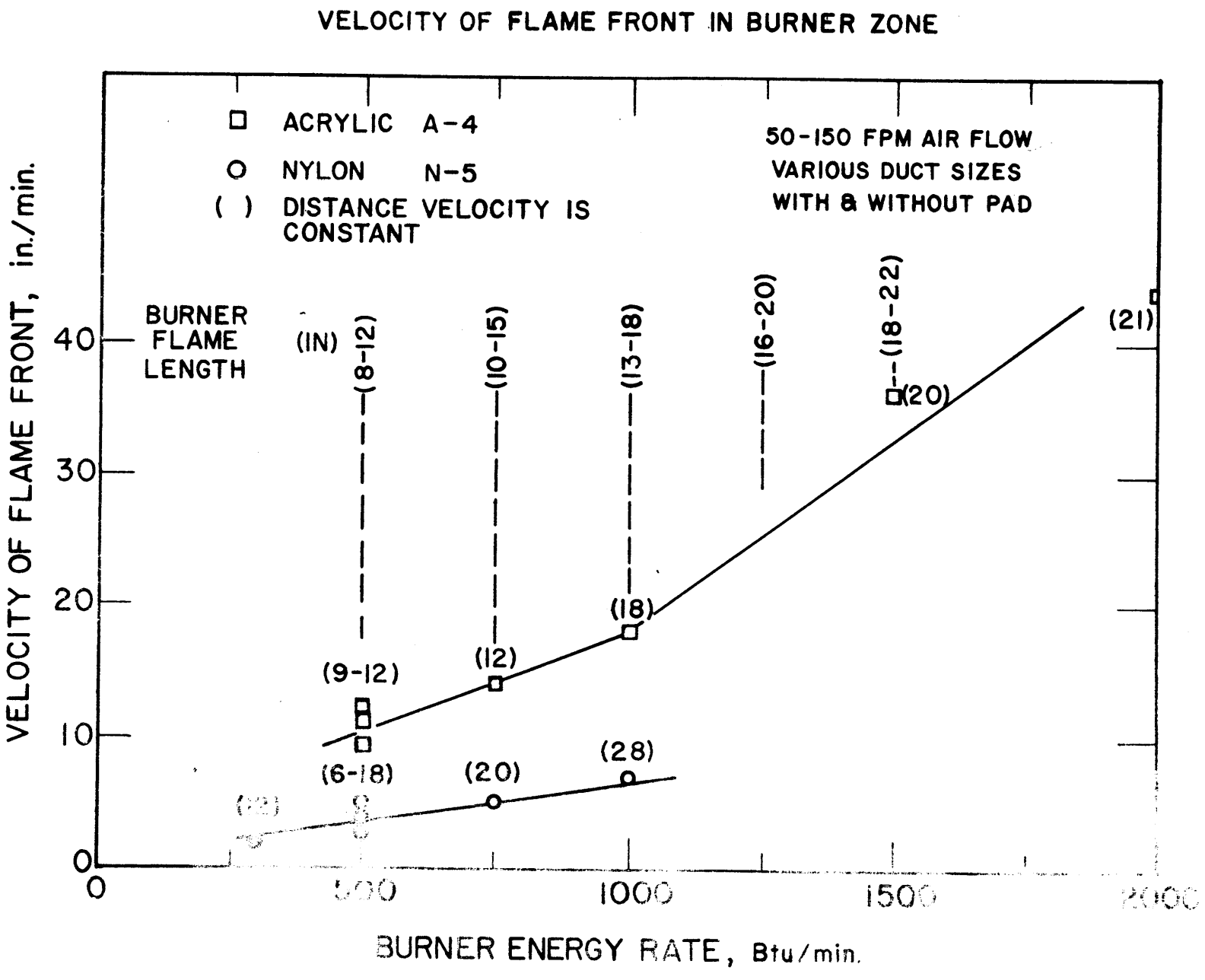

Figure [illegible]. Initial flame spread velocity for A-4 and N-5.

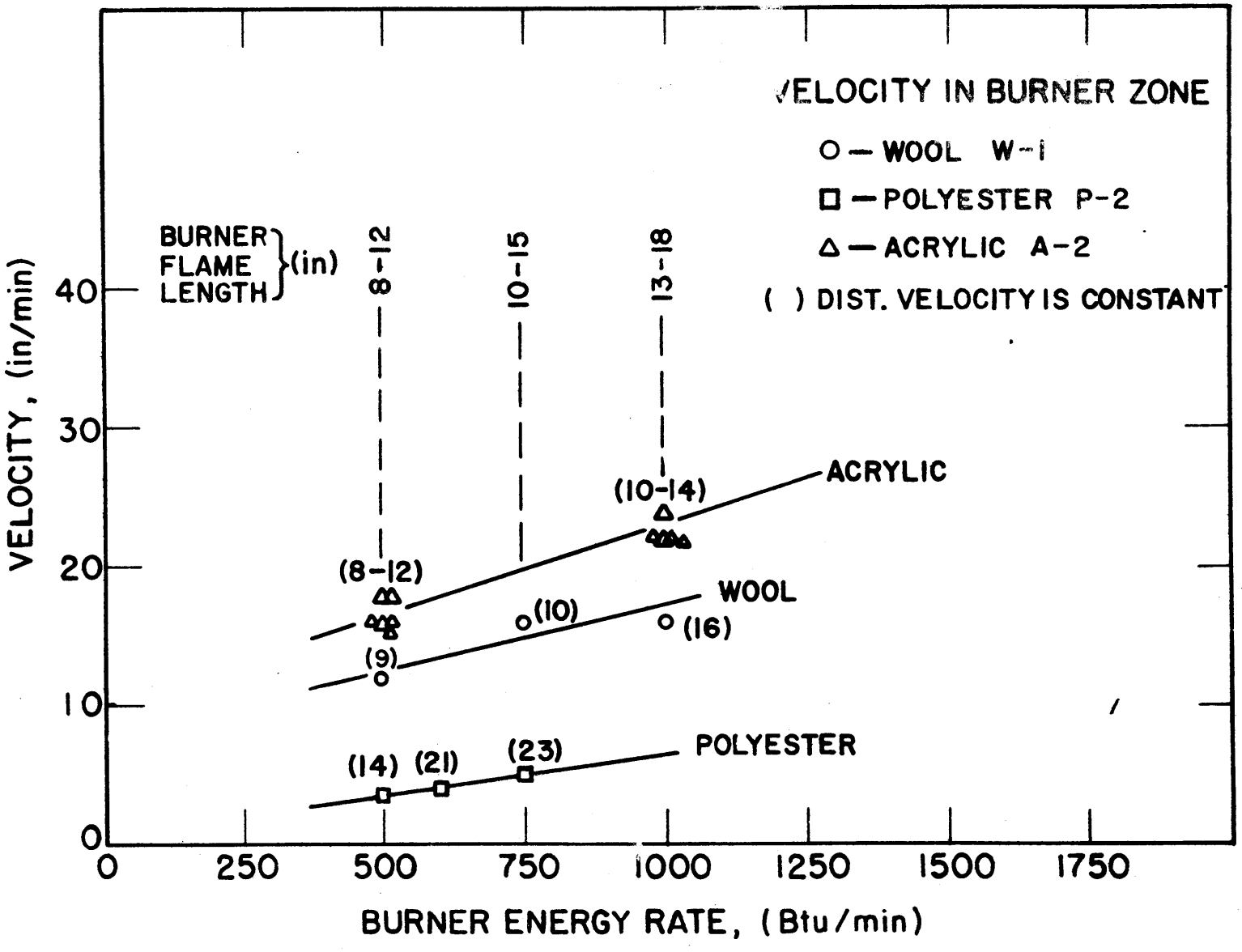

Figure 6-7. Initial flame spread velocity for W-1, A-2, and P-2.

convected downstream. Estimates on a "500 BTU/min" burner input suggested a maximum of a 10 percent conduction wall loss and a maximum of a 20 per cent radiation loss to the local surroundings.

The effect of burner flame on floor covering flame spread is to initiate a fairly constant flame spread and to contribute to downstream ceiling and wall heating. Carpet pile fibers which melt tend to maintain a constant flame spread rate for distances greater than the burner flame length, L_B; however, carpets which did not exhibit melting tended to maintain a uniform flame spread velocity up to L_B. Nylon carpets exhibit the former (see figure 6-4), while acrylic carpets exhibit the latter (see figure 6-5). The effect of burner energy input on initial carpet flame spread is shown in figures 6-6 and 6-7 for several representative carpets tested. The numbers in parenthesis represent the distance in inches over which the flame velocity maintained a constant value. These results are based on a sample of data ranging over initial conditions of 50-200 ft/min air velocity, 11 to 48 in. for height, 24 to 48 in. for width, and with and without pad underlay. It is significant that this initial flame spread is a strong function of burner flame length, L_B, and energy input, $\dot{E}_B$; while very weakly dependent (if at all) on duct size, air flow, and carpet underlay for the range of parameters investigated. Both $\dot{E}_B$ and L_B affect the extent of heat transfer to the floor material. Above a critical burner heat flux level, steady flame propagation would be expected to be monotonically increasing with flux. For the results presented in figures 6-6 and 6-7 it would not be correct to extrapolate back to $\dot{E}_B=0$ since a definite $\dot{E}_B > 0$ is required before steady flame spread is possible. The width of the initial burning zone is also controlled by the burner flame width, and flame spread to the sides of the duct is insignificant compared to forward flame motion. However, as flame acceleration ensues and flameover is approached, burning across the entire duct width is likely.

6.2 Air Flow

The air flow entering the test section was unidirectional, uniform, and laminar in character. The burner and sharp edge entrance of the test action presented local disturbances to the inlet laminar flow. Considering only air flow to the test section, the duct inlet Reynolds number (Re) for all run conditions was always greater than 2000. Hence fully developed flow should be turbulent. Since the boundary layer development is likely to be disturbed at the inlet a turbulent boundary layer should persist through fully developed turbulent duct flow which could occur within the test section length [17]. Because of the increase in kinematic viscosity with temperature, a heated flow would have a lower Reynolds number and could relaminarize. However, once the burner flame is introduced the inlet disturbance is increased tremendously and buoyancy becomes a dominant factor. In fact, smoke trace observations indicated reasonably laminar flow (V_∞ = 60 ft/min, H = 11 in., W = 24 in.) with no burner on up to a distance of 4 feet at the center line; however, with the burner on, laminar flow ceased at the flame plume. Thereafter the flow appeared turbulent.

Once the burner flame is ignited the inlet air flow is markedly disturbed. Air is entrained into the flame from all sides at varying degrees. For a spreading floor covering flame, air is swept in from the back and sides while the leading edge of the flame front is blown forward. This flow pattern is clearly discernible in figure 6-8.

Overall the air flow has a cooling effect on the combustion products which is clearly apparent if the average bulk gas temperature, T_g, is considered. Neglecting radiation or other losses this is

$$\frac{T_g}{T_\infty} = 1 + \frac{\dot{E}_B}{\rho_\infty c_p T_\infty W H V_\infty} \qquad (6\text{-}1)$$

(The symbols are defined in the Table of Nomenclature.) Clearly $\bar{T}_g$ decreases as V_∞ is increased. Although it is useful to think in terms of an average gas temperature, it is significant that the temperature distribution downstream of the flame zone is highly stratified with the hot gaseous products at the top of the duct. Variations in temperature also exist across the width of the duct due to the three dimensional character of the burning zone. However, these are not normally significant and diminish as distance increases from the flame zone. The vertical temperature stratification is illustrated in figure 6-9 in which is displayed equilibrium conditions in a duct with non-combustible materials. For these conditions the degree of stratification increases directly with $\dot{E}_B$. In general a dimensional analysis of the governing equations suggests that a Froude number parameter (Fr),

$$Fr = \frac{\rho_\infty V_\infty^2}{g \Delta\rho H}$$

is a suitable indicator for stratification. This follows since Fr is the ratio of inertia force to buoyant force. Hence a large Fr implies weak stratification. However, the above form for Fr is not convenient since $\Delta\rho$ is not an independent quantity. By introducing Ideal Gas laws and incorporating an average bulk temperature to characterize the temperature level it follows that an alternative expression is

$$Fr = \frac{V_\infty^3 \rho_\infty c_p T_\infty W}{g \dot{E}_B} \qquad (6\text{-}2)$$

Figure 6-8. Nylon carpet flame displaying three-dimensional flow pattern.

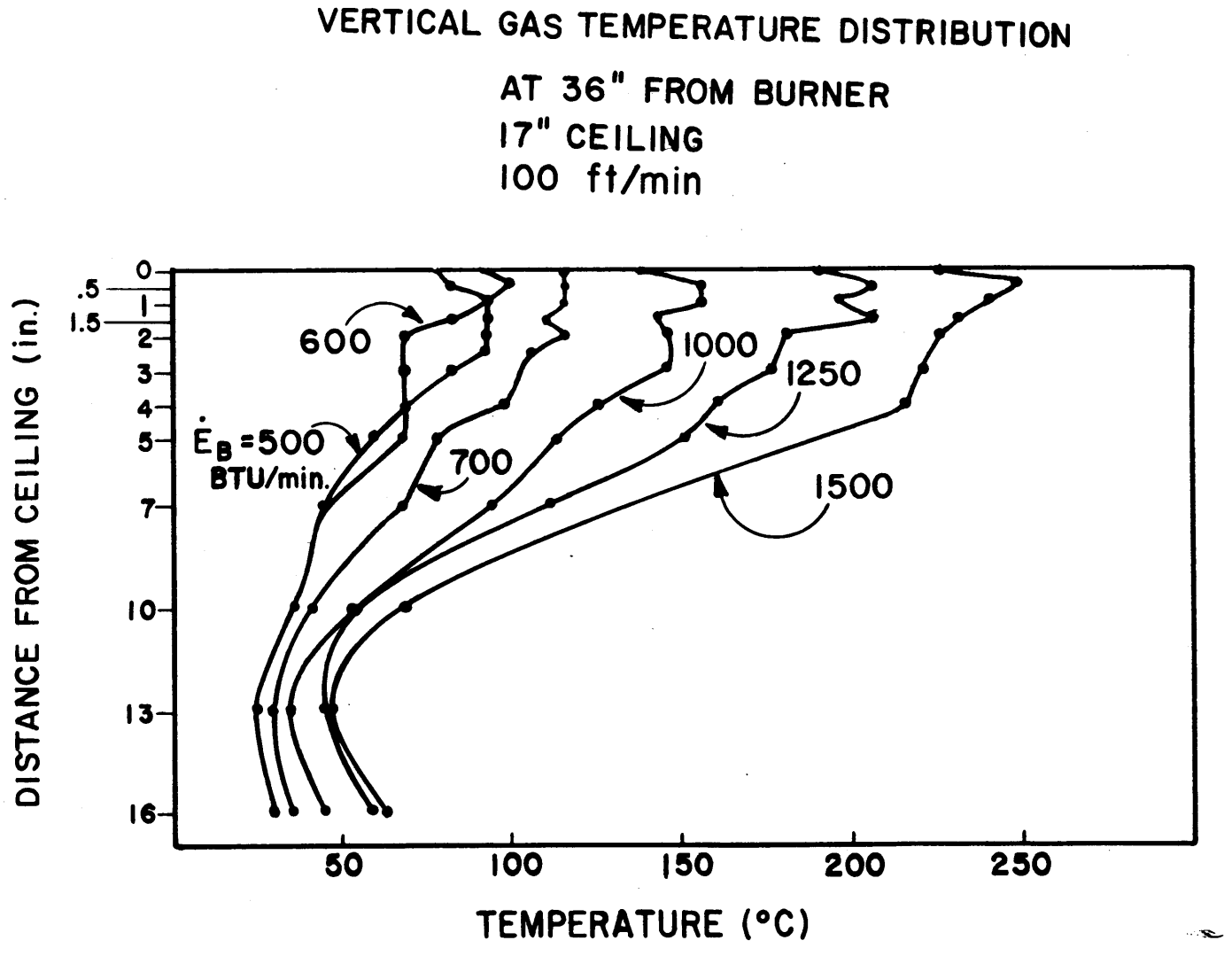

Figure 6-9. Vertical gas temperature profiles.

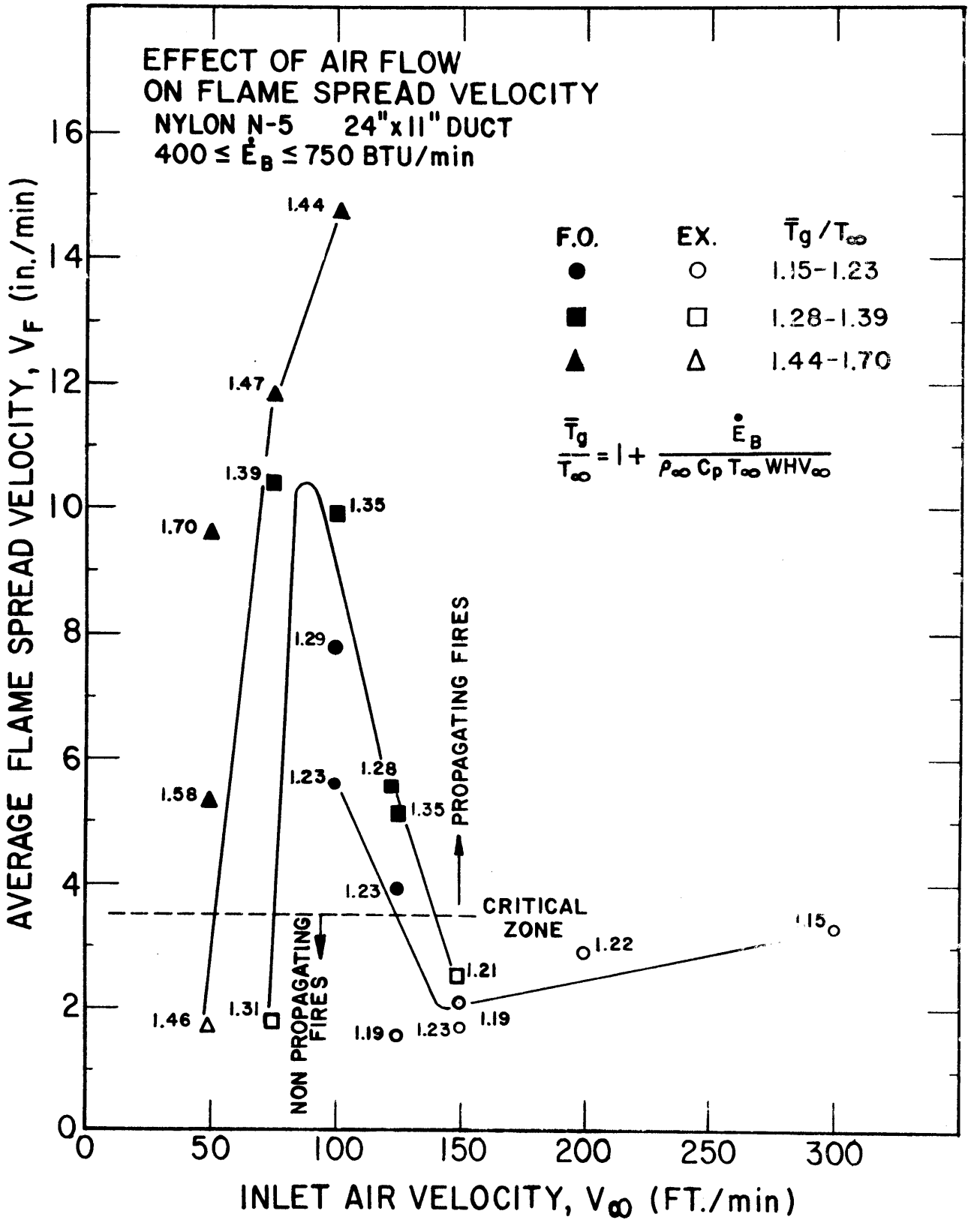

Figure 6-10. Effect of air flow on flame spread.

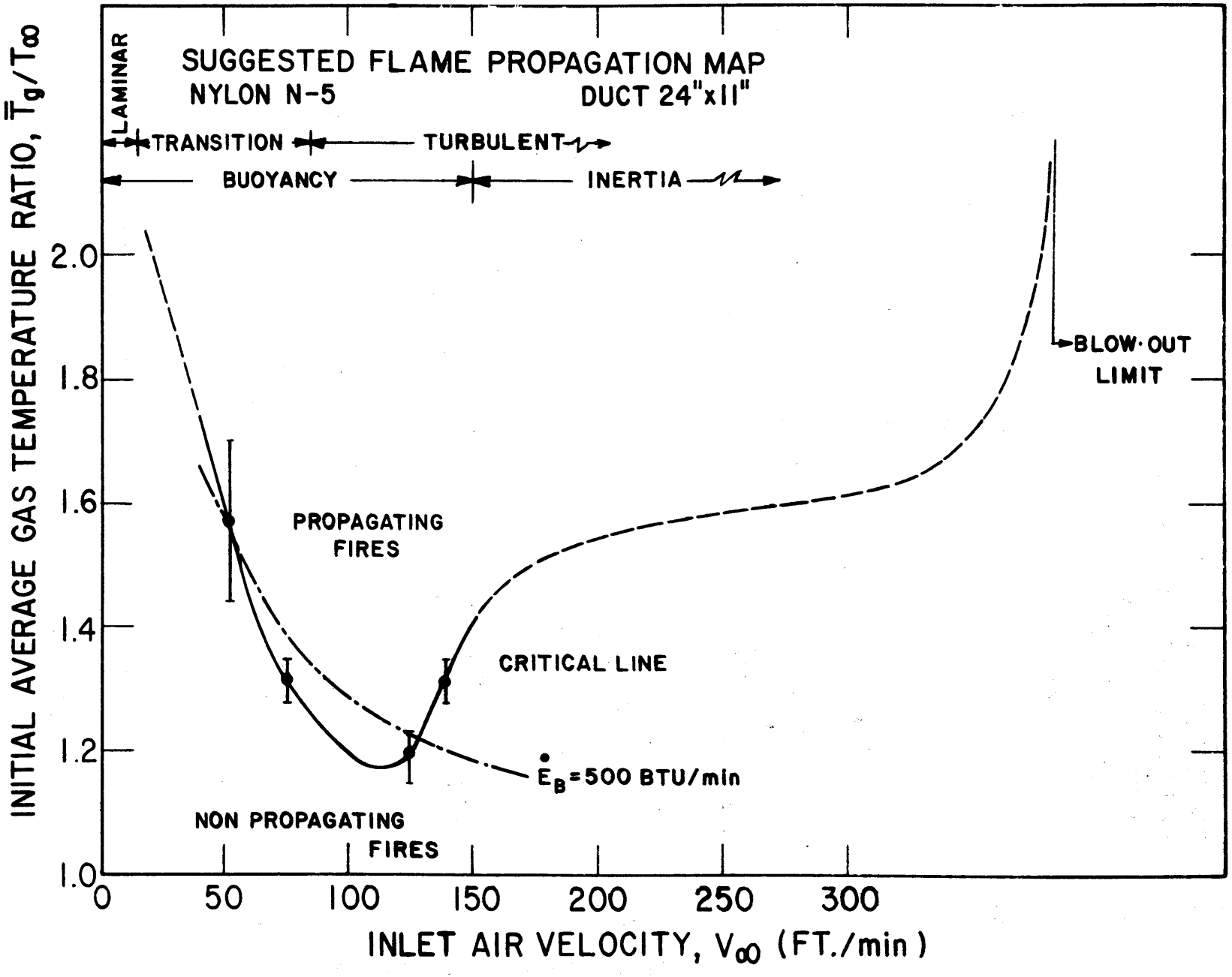

Figure 6-11. Flame propagation map.

For the data presented in figure 6-9, Fr ranges from 0.30 to 0.10.

The effect of air flow on flame spread is not completely understood but some thoughts and observations can be made. As reported by Rhodes and Smith [7], a critical velocity appears to exist for flame spread. This is illustrated in figures 6-10 and 6-11. The first figure displays the end result of tests for a nylon carpet at various air flows (V_∞) and burner settings ($\dot{E}_B$). In order to appropriately display propagating and non-propagating fires an average flame front velocity ($\bar{V}_F$) has been introduced as

$$\bar{V}_F = \frac{\text{Distance burned}}{\text{Time}}$$

Also an attempt has been made to draw a family of curves based on average initial gas temperature, $\bar{T}_g$. A critical zone is suggested and the intersections are used to plot figure 6-11. Physical reasoning led to the extrapolated curve shown as a dashed line. Also shown are flow characterizations based on Reynolds number and Froude number considerations. Finally a line of constant burner input ($\dot{E}_B$) is superimposed and following this line by varying the air flow illustrates how one can move from a propagating regime to a non-propagating regime. Although these results are restrictive to the particular conditions in these tests, it is suggested that the effect of air flow on duct flame spread has this same general character.

6.3 Energy Release Rate from Floor Covering

Due to the nature of the test at least a portion of every floor material which was under the influence of the burner flame would be consumed. Based on initial duct temperature levels for runs with and without floor combustibles during the same time period, it was reasoned that energy release rate of the burning carpets was significant when compared to that of the burner alone. Since this total initial energy input is critical for propagation an estimate of the carpet energy release rate was sought. This was accomplished by several techniques, but the general intent was to arrive at results of the correct order of magnitude. The effort was not intensive but the results are expected to be representative for carpets.

Carpet samples were tested in the NBS rate of heat release calorimeter [18]. The results of these tests for three sample carpets are shown in figure 6-12 [19]. The samples were burned for varying times under normal atmospheric conditions at an irradiation level of 6 watts/cm^2. The principal interest was energy release as a function of weight loss. By then determining the resultant weight loss during a model corridor experiment, the energy release could be deduced. This, of course, assumes identical burning characteristics in the chamber and the rate calorimeter. An alternative method was to determine the heat of combustion from an oxygen bomb calorimeter, and then repeat this procedure for residue following a model corridor fire. The higher heating values determined in the oxygen bomb by Kashiwagi [20] are

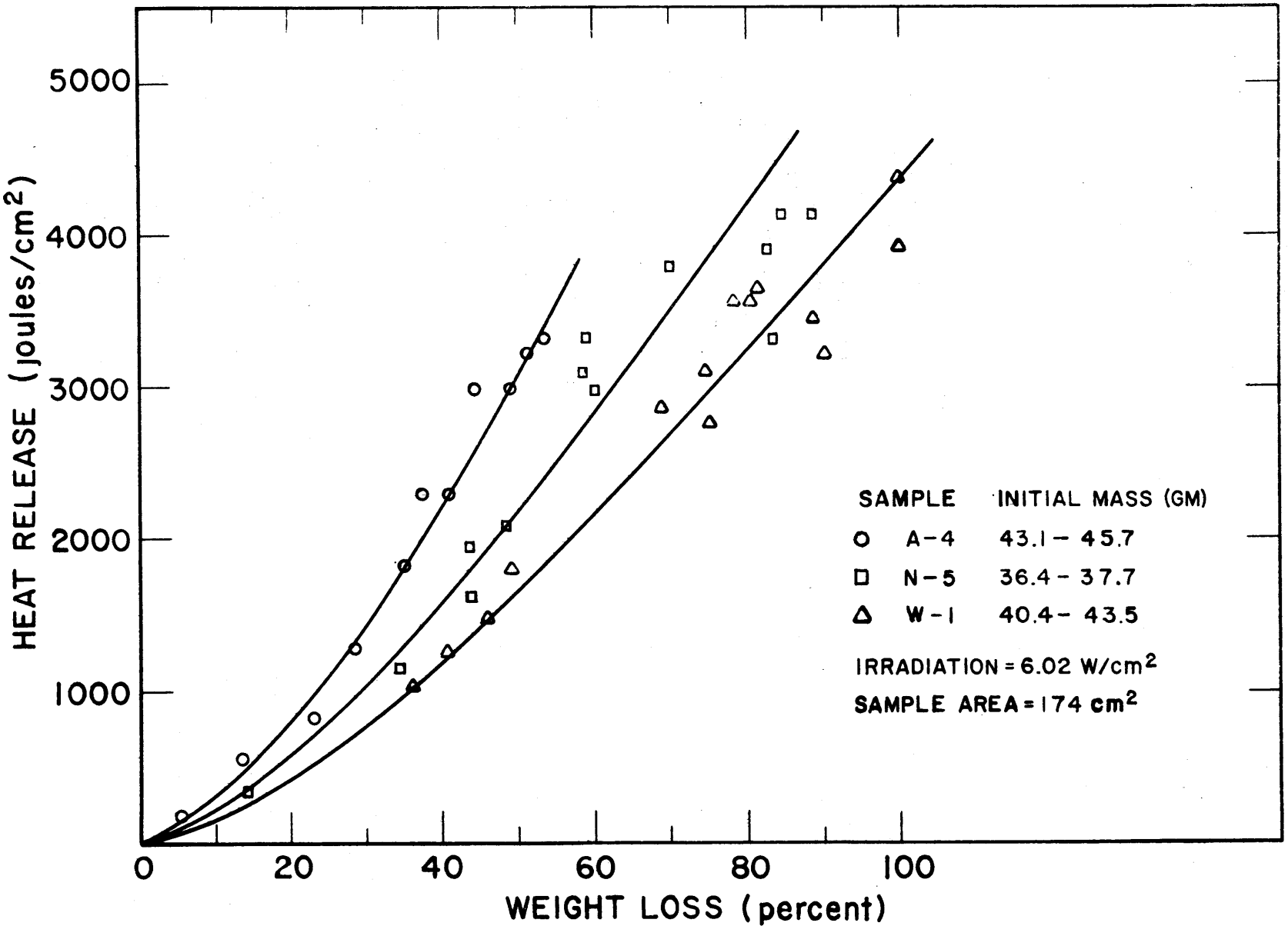

Figure 6-12. Energy release characteristics of carpets based on the NBS rate calorimeter.

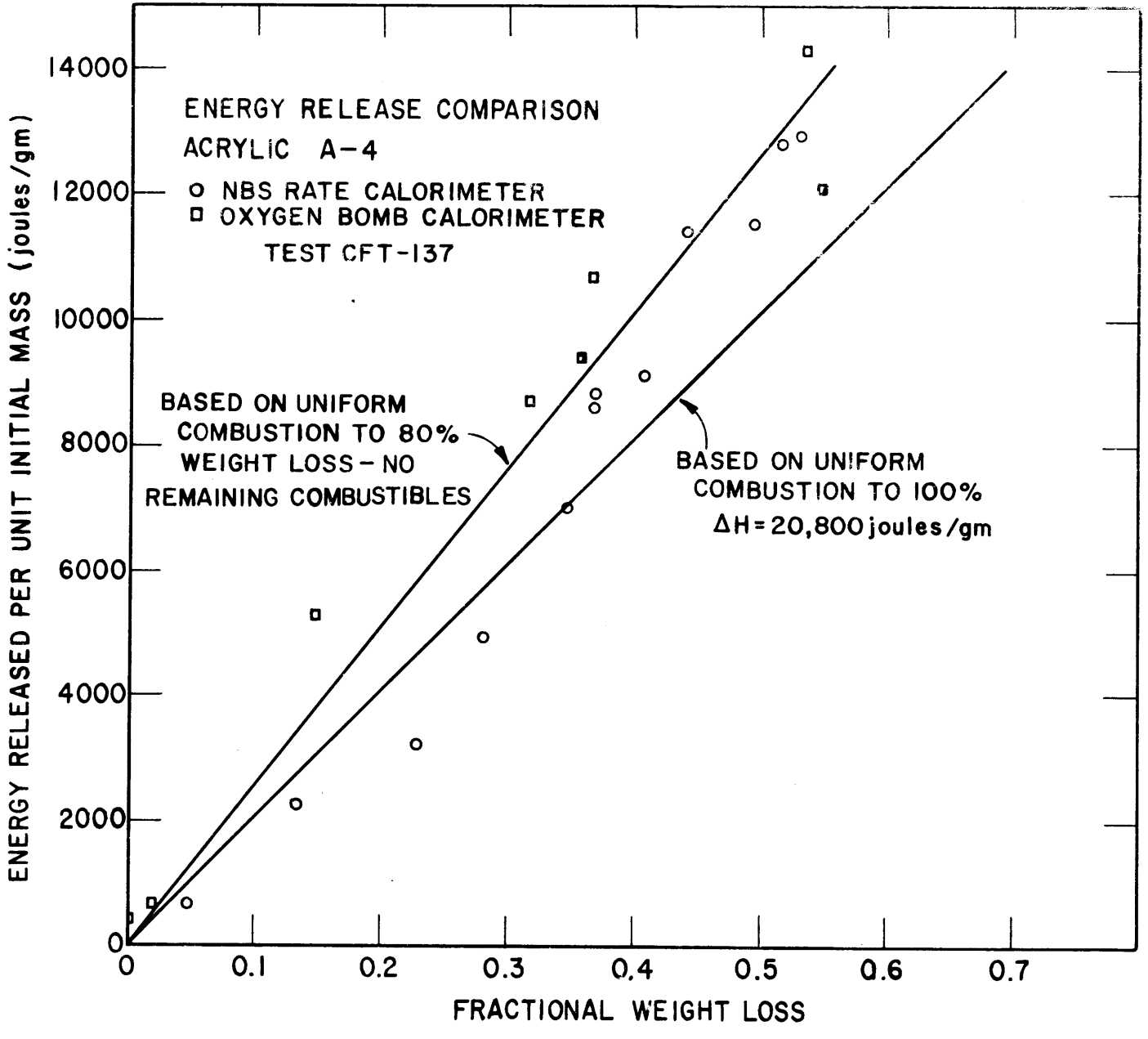

Figure 6-13. Energy release--comparison of NBS rate calorimeter and oxygen bomb.

TABLE 6-1

Oxygen Bomb Calorimeter Results for Carpets

No.	Material		Weight		Heat of Combustion (cal/gm)*		
	Pile	Backing	pile/total oz/yd^2	pile/total gm/cm	Pile	Backing	Total
A-1	Acrylic	Jute-Cotton	38/54	0.13/0.18	7080	5350	6030
A-2	Acrylic	PP-Jute	32/69	0.11/0.23	7090	3470	4780
N-1	BCF Nylon	PP-Foam Rubber	20/89	0.07/0.30	7270	3760	--
W-1	Wool	Jute-Cotton	38/76	0.13/0.26	4990	4640	4800
N-3	BCF Nylon	Jute-Jute	25/69	0.085/0.23	7340	3660	4590
N-4	Nylon	Jute-Jute	28/75	0.095/0.25	7370	3740	4920
N-5	BCF Nylon	Jute-Jute	16/64	0.054/0.22	7310	3400	4128
A-3	Acrylic	PP-PP	36/65	0.12/0.22	7100	5100	5150
A-4	Acrylic	Jute-Jute	36/80	0.12/0.27	7020	3580	4960
A-5	Acrylic	PP-Jute	30/66	0.10/0.22	7020	3780	4930

* Higher Heating Values

TABLE 6-2

Floor Covering Weight Loss in Model Corridor

(Following Flameover)

No.	Material	Weight Loss (%)
N-1	Nylon	64
N-2	Nylon	64
N-4	Nylon	74
N-5	Nylon	84
N-6	Nylon	67 - 82
A-1	Acrylic	42
A-4	Acrylic	47 - 49
A-6	Acrylic	45
P-1	Polyester	77*
P-2	Polyester	69
P-4	Polyester	77
O-1	Polypropylene	62
O-2	Polypropylene	43 - 100
O-3	Polypropylene	46
W-1	Wool	59* - 73*

* No flameover occurred

summarized in table 6-1. These values represent an upper limit for heat release. Based on residue samplings from a model corridor test (CFT-137) energy release per unit initial carpet mass was determined. These results are shown in figure 6-13 and are compared with the NBS rate calorimeter results. The two techniques are in general agreement except in the low mass loss regime. This is not surprising since the initial burning process is very different in the two methods and complete combustion is forced in the bomb (and water vaporization was not corrected for in the bomb). Because of non-combustible filler in the latex backing it is not uncommon to have a significant non-combustible residue in the bomb calorimeter. An 18 per cent residue was reported for Nylon N-5. It is noted that beyond a 30 percent weight loss for acrylic A-4 a uniform combustion line based on 80 per cent maximum weight loss agrees well with the data. Maximum weight loss of floor covering samples following a model corridor burn is presented in table 6-2. These results are consistent with maximum weight loss found in the NBS rate calorimeter as indicated by the upper limit of the data presented in figure 6-13.

In order to translate these energy results into an average release rate, average burning time (Δt_b) must be known. The quantity Δt_b is defined as the duration of flaming for a fixed position on the floor covering. Although the weight loss result for a material may be invariant following a fire above a critical intensity, the burning time is likely to be more sensitive to surface boundary conditions (both top and bottom). If Spaldings formulation [21] is adopted for a burning material (directly applicable to a liquid below its vaporization temperature), then the effect of variables on burning time can be recognized. For a material of mass per unit surface area m_i'', with a burning mass flux $\dot{m}''$, then

$$\Delta t_b = \frac{m_i'' \phi}{\dot{m}''} \tag{6-3}$$

where ϕ is the fractional mass loss. From Spalding's formulation

$$\dot{m}'' = gB \tag{6-4}$$

where g includes the convective effects (h/c_p) and B is the driving force for the flux transport.

$$B = \frac{i_\infty - i_s}{\Delta i_{vap} + \dot{q}_L''/\dot{m}''} = \frac{(Y_{o,\infty} \Delta H_f / r) + \int_{T_s}^{T_\infty} c\, dT}{\Delta i_{vap} + \dot{q}_L''/\dot{m}''} \tag{6-5}$$

where i_∞ = free stream enthalpy

i_s = surface enthalpy

$\frac{Y_{o,\infty} \Delta H_f}{r}$ = energy of reaction per unit mass of gas mixture

In addition if radiation is significant at the surface then it must be appropriately added to the equation (6-4). Although a floor covering is usually thermally thick, a rough estimate of a conductive heat loss to the substrate material below can be assessed from

$$\dot{q}_L'' = \frac{2\sqrt{\gamma}\,(T_s - T_\infty)}{\sqrt{\pi}\,\sqrt{t}} \qquad (6\text{-}6)$$

where $\gamma = (k\rho c)_{substrate}$. This followed by considering a thin material of constant temperature T_s on an infinitely thick substrate of initial temperature, T_∞. Thus the greater γ is for the substrate, the lower the burning rate should be. Several conclusions can be reached from the above modeling. Since the numerator in eq. (6-5) and m_i'' are probably similar for carpets, it follows that burning time Δt_b is directly proportional to fractional weight loss, ϕ; effective vaporization energy, Δi_{vap}; and thermal inertia of the substrate, $k\rho c$; and inversely, proportional to air flow, V_∞ (as reflected by h). Table 6-3 is a first attempt to categorize burning time for the floor samples tested in terms of the major variables suggested by the model. At a cursory examination it appears that the burning is erratic, however, this is not surprising since the initial burning process is transient and unstable. Moreover, it should be pointed out that the times are based on thermocouple response - the duration between a rapid rise and a pronounced drop in temperature. This has not been correlated with observed flaming. A more thorough review of the data should show consistent results at distances beyond the burner influence and for runs resulting in flameover.

A simple model will now be presented which is empirical in nature and based on laboratory data and test observations. Assuming uniform burning, the energy release flux, $\dot{E}_c''$ is

$$\dot{E}_c'' = \frac{1}{A}\frac{dE_c}{dt} \qquad (6\text{-}7a)$$

where

$$\frac{dE_c}{dt} \simeq \frac{E_{c,f}}{\Delta t_b} \qquad (6\text{-}7b)$$

TABLE 6-3

Duration of Burning, Δt_b, at Various Distances, x

CFT.	No.	Material	Air Velocity	Substrate	Final Result	Burning Time at		(sec)
			ft/min			X=1	X=2	X=4 ft
50	A-3	Acrylic	100	Pad	F.O.	160	100	200
43	A-3	Acrylic	100	ASB.*	Ex	30	30	-
35	A-3	Acrylic	100	ASB.	Ex	40	-	-
127	A-4	Acrylic	100	Pad	F.O.	180	240	130
129	A-4	Acrylic	100	Pad	F.O.	210	240	120
126	A-4	Acrylic	100	Pad	F.O.	-	160	180
49	A-4	Acrylic	100	Pad	F.O.	160	200	160
68	A-4	Acrylic	100	Pad	F.O.	260	240	330
114	A-4	Acrylic	100	Pad	F.O.	360	160	160
113	A-4	Acrylic	100	Pad	Ex	340	160	-
76	A-4	Acrylic	100	Pad	Ex	240	-	-
42	A-5	Acrylic	100	ASB.	F.O.	50	20	-
36	A-5	Acrylic	100	ASB.	Ex	30	-	-
214	A-1	Acrylic	100	Pad	Ex	110	110	-
12	A-2	Acrylic	100	Pad	F.O.	120	120	120
13	A-2	Acrylic	100	Pad	Ex	180	-	-
142	N-3	Nylon	100	ASB.	F.O.	510	260	260
141	N-3	Nylon	100	ASB.	Ex	480	270	-
28	N-3	Nylon	100	ASB.	Ex	240	-	-
27	N-4	Nylon	100	ASB.	Ex	240	180	-
32	N-4	Nylon	100	ASB.	Ex	330	270	-
57	N-4	Nylon	100	ASB.	F.O.	300	150	225
215	N-4	Nylon	100	Pad	F.O.	-	130	-
130	N-5	Nylon	100	Pad	F.O.	150	270	180
64	N-5	Nylon	100	Pad	F.O.	200	270	110
65	N-5	Nylon	100	Pad	F.O.	230	330	90
66	N-5	Nylon	100	Pad	F.O.	215	240	210
40	N-5	Nylon	100	ASB.	Ex	180	-	-
105	N-1	Nylon	100	Foam	Ex	285	210	-
60	O-1	Polypropylene	100	Pad	Ex	105	375	-
59	O-1	Polypropylene	100	Pad	F.O.	120	290	120
217	O-1	Polypropylene	100	Pad	F.O.	-	260	170

* ASB. indicates carpet is laid to asbestos board floor

and $E_{c,f}$ is the energy released at the final fractional weight loss, ϕ_f. Or rearranging

$$\dot{E}_c'' = m_i'' \left(\frac{E_{cf}}{m_i}\right) \Big/ \Delta t_b \qquad (6\text{-}8)$$

where m_i'' is the initial carpet mass per unit area, and $(E_{c,f}/m_i)$ is the maximum energy release corresponding to the representative final weight, ϕ_f, as given in table 6-2.

. In order to determine a rate of energy release by the floor material, E_c, the burning area must be known. Two cases will be considered. Case I assumes the principal carpet energy release occurs in the ignition region under the burner influence. This initial energy input plus the contribution from the burner is significant to the outcome of the test. If a critical input is exceeded flameover will occur. Case II addresses the slower burning materials which tend to propagate substantially beyond the burner's influence then may cease to propagate. In both cases a constant flame front velocity, V_F, will be assumed. This is justified in view of the comments made covering figures 6-4 and 6-5. For Case I the flame front is restricted to the burner regime denoted by flame length L_B and width W_F.

The results follow:

Case I: Flame spread restricted to burner regime.

$$\alpha \equiv \frac{L_B}{V_F \Delta t_b} \qquad (6\text{-}9)$$

a. $\alpha < 1$

$$\left.\begin{aligned} \dot{E}_c &= \dot{E}_c'' W_F V_F t \;, \quad t < L_B/V_F \\ \dot{E}_c &= \dot{E}_c'' W_F L_B \;, \quad \frac{L_B}{V_F} < t < \Delta t_b \\ \dot{E}_c &= \dot{E}_c'' W_F \left[L_B - V_F(t - \Delta t_b)\right], \quad \Delta t_b < t < \frac{L_B}{V_F} + \Delta t_b \end{aligned}\right\} \qquad (6\text{-}10a)$$

Equation (6-10a) was then averaged over the time interval $\frac{L_B}{V_F} + \Delta t_b$ to yield

$$\dot{E}_{c,avg.} = \frac{\dot{E}_c'' W_F L_B}{\alpha + 1} \;. \qquad (6\text{-}10b)$$

b. $\alpha > 1$

$$\left.\begin{aligned} \dot{E}_c &= \dot{E}_c'' W_F V_F t, \quad t < \Delta t_b \\ \dot{E}_c &= \dot{E}_c'' W_F V_F \Delta t_b, \quad \Delta t_b < t < \frac{L_B}{V_F} \\ \dot{E}_c &= \dot{E}_c'' W_F V_F \left[\Delta t_b + \frac{L_B}{V_F} - t\right], \quad \frac{L_B}{V_F} < t < \frac{L_B}{V_F} + \Delta t_b \end{aligned}\right\} \quad (6\text{-}10c)$$

$$\dot{E}_{c,avg.} = \dot{E}_c'' W_F L_B \left[\frac{1 + 1/\alpha}{2} - \frac{1}{1 + 1/\alpha}\right] . \quad (6\text{-}10d)$$

Case II: Steady continuous flame spread

$$\left.\begin{aligned} \dot{E}_c &= \dot{E}_c'' W_F V_F t, \quad t < \Delta t_b \\ \dot{E}_c &= \dot{E}_c'' W_F V_F \Delta t_b, \quad t > \Delta t_b \end{aligned}\right\} \quad (6\text{-}11)$$

To illustrate the procedure Case I is considered for Acrylic A-4 under conditions of V_∞ = 100 ft/min and $\dot{E}_B$ = 500 BTU/min.

L_B = 10 in. (Fig. 6-2)

V_F = 11 in/min (Fig. 6-6)

$\Delta t_b \approx$ 250 sec. (Table 6-3)

Then

$$\alpha = \frac{L_B}{V_F \Delta t_b} = 0.218 < 1 .$$

From equation 6-8, table 6-2, and figure 6-13,

$$\dot{E}_c'' = m_i'' \left(\frac{E_{c,f}}{m_i}\right) / \Delta t_b$$

$$= \frac{(0.27 \text{ gm/cm}^2)(11650 \text{ j/gm})}{(250 \text{ sec})} \times 60 \frac{\text{sec}}{\text{min}} \times 9.48 \times 10^{-4} \frac{\text{BTU}}{\text{joule}}$$

$$= 0.717 \text{ BTU/cm}^2 \cdot \text{min} .$$

Finally from equation 6-10b,

$$\dot{E}_{c,avg.} = \frac{(0.717\ \text{BTU/cm}^2\cdot\text{min})(8\ \text{in.})(10\ \text{in.})}{1+0.218} \times \left(2.54\ \frac{\text{cm}}{\text{in.}}\right)^2$$

$$= 285\ \text{BTU/min.}$$

(Note that an 8 inch flame zone was assumed. This is consistent with the burner characteristics). The fact that this energy release, rate is significant when compared to $\dot{E}_B$ = 500 BTU/min is important. Thus this initial energy input by the carpet must be considered as a contributing factor in evaluating the critical energy rate required for flameover. If Case II is considered with the same V_F and W_F values, then, at most,

$$\dot{E}_c = \dot{E}_c'' W_F V_F \Delta t_b$$

$$= \left(0.717\ \frac{\text{BTU}}{\text{cm}^2\cdot\text{min}}\right)(8\ \text{in.})(11\ \text{in/min})(250\ \text{sec}) \times \left(2.54\ \frac{\text{cm}}{\text{in}}\right)^2 \times \left(\frac{1\ \text{min}}{60\ \text{sec}}\right)$$

$$= 1700\ \text{BTU/min. for } t > 250\ \text{sec.}$$

In this case the flame front would reach $x = L_B$ in $t = L_B/V_F = 54$ seconds. For acrylic carpets (see figure 6-5) the flame front would normally slow down considerably for $x > L_B$ until flameover ensues. Hence an $\dot{E}_c$ slightly greater than 285 but much lower than 1700 BTU/min would be representative of the carpet's contribution. In any case the energy release from the initial burning of the carpet cannot be neglected.

6.4 Radiant Preheating

A dominant factor determining whether a propagating fire will occur was found to be preheating of the floorcovering surface extending over several feet from the flame front. In close proximity to the burner flame both radiation (figure 6-2) and convection (figure 6-3) are important; however, downstream of the burner zone (figure 6-9) radiant heating of the floor material is caused by the hotter ceiling temperatures. Unfortunately no single device was consistently used in the testing to accurately monitor the flame and ceiling induced floor heat flux. Gardon type heat flux sensors were used with sapphire windows to shield out convective heating. However, sapphire is a poor transmitter of long wavelength radiation which predominates for relatively low temperature sources (200-600°C) encountered. Moreover, once the flame front passed over the sensor the heated window reradiated to the sensor element causing an erroneous radiant heat flux measurement. Hence an indirect method of calculating the local floor flux from

ceiling temperature measurements was resorted to. Before this is fully discussed, some approximate results from a water flow designed total heat flux gage will be reported. A 0.005 inch thick stainless steel tube 6 inches long and 1/8 inch o.d. (A 1/8 in. o.d. with a 3/64 in. wall thickness Cu-tube was also used) was inserted along the carpet surface aligned normal to flame propagation. A controlled water flow passed through the tube and a calibrated differential thermocouple monitored water temperature rise. Assuming one-half of the tube circumference was exposed to incident heat flux (the tube was blackened with a high emissivity paint), the total heat flux could then be determined. For a water flow of about 10 ml/min, a 1/32 to 1/8 in I.D. tube has a response time of 2 to 15 seconds. Figure 6-14 displays the results for one run. It appears that the effect of the flame is felt when it is within about 10 inches of the sensor. Previous flux levels are soley due to radiant heating from the ceiling. Although the cooled tube sensor probably inhibits the flame to some extent, the maximum value recorded 1.5 BTU/ft^{2}sec. is comparable to 1.77 BTU/ft^{2}sec determined by Parker [22] for downward flame propagation along thin cellulosic materials.

Since the primary long term radiation originates from the heated ceiling a calculation was made to determine the incident floor flux along the centerline of the floor. Seven ceiling temperature measuring stations were used to determine the radiant flux. The ceiling was assumed to be a blackbody with uniform temperature across its width. (Asbestos board and soot deposited on a solid surface both have emissivities of 0.93 - 0.95 up to 400°C [23].) The incident floor flux was then determined by considering the emitted flux from a diffuse surface, and geometric considerations. The result is given in figure 6-15. Integration was accomplished by using an Aitken one-degree interpolation for the ceiling temperatures and Simpson's Rule with a 40 point step division. The floor flux was then determined for several tests using seven ceiling thermocouples and found as a function of distance and time.

Having made these calculations, two points of view were taken to examine the effect of radiant flux. The first was to view it as an instant additive of direct forward heat transfer by the flame front. Then, using the calculated flux and recognizing the position of the flame front permitted the ceiling induced radiant flux to be derived at the moving flame front. This is illustrated in figure 6-16 where two similar runs are compared. They differed only in ceiling height and had two distinct outcomes. At the time of incipient flameover in run 68 the flux attained 0.5 watts/cm^2, while the flux never exceeded 0.15 watts/cm^2 for run 76. Adopting the second point of view the calculated flux is examined at a fixed point downstream of the burner flame influence. Again the two runs show distinct differences in the resulting flux. If the carpet surface temperature is also compared a distinct correlation is seen with the radiant flux calculations implying a cause and effect relationship. Moreover, gas temperatures 1 inch above the surface considerably lag the surface temperatures, supporting the contention that direct radiation causes surface temperature rise. (Run 49 is shown since it is identical to run 68 to illustrate the lagging gas temperature. The

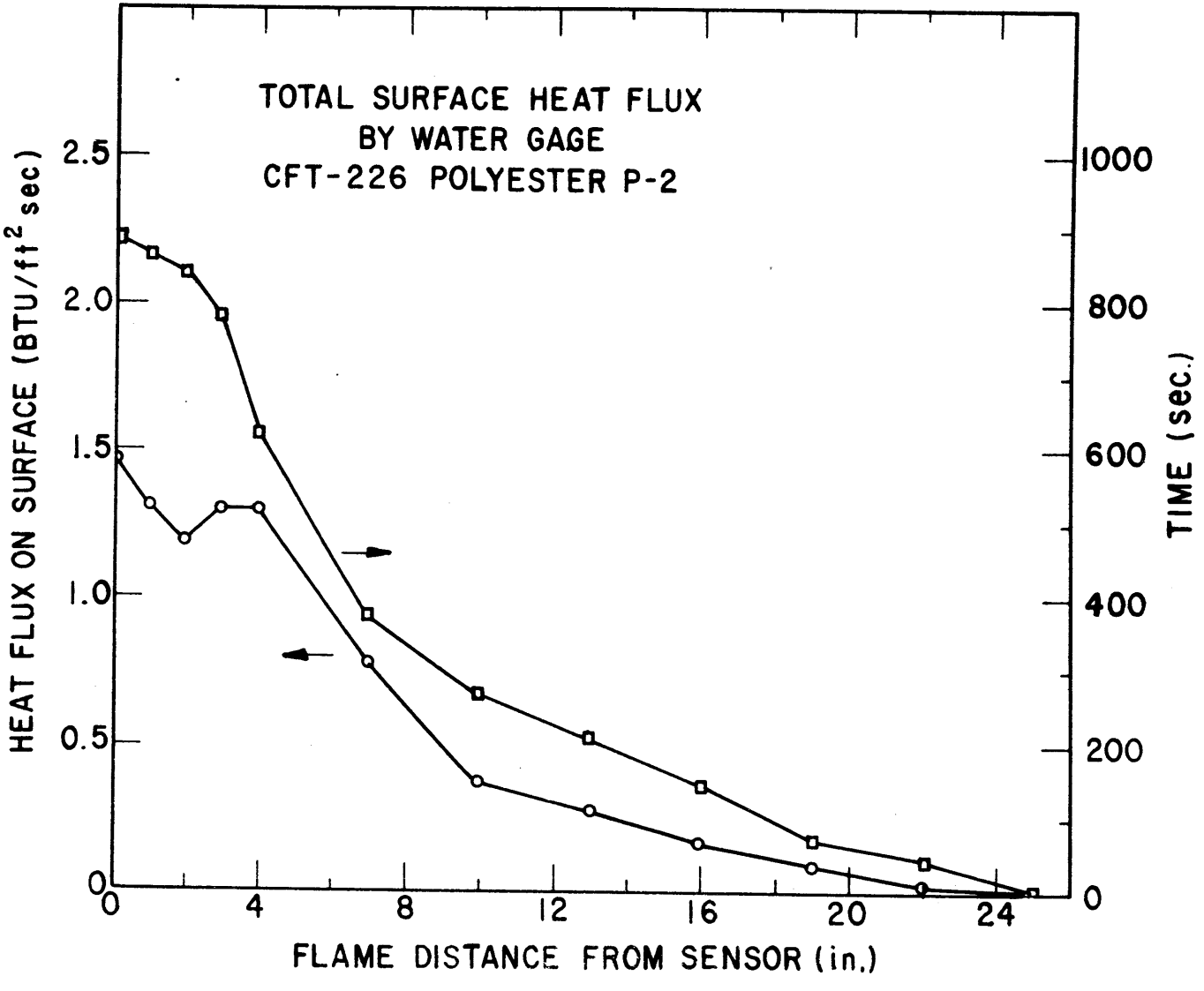

Figure 6-14. Carpet incident heat flux as a function of flame position.

CALCULATED INCIDENT CARPET RADIANT HEAT FLUX, $\dot{q}''_1$

(CEILING SOURCE ONLY)

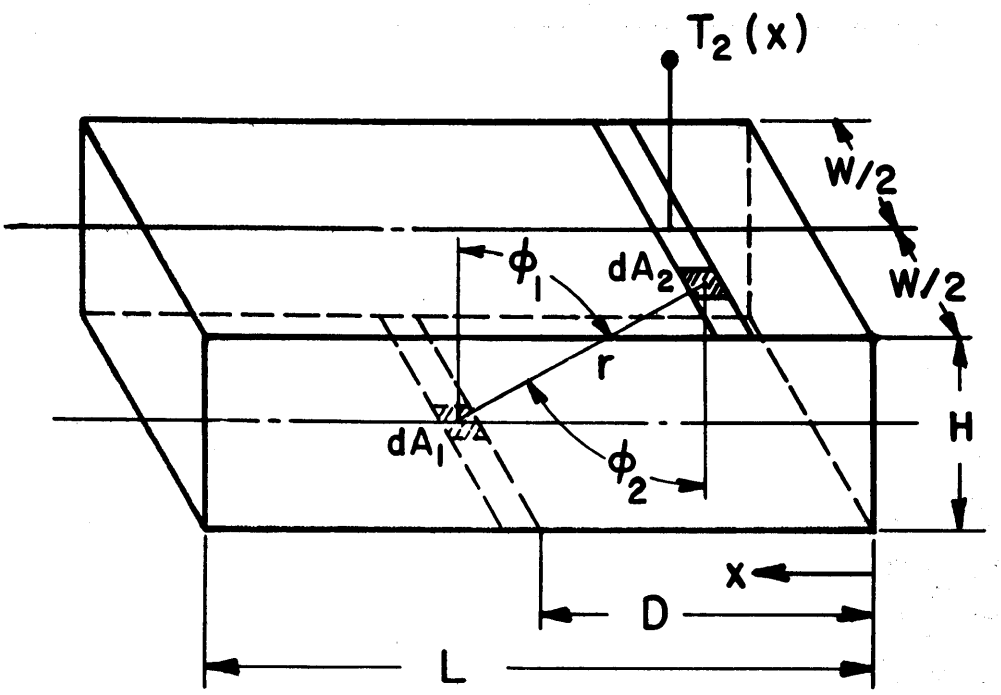

$$\dot{q}''_1 = \iint_{A_2} \frac{\sigma T_2^4}{\pi} \cdot \frac{\cos\phi_1 \cos\phi_2}{r^2} \, dA_2$$

$$\dot{q}''_1 = \frac{\sigma H^2}{\pi} \int_0^L \left\{ \frac{W/2}{M\left[M+\left(\frac{W}{2}\right)^2\right]} + \frac{\tan^{-1}\left(\frac{W/2}{\sqrt{M}}\right)}{M^{3/2}} \right\} T_2^4(x)\,dx$$

WHERE $M=(D-x)^2+H^2$

Figure 6-15. Calculated incident radiant heat flux.

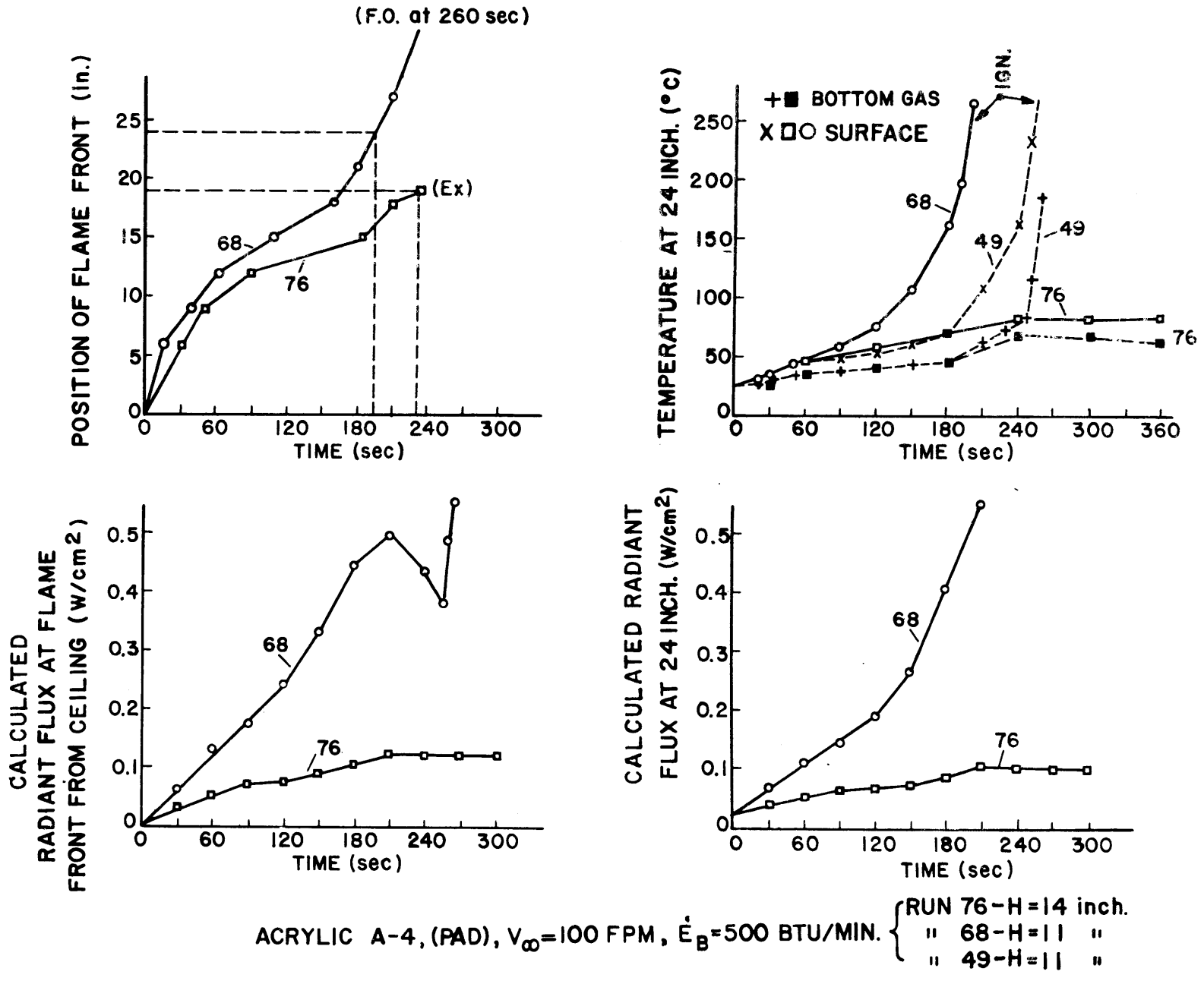

Figure 6-16. Flame spread as a function of calculated incident radiation.

50 second shift is most likely due to differences in initial conditions.) To support the radiant induced surface temperature response, a one-dimensional heat conduction model was considered for run 68 at x=24 inches. The radiant heat flux was approximated as a linear function of time up to the point of ignition. Three cases were considered - a thermally thin carpet (back insulated), a thermally thin pile (back insulated) and a thermally thick carpet. The details are presented in Appendix B. The results are shown in figure 6-17. Although the temperature is generally overestimated, it is apparent that the flux level is more than adequate to cause the temperature rise observed. Some additional runs were examined for the same carpet (Acrylic A-4). The flux at the flame front appears to be in excess of 0.3 watts/cm^2 to permit a propagating fire (see figures 6-18 and 6-19).

A semi-quantitative model is described to link flame spread to radiation pre-heating. A thin bed horizontal steady state flame spread is considered. A suitable representation is expressed as

$$\frac{ds_F}{dt} = V_F \cong \frac{k_g}{\rho c_p \delta}\left(\frac{T_F - T_{VAP}}{T_{VAP} - T_o}\right) \qquad (6\text{-}12)$$

derived by de Ris [24] or Parker [22] prefixed by a constant of about 1.5. Assume the gas phase transport processes are fast compared with radiant preheating. In this quasi-steady approximation T_o is the fuel bed temperature "far" ahead of the flame which is responding to a uniform and constant radiant flux $\dot{q}''_r$. For no heat losses the radiant preheat model yields

$$T_o - T_\infty = \frac{\dot{q}''_r t}{\rho c_p \delta} . \qquad (6\text{-}13)$$

Substituting for T_o and solving for the flame position as a function of time yields

$$s_F = \frac{k_g (T_F - T_{VAP})}{\dot{q}''_r} \ln\left[\frac{1}{1 - \frac{\dot{q}''_r t}{\rho c_p \delta (T_{VAP} - T_\infty)}}\right] . \qquad (6\text{-}14)$$

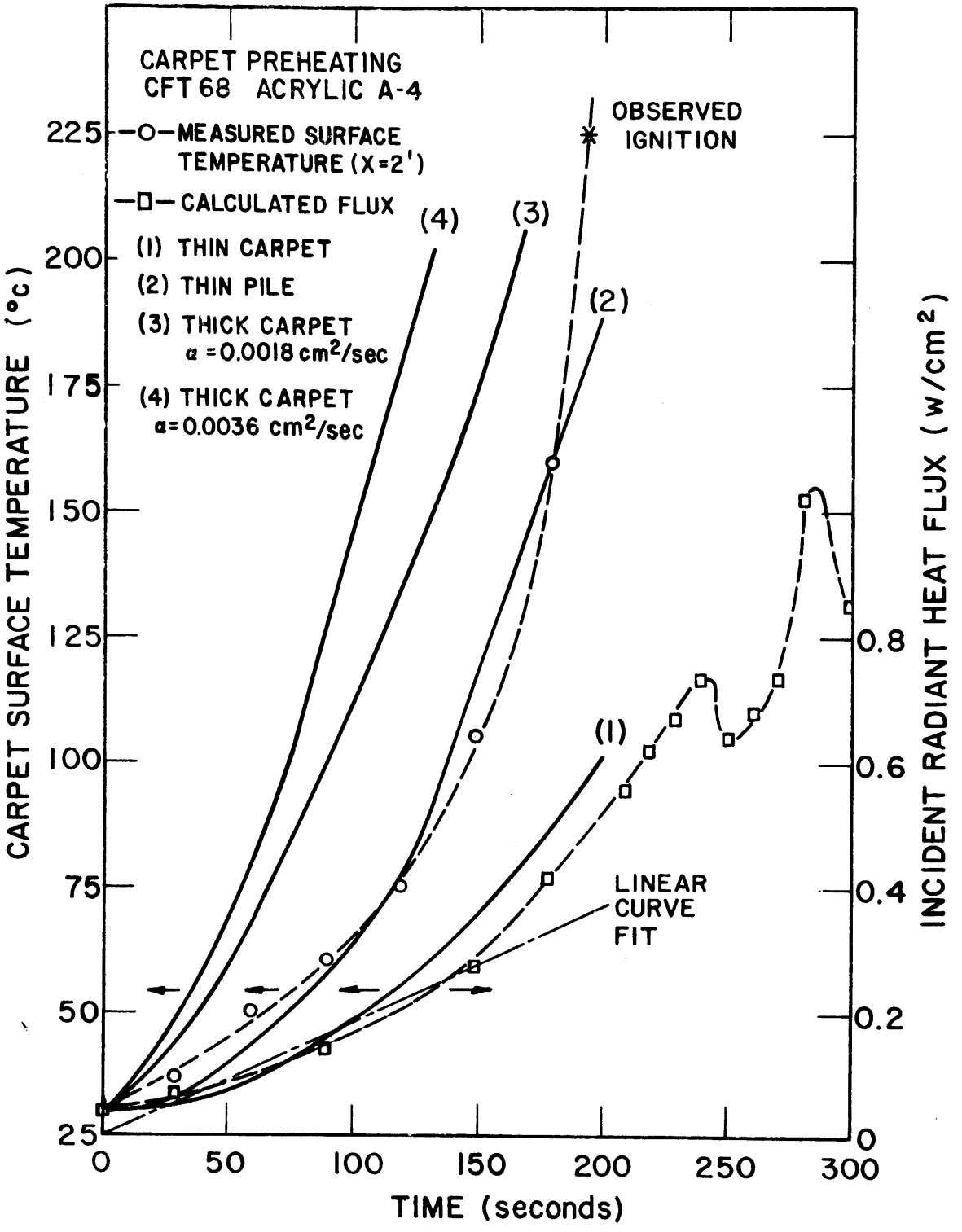

Figure 6-17. Carpet preheating characteristics.

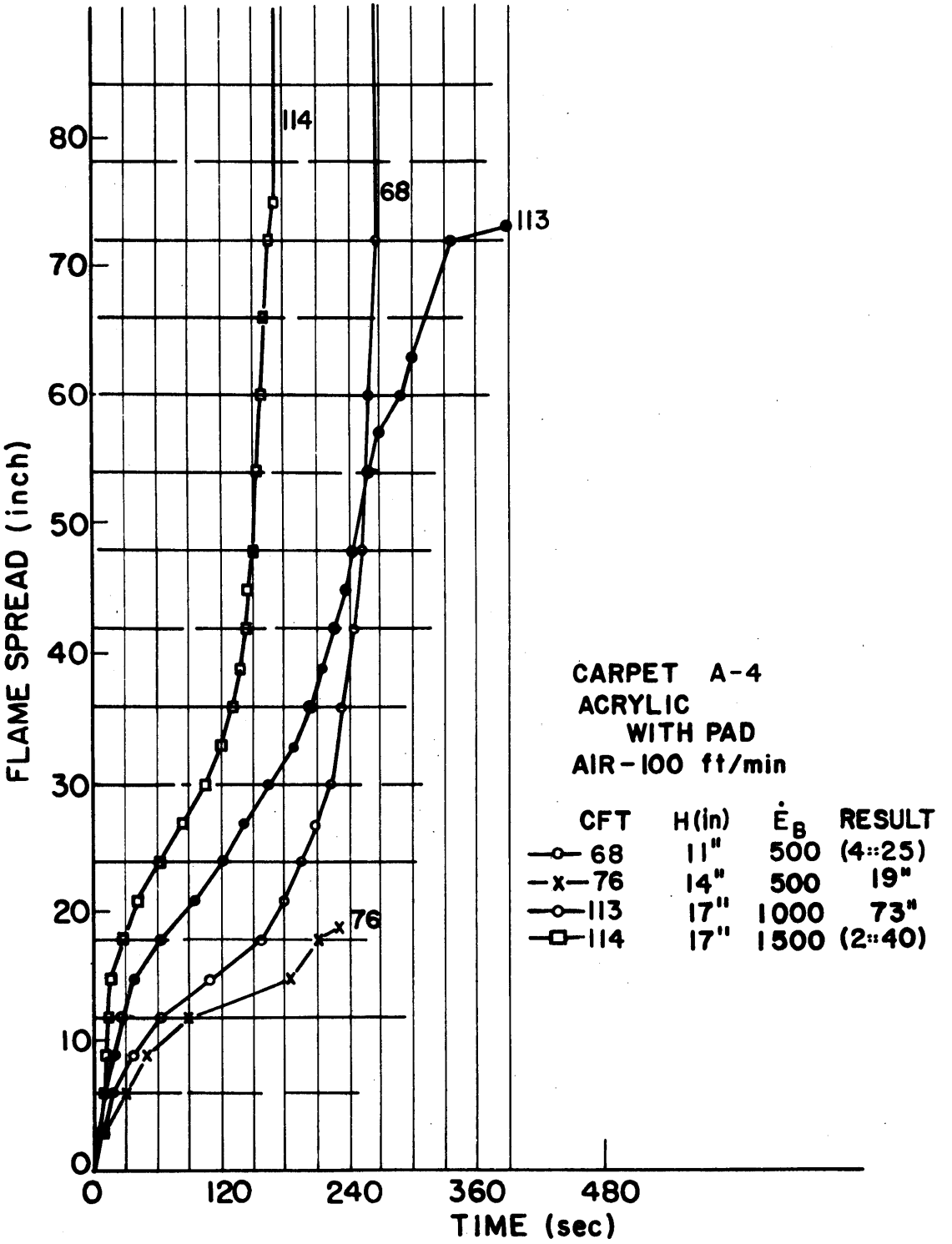

Figure 6-18. Flame spread--radiation analysis.

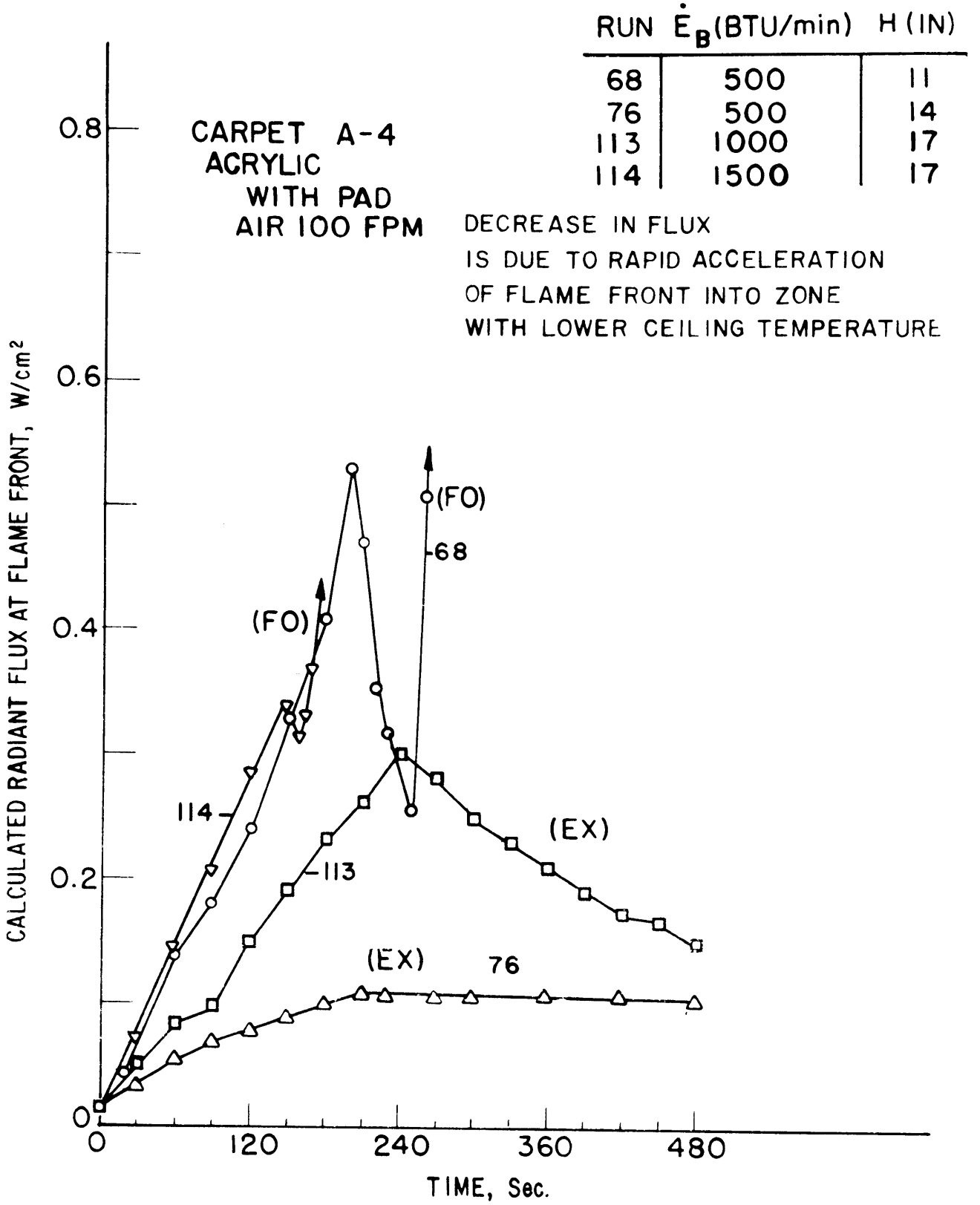

Figure 6-19. Calculated radiant flux at flame front.

For a reasonable choice of parameters the model gives the results as shown in figure 6-20. Of course, the carpet is not a thin bed and an infinite flame spread rate is impossible. Moreover, the quasi-steady assumption and preclusion of losses must be questioned at some point before the physically impossible solution is reached. However, the character and magnitude of the results has a striking similarity to the observed phenomenon (see figure 6-5). The model, of course, does not include the burner effect on flame spread; however, this could be included by a step change in flux level over the thin bed to simulate the initial burner input.

Several other observations and facts should be pointed out. Carpet fibers which form a melt (nylon, polypropylene, polyester) upon exposure to heat displayed a noticeable melt leading the flame front by 1 to 2 inches. Carpet fibers which basically char (acrylic, wool) displayed a much shorter decomposition front ahead of the flame front. No further evidence of carpet transformation was apparent ahead of the flame front up to the start of flameover. Also insignificant fuel contribution could be attributed to the pad substrate before flameover. Carpet fiber pyrolysis analysis by McCarter [25] indicated the results shown in table 6-4 based on a heating rate of 60°C/min. In general the observed carpet surface temperatures preceding ignition were always below the fiber decomposition (vaporization) temperatures. This supports the observation that carpet degradation occurs only over a short distance ahead of the advancing flame. That is, pyrolysis products are not evolved as a direct result of carpet preheating "far" ahead of the flame.

Since radiation was found to be a dominant factor in this work, and radiation is felt to be important in the NBS corridor fire studies, some similarly calculated floor fluxes were determined from the corridor ceiling temperature data. Because of the low scanning rate of the data system (30 sec) it was not possible to determine a distinct correlation with flame spread. In addition the response of carpet surface thermocouples indicated possible pyrolysis ahead of the flame front. From the results of the NBS corridor studies [15] 333, 337, 340, 342-345, a calculated floor flux at the time the carpet surface temperature attained 200°C ranged from 0.30 to 1.70 watts/cm^2 and averaged about 0.60 watts/cm^2. The flux usually steadily increased then accelerated rapidly to values as high as 3 watts/cm^2. It is significant that the same radiant flux levels precede flame spread in the model corridor test work.

6.5 Heat Balance Analysis

An attempt was made to monitor the heat transport and energy source processes during several test runs. This is difficult due to the rapdily transient behavior and sharp thermal variations within the system. The test duct was modified with baffles and a square 5 in x 5 in orifice at the exit. This did not affect initial air flow and produced a well mixed flow at the exit. The exit orifice did cause a substantial decrease in inlet air flow just before flameover or with a fire which propagated more than 24 inches. High temperature thermopile type heat

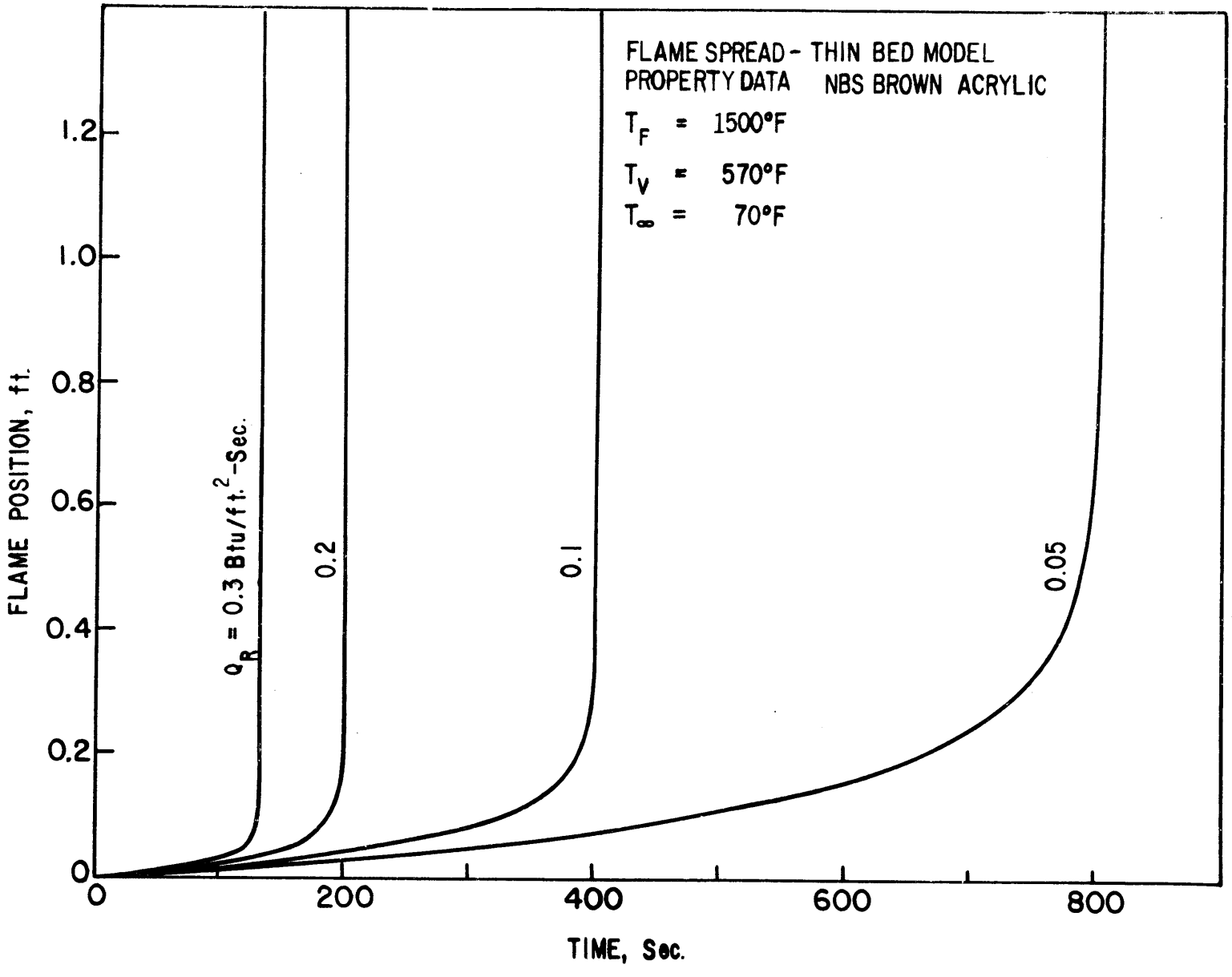

Figure 6-20. Theoretical flame spread with radiant heating.

TABLE 6-4

Fiber Decomposition Characteristics

No.	Fiber	Temperature at detection of combustible gas	Temperature after 5% of total com. gas has evolved	Initial pyrolysis sample mass	Residue after pyrolysis	Observed carpet surface temp. preceeding ignition in model corridor
		°C	°C	mg	mg	°C
A-1	Acrylic	290	345	21.6	11.2	≤ 260
A-1	Acrylic	300	345	20.4	10.2	≤ 200
W-1	Wool	245	285	20.2	2.8	≤ 180
N-1	Nylon 6,6	405	450	20.0	0	≤ 300
O-5	Polypropylene	350	435	18.1	0	-
O-4	Polypropylene (FR)	325	465	20.1	0	-
P-1	Polyester	420	440	21.1	4.0	-

flux sensors were used to examine heat transfer through the walls, floor, and ceiling. They can be regarded as within 20 per cent accurate at high temperature and have a response time of about 10 seconds. The sensors were positioned as shown in figure 6-21. By applying mass and energy conservation equations to a control volume enclosing the duct space and the floor covering (carpet only) the following equations result:

MASS

$$\frac{dm_c}{dt} = \dot{m} - \dot{m}_\infty - \dot{m}_B = \dot{m}_b \text{, burning rate} \qquad (6\text{-}15)$$

ENERGY

$$\left(\frac{dU}{dt}\right)_c + \dot{m}c_p(T-T_\infty) = \dot{E}_B + \dot{E}_c - \dot{q}_{r,o} - \dot{q}_k \; . \qquad (6\text{-}16)$$

Combining and rearranging, yields

$$\begin{aligned} \Delta\dot{E}_{net} &\equiv \dot{E}_c - \dot{q}_{r,o} - (\dot{m}_b + \dot{m}_B)c_p(T-T_\infty) - \left(\frac{dU}{dt}\right)_c \\ &= -\dot{E}_B + \dot{q}_k + \dot{m}_\infty c_p(T-T_\infty) \; . \end{aligned} \qquad (6\text{-}17)$$

The terms on the right-hand side could be determined.

$\dot{E}_B$ = burner energy release rate

$\dot{q}_k$ = wall conduction loss measured by heat flux sensors

$\dot{m}_\infty c_p(T-T_\infty)$ = convected energy rate

The terms on the left-hand side could only be inferred not determined directly.

(a) $\dot{E}_c$ = carpet energy release rate

(b) $\dot{q}_{r,o}$ = radiation loss out ends of duct

(c) $(\dot{m}_b + \dot{m}_B)c_p(T-T_\infty)$ = convected energy rate of burner and carpet fuel

(d) $\left(\frac{dU}{dt}\right)_c$ = energy rate increase of carpet

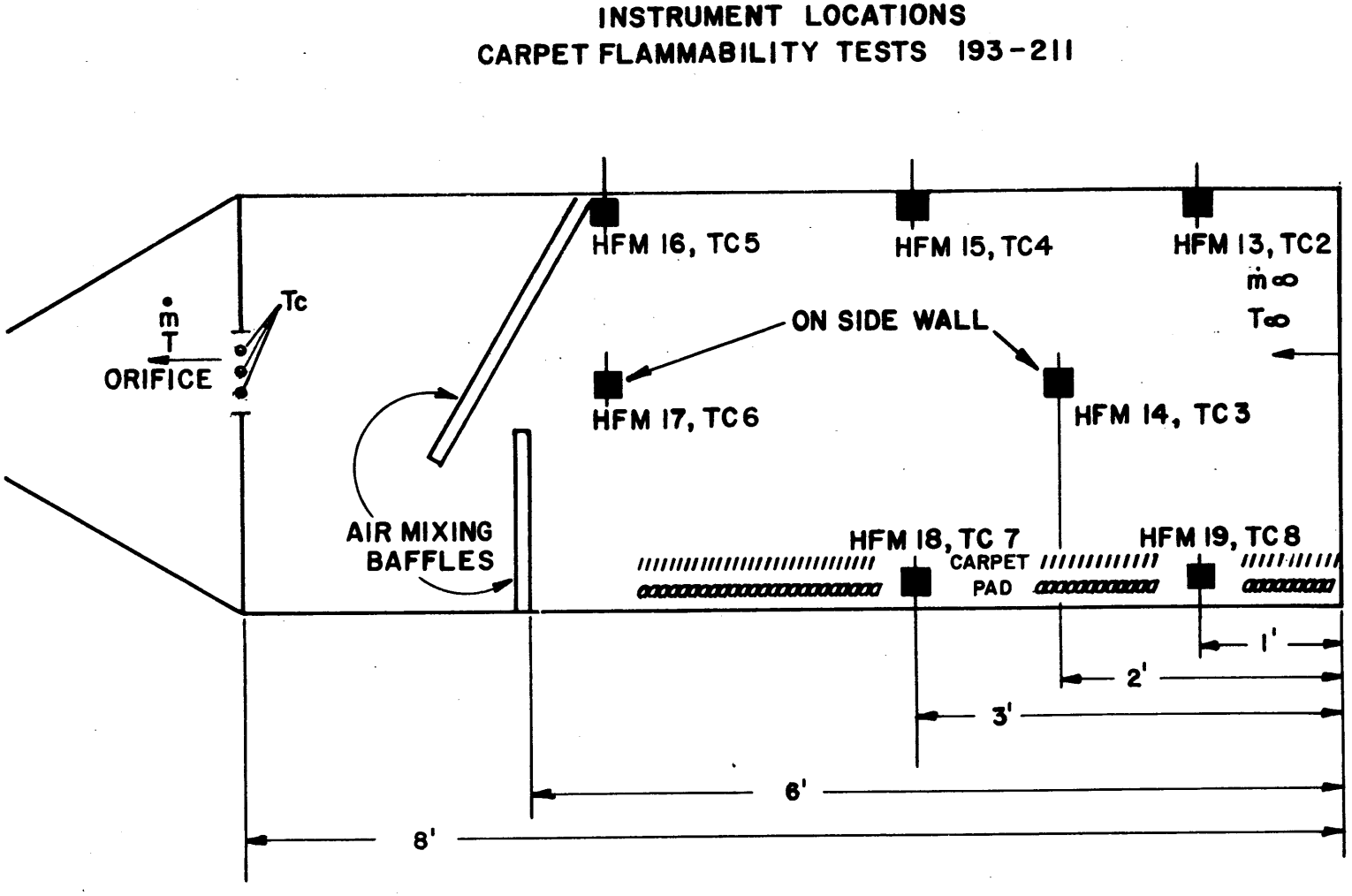

Figure 6-21. Sensor locations for energy balance analysis.

Terms (a) and (d) are probably dominant. Some results are shown plotted in figure 6-22. The blank run falls below the zero datum due to radiation losses ($\dot{q}_{r,o}$) and unaccounted conduction losses (no heat flux sensor covered the last 8 ft^2 of the floor area). An oxygen cell was used in several runs to measure oxygen concentration in the exhaust gases. Difficulty was encountered with calibration and determination of response time for this cell. However, it can be stated that for no flameover (CFT 190) O_2 concentration did not fall below 15 per cent while near the time of flameover (CFT 191) the O_2 concentration dropped below 5 per cent. It appears that flameover can lead to a fuel rich fire propagation domain.

7. OVERALL ANALYSIS AND SCALING RELATIONSHIPS

In the previous sections both quantitative and qualitative characteristics of the test system and floor covering flammability have been addressed. Here a simple model to characterize the system behavior will be considered. It will be concerned with the development processes which lead to flameover, and couched in terms of a "critical" preheating temperature to sustain a propagating flame. Hence heat transfer mechanisms will be emphasized and not the thermophysical and chemical processes directly connected with flame spread. Thus a first order overview will be achieved and effects such as carpet construction, phase transition and pyrolysis, and gas phase composition and kinetics will be put off to future analyses. Assuming that the factors ignored are independent of scale changes, then any scaling relationships developed from such a model will have wide spread application. In the least, it will present a more concise view of the variables involved.

Basically, the simplified model considers a wind blown flame plume emanating from a line source which heats the duct ceiling which in turn heats the duct floor covering via radiation. This idealization is portrayed in figure 7-1. As an analysis is developed additional assumptions will be introduced as the need arises. The goal is to arrive at an approximate relationship for floor covering temperature during preheating. Then the dimensionless groups contained in this relationship will be assessed. The dominant groups can then be used to determine scaling relationships.

The first step in analyzing this model is to develop a relationship for the plume temperature at the point it intersects the ceiling. This is based on a simplification of the work of Escudier [26]. His analysis is based on two entrainment constants α and β for a one-dimensional turbulent plume in a uniform cross wind, V_∞. The constant α is associated with the relative tangential external wind flow and reduces to the pure free convection entrainment constant for no wind flow. The constant β is associated with the normal wind velocity component and accounts for vortex mixing within the plume. Further discussion and details of the derivations of the results can be found in Appendix C. The results given here in dimensionless form for the gas temperatures at ($z = H$) are:

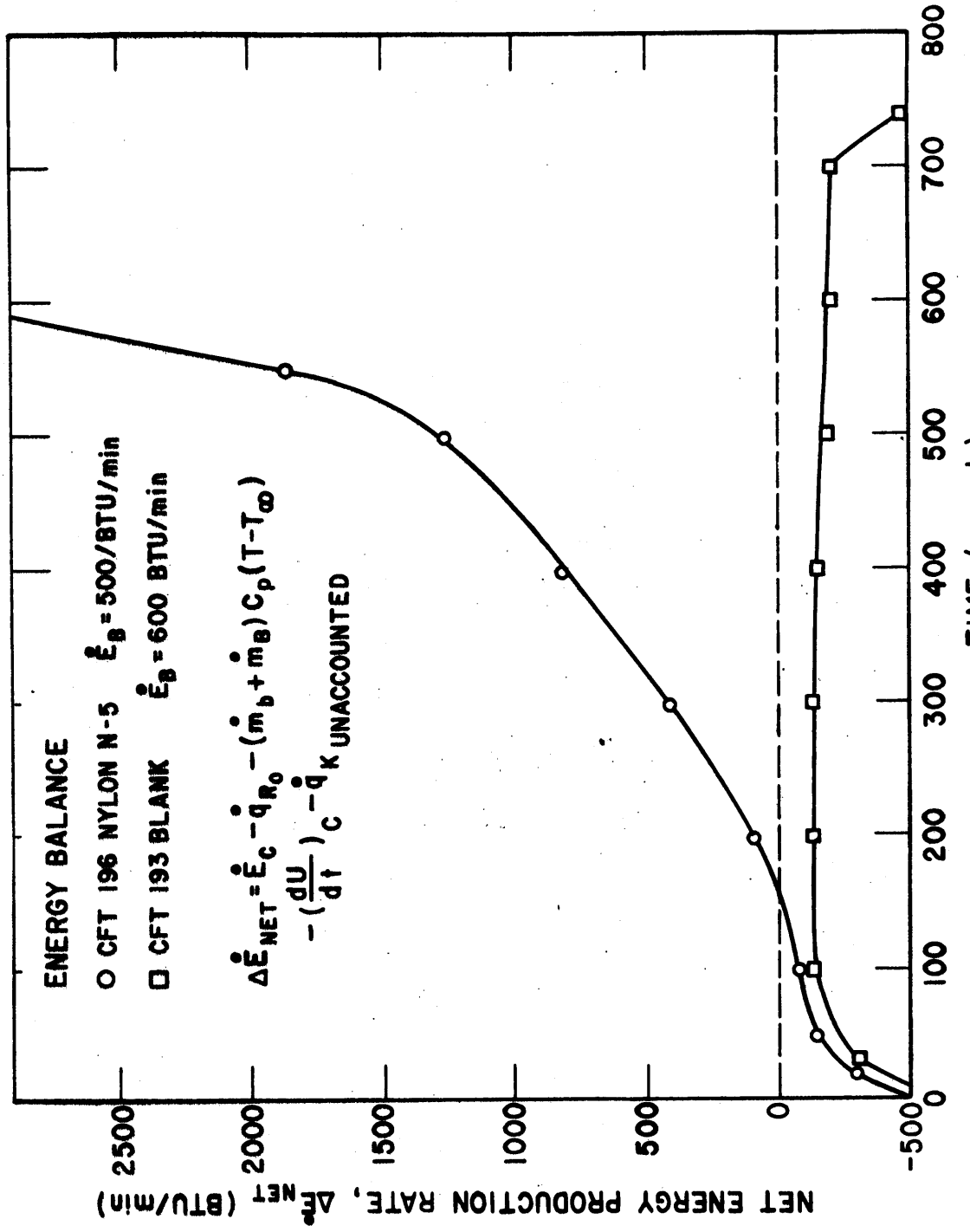

Figure 6-22. Some results of an overall energy balance.

SIMPLIFIED PREHEATING MODEL

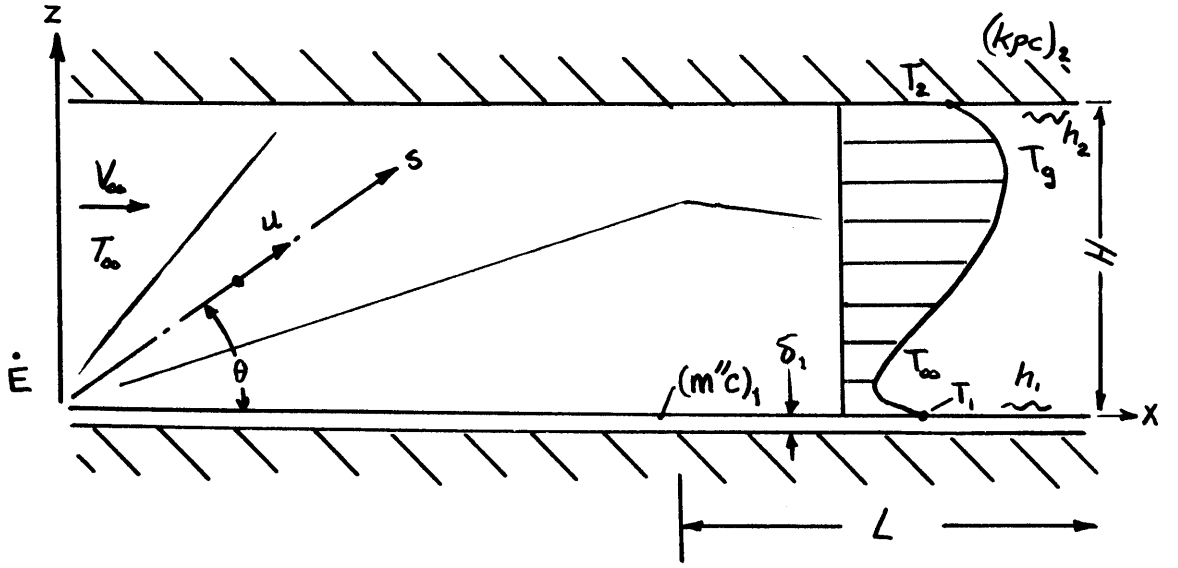

ASSUMPTIONS:

1. Preheat length, $L \rightarrow \infty$
2. Carpet thermally thin, insulated back.
3. Ceiling semi-infinite.
4. Blackbody surfaces.
5. Surrounding walls cold, T_∞
6. Energy rate from a line source and constant.
7. Flow thermally stratified and invariant over L.

Figure 7-1. Simplified preheating model.

$$\Theta_g \equiv \frac{T_g - T_\infty}{T_\infty} = \frac{Co}{2\beta'} \tag{7-1a}$$

where

$$Co \equiv \frac{\dot{E}}{T_\infty \rho_\infty c_p W_F H V_\infty} \tag{7-1b}$$

$$\beta' \equiv \alpha \tan\theta + \beta \tag{7-1c}$$

$$\tan\theta = f(\alpha, \beta)\, Fr^{-n}$$

or

$$\tan\theta = \begin{cases} \frac{1}{(2\alpha)^{1/3}}\, Fr^{-1/3}, & Fr \sim \text{small} \\ \frac{1}{(2\beta)^{1/2}}\, Fr^{-1/2}, & Fr \sim \text{large} \end{cases} \tag{7-1d}$$

and

$$Fr \equiv \frac{\rho_\infty c_p T_\infty V_\infty^3}{g(\dot{E}/W_F)} \tag{7-1e}$$

The "Combustion number" (Co) represents the ratio of the rate of energy released during combustion to the rate of convective transfer of energy. The Froude number, Fr, has been defined before as the wind to buoyancy effect.

The ceiling temperature will now be determined as a result of the plume intersecting the ceiling. Assume that the temperature is independent of x and that the expansion of the ceiling jet fills the full width, W, of the duct. The latter effect will be accounted for by replacing W_F with W in (7-d). The ceiling is considered infinite in thickness and an approximate conduction analysis is employed. The conductive flux is given by:

$$\dot{q}''_k \cong \frac{(\rho c)_2}{2} \frac{d}{dt}\left[(T_2 - T_\infty)\delta\right]$$

$$\delta \cong 2\sqrt{a_2 t} \,. \tag{7-2}$$

It is further assumed that the ceiling radiates as a blackbody to surroundings which are at temperature T_∞. An energy balance at the ceiling surface yields

$$h_2(T_g - T_2) = \frac{(\rho c)_2}{2} \frac{d}{dt}\left[(T_2 - T_\infty)\delta\right] + \sigma(T_2^4 - T_\infty^4). \tag{7-3}$$

In dimensionless form, the solution is:

$$\Theta_2 \equiv \frac{T_2 - T_\infty}{T_\infty} = \frac{\Theta_g}{1 + \frac{1}{2\sqrt{\tau}} + 4\frac{\sigma \bar{T}_\infty^3}{h_2}} \tag{7-4a}$$

where

$$\tau \equiv \frac{t}{\left(\frac{k\rho c}{h^2}\right)_2} \tag{7-4b}$$

and the non-linear radiation term has been linearized for convenience.

The ceiling heat-up time is usually more rapid than the floor heating so that a mean temperature, $\bar{\theta}_2$, will be used to decouple the floor heating problem from the ceiling temperature. Assuming the floor is a thin bed and $L \to \infty$, then:

$$h_1(T_\infty - T_1) + \sigma F_{12}(T_2^4 - T_1^4) + \sigma F_{1\text{-}S}(T_\infty^4 - T_1^4) = (m''c)_1 \frac{dT_1}{dt} \quad (7\text{-}5a)$$

where

$$F_{12} = F_{21} = 1 - F_{2\text{-}S} = \sqrt{1 + \left(\frac{H}{W}\right)^2} - \left(\frac{H}{W}\right) \quad (7\text{-}5b)$$

The solution in dimensionless form is

$$\Theta_1 \equiv \frac{T_1 - T_\infty}{T_\infty} = \bar{\Theta}_2 \cdot F_{21} \cdot \left[\frac{4\left(\frac{\sigma T_\infty^3}{h_1}\right)}{1 + 4\left(\frac{\sigma T_\infty^3}{h_2}\right)}\right] \cdot \left[1 - \exp \frac{-\left[1 + 4\left(\frac{\sigma T_\infty^3}{h_1}\right)\left(\frac{k\rho c}{h^2}\right)_2 \tau\right]}{\left(\frac{m''c}{h}\right)_1}\right] \quad (7\text{-}6)$$

These equations, 7-1, 7-4, and 7-6, form the solution for the preheating problem. In general (neglecting flame radiation, and thermal non-uniformities):

$$\Theta_1 = \text{function}\left(\frac{H}{W}, Co, Fr, \tau, \left(\frac{k\rho c}{h^2}\right)_2 \Big/ \left(\frac{m''c}{h}\right)_1, \frac{\sigma T_\infty^3}{h_1}, \frac{\sigma T_\infty^3}{h_2}\right) \quad (7\text{-}7)$$

The heat transfer coefficients, h_1 and h_2, are not explicitly independent since they must be calculated. For this reason it is convenient to eliminate h from all but one of the dimensionless groups. Where h occurs, it can be considered as proportional to $\rho c_p V$ which holds for rough wall turbulent flows. A new set of dimensionless groups is given as

$$\Theta_1 = \text{function}\left(\frac{H}{W}, \frac{\dot{E}}{\rho_\infty T_\infty c_p W g^{1/3} H^{3/2}}, \frac{V_\infty}{(gH)^{1/2}}, \frac{t(\sigma T_\infty^3)^2}{(k\rho c)_2}, \right. \quad (7\text{-}8)$$

$$\left. \frac{(k\rho c)_2}{(m''c)_1 \sigma T_\infty^3}, \frac{\sigma T_\infty^3}{h}\right)$$

This form has the advantage of separating out the velocity effect, and the second parameter is directly related to the gas temperature for a line plume with no wind.

Assume now that a "critical" floor temperature is required to sustain flame spread. Consider the floorcovering material as fixed and the duct material fixed. Then some observations can be made. The first three dimensionless parameters are compared for several flammability tests and full scale experiments of real fires in table 7-1. The time scale is identical for all cases provided h is assumed to be invariant. For similarity with real fires the three parameters must be equal to their counterparts in the flammability tests. For ASTM E84 to be applicable in this comparison the test sample is considered to be floor mounted. Moreover, the energy contribution from the test sample in small scale experiments may be comparable to the burner values listed in table 7-1 and should be absorbed into E for a correct comparison. Thus, a more rational form of comparing test methods to full-scale fire conditions is presented.

Partial use of the scaling relationships were applied to some of the model corridor data which represented a wide range of experimental conditions. A presentation of this analysis was motivated by equation (7-6) and flame spread was expressed as final distance burned (D_b) divided by burner flame length (L_B). The dependent dimensionless parameter was based on the product of the first two terms on the right-hand-side of eq. (7-6). This parameter, ϕ , is based on plume temperature and radiation exchange. It is reasoned that these factors are strong variables compared with the other parameters in eq. (7-6). The results of this approach is shown in figure 7-2 for nylon carpet N-5/U and in figure 7-3 for acrylic carpet A-4/U. Each designated point on the figures represents the outcome of experiments summarized in tables 4-2 and 4-3. It is apparent that when flameover does not occur, the distance burned is primarily influenced by the length of the burner flame. Also the results clearly demonstrate a critical region beyond which flameover will occur for the appropriate combination of energy input rate and geometry. Moreover this critical value for ϕ is seen to be dependent on the material properties of the test specimen as one would expect. An increase in ϕ beyond its critical value should lead to flameover in shorter time, however, this trend is not completely evident. Finally this use of partial scaling appears to be helpful in generalizing the data. However, general extrapolation of these results will have to await more extensive scaling studies.

8. CONCLUSIONS

An experimental model corridor facility was designed, constructed and instrumented. Good control of selected variables was obtained. A testing procedure was developed that has given reliable results.

Using the model corridor many of the factors which control flame spread on carpets have been defined and are reasonably well understood. The dominant factor is radiant preheating of the carpet surface ahead of the flame front. If the critical level of preheating is exceeded an accelerating flame front will develop and the total length of sample becomes involved. This phenomenon has been termed flameover. If sufficient preheating does not occur, a decelerating flame front develops

TABLE 7-1

Comparison of Test Methods and Fire Conditions

Based on Scaling Relationships

Parmeter	Proposed Model Corridor Test	UL Chamber Test	ASTM E-84 Tunnel Test	Full* Scale Corridor
E (BTU/Min)	600	500	5,000	100,000
V_∞(FT/Min)	100	100	240	200
H (FT)	1.33	1	1	8
W (FT)	1.33	2	1.5	8
$[\dot{E}/WH^{3/2}]$	293	250	3,330	550
$[V_\infty/H^{1/2}]$	87	100	240	71
[H/W]	1	0.5	0.667	1

* Based on energy estimates of real fires by Waterman and Christian [14]. Air flow is based on extreme ventilation conditions [27,28].

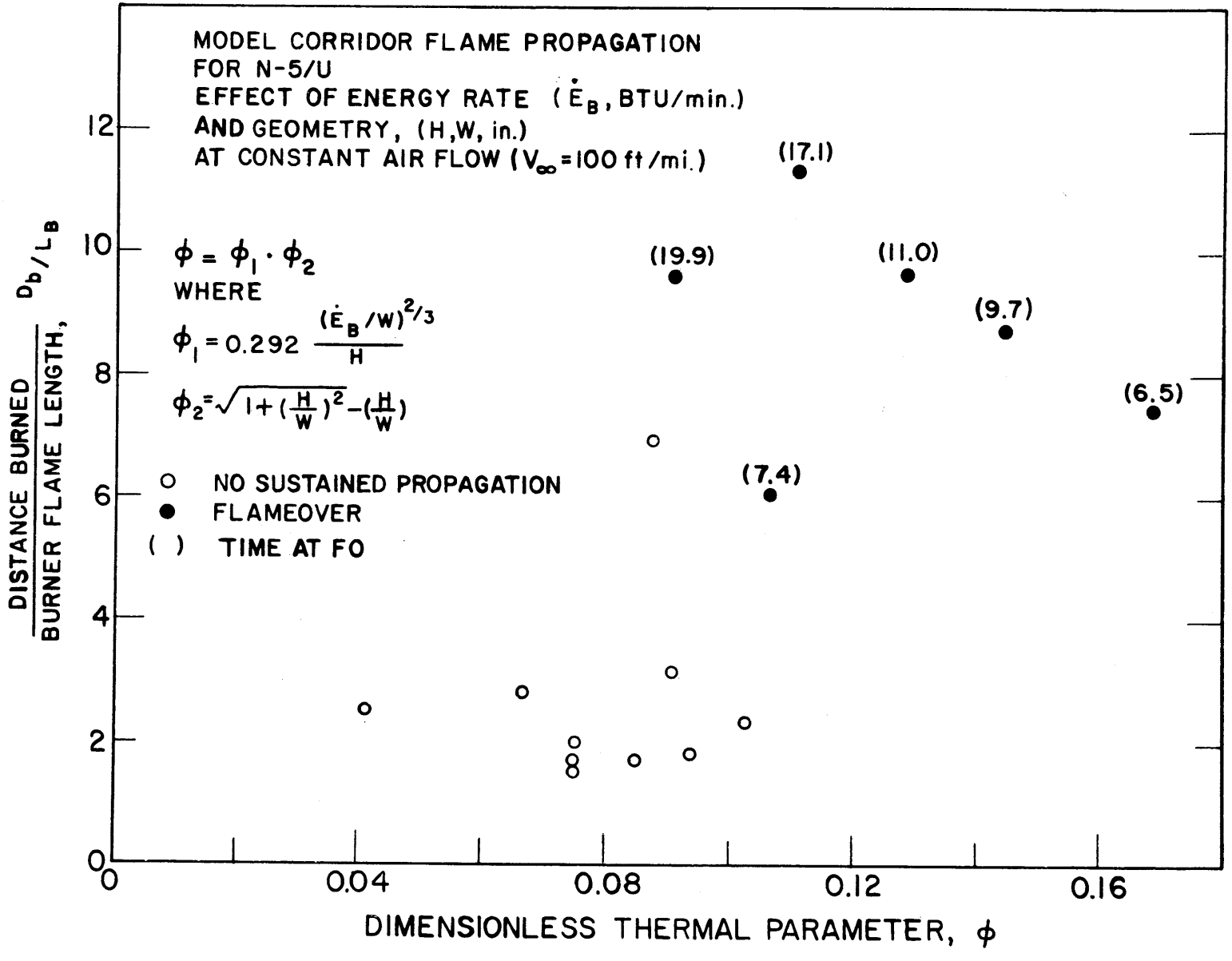

Figure 7-2. Partial scaling applied to model corridor flame spread for nylon carpet N-5/U.

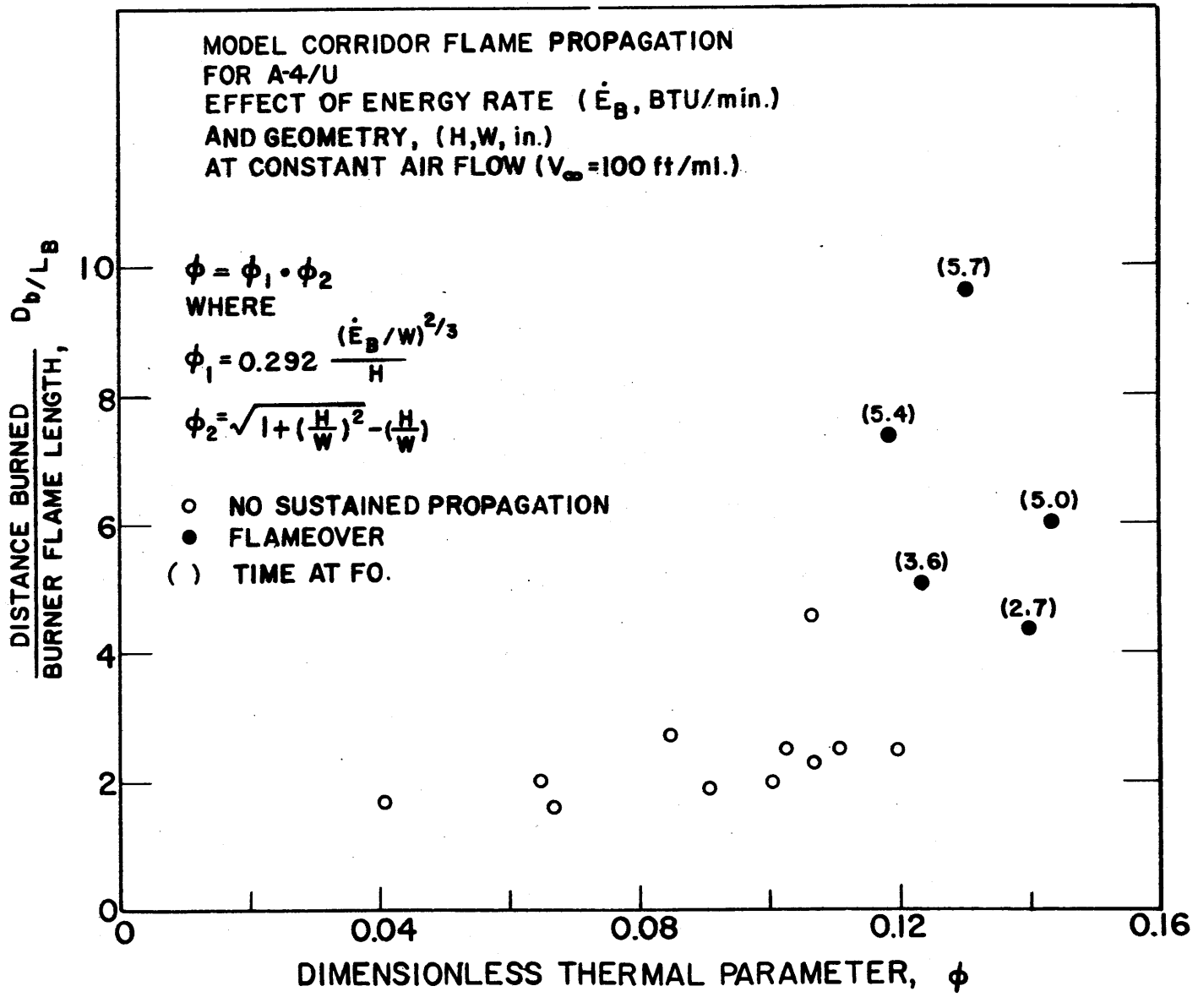

Figure 7-3. Partial scaling applied to model corridor flame spread for acrylic carpet A-4/U.

which leads to very slow burning or extinguishment. The intensity of the radiant preheating is related to the energy supplied both from an external source and the burning carpet, the cross-sectional dimensions of the model corridor and air velocity.

The total floor covering assembly is shown to affect flame spread behavior. The thermal insulation provided by an underlay can increase severity and a "bonded" installation can reduce severity. This suggests that a test method should be designed to evaluate total floor covering assemblies and not components.

Mathematical modeling yields scaling relationships which allow the model corridor to be compared, with some qualifications, to the burning characteristics of floor covering materials in full-scale situations.

Several factors remain to be clarified. The effect of air velocity in the model corridor, and its relationship to real situations, is not clearly understood. In the model corridor the heat released by the initially burning carpet is a significant part of the total energy. It is not known whether this is the case in real fires. It is recommended that further experimentation be directed to these questions.

Dr. Clayton Huggett [32] of the National Bureau of Standards characterized carpet behavior in building fires as follows:

1. Rapid flame spread over the pile surface is the primary hazard mechanism.

2. This flame spread is controlled by a time and intensity dependent energy input to the carpet surface ahead of the flame front.

3. This energy is supplied by the ignition source and feedback from the burning carpet.

4. The magnitude of the energy input necessary to cause rapid flame spread is a measure of hazard potential.

This behavior is supported by findings of the full-scale corridor program being carried out at the National Bureau of Standards, results of previous corridor and duct experiments, and by reports from witnesses to real building fires. It describes well the findings of this program, although correlation has not yet been established between the results obtained in the model corridor and full-scale experiments.

It is concluded that the major hazard that should be addressed by a test method is the rapid total involvement or flameover of a carpet assembly. Radiant preheating of the carpet surface, which is controlled by the energy supplied by both the ignition source and energy released by the burning carpet, determines whether flameover will occur. The energy input to a model or test facility can be scaled to simulate full-scale real life conditions.

9. SUGGESTED TEST METHOD

Based on the findings reported, it seems practical to develop a test facility and procedure that can provide a measure of the potential hazard of floor coverings in building fires. The following design and operating conditions are suggested for consideration.

1. A test section with cross-sectional dimensions of 16" x 16" and 8 ft. in length. This shape will be similar to real corridors.

2. Construction materials for the test section that have thermal properties similar to materials used in real corridors and that provide rapid cooling to facilitate short time between tests. Asbestos board (conforming to Canadian specification 34-g p. 18) is suggested for this material.

3. Water cooled curbs to inhibit edge burning.

4. A forced air flow with adequate control to insure a stable, uniform flow during testing. An air velocity of 100 ft/min is suggested. This is higher than scaling relationships suggest but practical if good flow control is desired.

5. A heat input to the test section supplied by a diffusion flame gas burner mounted to impinge on the surface of the floor covering material. A heat input of 600 BTU/min is suggested. Using the scaling relationship, $\dot{E}/WH^{3/2}$ this would simulate about 53,000 BTU/min in a real corridor with cross-sectional dimensions of 8 ft x 8 ft and about 93,000 BTU/min in a corridor 10 ft x 10 ft. If consideration is given to energy release by the floor material in the test, then higher full-scale values for $\dot{E}$ will be estimated.

6. Preconditioning of samples and control of intake air temperature and humidity should be considered and studied in future work.

7. A test time of 12 minutes with the burner "on" followed by 12 minutes with the burner "off".

8. Testing of total floor covering assemblies as they are to be used in actual situations. This would include both the use of underlayments and bonded installations.

9. The test result should be a "pass-fail" decision. This is consistent with the results of the program and should be based on whether or not the test specimen burns the entire 8 foot length in the 24 minute test time.

Some of these parameters are not fully quantified at this time. As additional results of full-scale and laboratory experiments become available, some test conditions could be modified to more closely approximate true hazard conditions. It is not anticipated that major changes in the test facility or procedure would be required.

It is suggested that a test method, based on the concepts presented in this report, would be suitable for use in regulating floor covering materials to be used in corridors and exitways of institutional buildings. To accomplish this recommendation it is suggested that one such test facility be designed and constructed. With this unit, the concept presented could be confirmed and repeatability established. Following this, several additional test facilities would be required so that inter-laboratory reproducibility could be established.

APPENDIX A. REVIEW OF LITERATURE ON DUCT AND CORRIDOR FIRES

Past studies motivated by mine fire considerations and flammability test development projects have been concerned with flame spread in ducts. Typically these ducts have varied in size, have been oriented horizontally, have involved forced air flow, and have included a variety of ignition sources and arrangements of fuel loadings. Although the conditions may differ, there is sufficient commonality upon which to base some general conclusions.

Rhodes and Smith [7][1] describe experiments with model mine fires. The test duct was 48 feet long and had a cross section of 6.5 by 4.75 inches. The ignition source was small and only when wood lagging covered both sides and roof did a fire propagate the full fuel length. Floor fuel covered ducts did not propagate beyond 7 feet. They also found that for hardwood fuel lagging along the duct sides and roof air flow had a marked effect on fire propagation. This is shown in figure A-1 in which a critical air flow speed is apparent for fires which propagate. They explained this critical zone as associated with the fully developed transition Reynolds number for laminar to turbulent flow.

Roberts and Clough [8] conducted similar experiments in a wood lined passage 30 cm square and about 30 meters long. They studied steady propagating fuel rich fires. These fires produce an excess of fuel gases due to intense preheating downstream of the flame zone, consume all available oxygen in the air stream, and propagation rate depends on ventilation air speed. The fuel rich case developes from an oxygen rich fire which in turn requires a critical ignition source to be sustained. They put forth a one-dimensional flame spread model which incorporates convective preheating to develop a pyrolysis zone ahead of the flame zone. Basically they found that if the ignition source is insufficient to generate a critical rate of fuel per unit rate of air flow then no propagation or an oxygen rich propagation mode is possible. On the other hand, above this critical condition, acceleration to the more intense fuel-rich steady propagation limit would result. In this fuel-rich zone an increase in air flow would lead to an increase in flame propagation. Roberts [9] has re-iterated these findings along with additional experimental investigations of duct fires.

de Ris [10] has presented a detailed analysis of fuel-rich duct fires, and his predicted results are in reasonable agreement with some of the findings of reference [8]. de Ris correctly qualifies his analysis to cases excluding secondary backflow upstream or downstream of the combustion zone, and excluding stratification which permits oxygen to bypass the fire. He adopts the criterion

$$\frac{\Delta \rho g H}{\rho_\infty V_\infty^2} < 1$$

1 Figures in brackets indicate literature references at the end of this report.

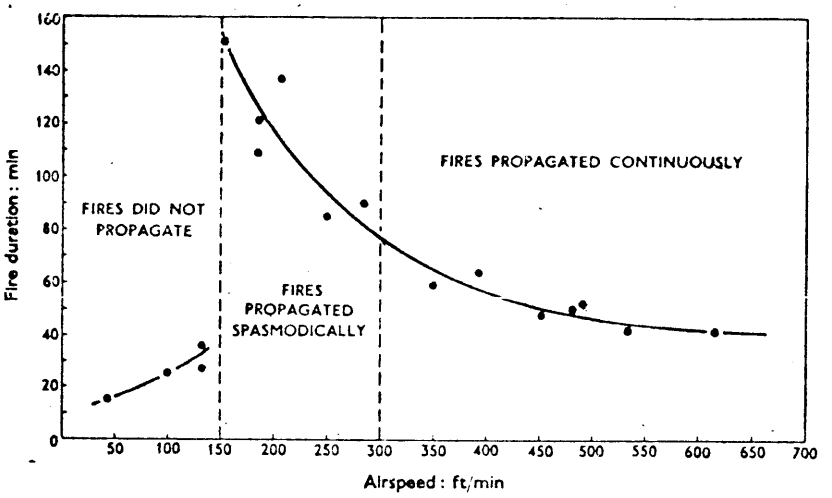

Figure A-1. Model mine fire characteristics [7].

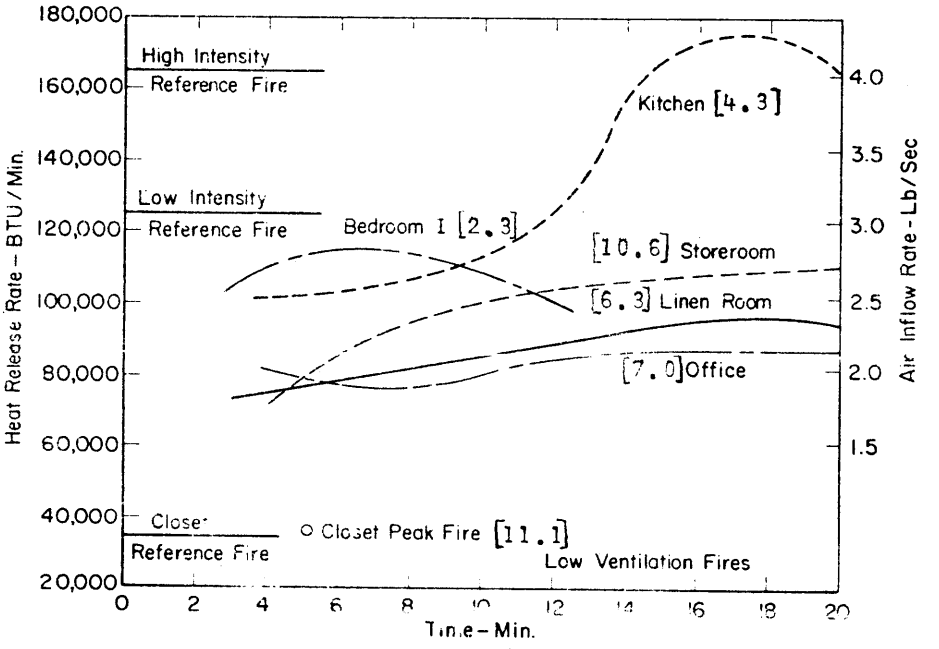

Figure A-2. Estimated energy release rate from fires of various occupancies [14].

to insure that no backflow or stratification occurs. P. H. Thomas [11] used a similar criterion; i.e.

$$\frac{g\dot{E}}{\rho_\infty T_\infty c_p V_\infty^3} < 1$$

to denote the onset of upstream movement of smoke from a line fire in a ventilated duct. The two relationships should be regarded as estimations and not as exact, and they are essentially equivalent.

Although the duct flow literature is closest in physical scale to the study herein, the ultimate application is fire propagation in building corridors. Corridor studies have typically been full scale and have investigated the effect of a room fire on adjoining corridor. All studies, generally, have had a similar configuration. A doorway connects the fire room to the corridor, and the corridor has a window at its far end. Vents have been distributed in various locations, and usually no forced air flow has been imposed. Although much data gathering and categorizing has been done here, no detailed analysis has been put forth, and only one study been primarily directed to floor covering materials.

McGuire [12] reports on full-scale and quarter-scale model results in which various lining materials have been used along walls, floor, and ceiling. He also displays the ratings given to the various materials used as determined by ASTM E-84 and ASTM E-162 flammability tests. He concludes that floor coverings with a rating below 220 made little contribution to fire spread in the full scale corridor but were more significant in the quarter-scale work. The critical rating for ceiling material appeared to be 130 and for wall linings 35.

Tests conducted at the Danish State Testing Laboratory in Denmark are reported on by Christensen, Lohse, and Malmstedt [13]. The room and corridor were full scale and no combustible floor materials were investigated. Although no floor covering materials were studied, their overall results are of direct relevance here if one is to understand real fires versus controlled fires. With caution, some of their conclusions have been abstracted as follows:

(1) Wood crib fires have different developments than furnished rooms.

(2) The ignition process depends not only on a time-gas temperature relationship but also on the heat transfer and thermo-physical conditions of the ignition environment.

(3) "Comparison between various small scale laboratory methods disclosed such great differences between the results found by these methods that it must be established that they neither reflect the regularity found in the full-scale tests nor the limitation of influences.

It must be an indispensable requirement to the applicability of a testing method that it depends on effects that are probable in practice, and that it affords a criterion of the degree of ignitability that is connected with one of the thermo-physical conditions to which the materials may be brought by influences existing in practice."

The room and corridor experiments of Christian and Waterman [14] appear to be the only reported work which attempts to classify the energy output of fully developed room fires for various occupancies. Although much data was gathered in these tests, it is significant to review the energy release rates for the rooms. This is displayed in figure A-2. The numbers [ ] indicate fuel loading in lb/ft^2 of floor area, and all the rooms had a volume of 1200 ft^3 except the closet which was 72 ft^3. In addition gas temperature measurements imply a fire duration of about 30 minutes. It should be emphasized that these energy release rates were calculated from air flow measurements and involve several assumptions on fuel type and fuel-air mixing. Thus they should not be accepted as exact but only approximate.

Finally, work is in progress at NBS [15] to characterize room-corridor fires and assess the fire hazard with respect to floor covering materials.

In summary several observations can be made with respect to both duct and corridor fires. The strength of the ignition source is significant. With respect to the room-corridor arrangement, the room is the primary ignition source with regard to corridor flame spread. A critical input energy is required to sustain flame spread in a corridor or duct. The flame spread has a potential to propagate indefinitely if it becomes a fuel rich fire. Flame spread in ducts and corridors is more likely with wall or ceiling combustible linings than combustible floor coverings. Insufficient quantitative data and analysis have been put forth to generalize the spectrum of real fires and to provide a direct relationship to any established flammability test.

APPENDIX B. RADIANT PREHEATING CALCULATIONS

In order to determine if the observed incident radiant heat flux is sufficient to cause the measured surface temperature rise on the carpet pile some calculations were made. Two models were considered. The first considered a thermally thin floor material. Although this is not a good assumption based on the low thermal conductivity of carpets, in depth radiant absorption in the pile fibers would tend to result in a uniform temperature distribution in depth. Moreover a thermally thin assumption is a limiting case in which all the energy is distributed uniformly in depth. Alternately, the second model considers an infinitely thick material. In both models the material is assumed to have uniform properties, is an opaque black body, and is subjected to incident radiant heating with convective cooling. No other losses, such as reradiation or conduction into the underlay, are accounted for. A linearly varying radiant flux was prescribed.

B.1 Thin Bed Model

The energy equation is

$$m'' c \frac{dT}{dt} = \dot{q}''_r - h (T-T_\infty) \qquad \text{(B-1)}$$

where m'' = mass per unit area
c = specific heat
T = surface temperature
T_∞ = gas temperature and initial temperature
h = convective heat transfer coefficient
$\dot{q}''_r$ = incident radiant heat flux

The radiant heat flux is specified by

$$\dot{q}''_r = q_o + q_1 t. \qquad \text{(B-2)}$$

The solution is given by

$$T-T_\infty = \frac{q_o}{h}\left[1-e^{-\gamma t}\right] + \frac{q_1}{m''c\gamma^2}\left[\gamma t - (1-e^{-\gamma t})\right] \qquad \text{(B-3)}$$

where $\gamma = h/m''c$

B.2 Thick Bed Model

In the interest of expedience, reference is made to solutions given in Carslaw and Jaeger [29] as special cases of the more general problem specified earlier.

For constant heat flux with convective cooling,

$$\text{i.e.} \qquad \dot{q}''_r = q_o .$$

The surface temperature is given by

$$T_s - T_\infty = \frac{q_o}{h}\left[1 - e^{\beta^2}\operatorname{erfc}\beta\right] \tag{B-4}$$

where

$$\beta \equiv \frac{h}{k}\sqrt{\alpha t} .$$

If β is small, then

$$T_s - T_\infty \cong q_o \frac{2}{\sqrt{\pi}} \cdot \frac{\sqrt{\alpha t}}{k} . \tag{B-5}$$

This corresponds to the uniform heating with no convective cooling. For the case where

$$\dot{q}''_r = q_1 t ,$$

$$T_s - T_\infty = \frac{q_1 \sqrt{\alpha}\, t^{3/2}}{1.33\, k} \tag{B-6}$$

These results will be applied to acyrlic carpet A-4 in CFT 68. The incident radiant heat flux preceding ignition will be approximated by

$$q_o = 0$$

and

$$q_1 = 4.3 \times 10^{-4} \text{ cal/cm}^2\text{sec}^2$$

Based on fully developed turbulent flow in a duct the convective coefficient was estimated as $h = 0.6 \times 10^{-4}$ cal/cm^2 sec°C. Carpet properties are taken from measurements by Kashiwagi [20] and G. Robinson [30].

$k = 0.174 \times 10^{-3}$ cal/sec cm°C, Ref. [30]

$\alpha = 3.6 \times 10^{-3}$ cm^2/sec, Ref. [30]

$m'' = 0.286$ gm/cm^2

$m''_{pile} = 0.121$ gm/cm^2

$c_{pile} = 0.45$ cal/gm $^{\circ}$C, Ref. [20]

Kashiwagi has generally found α values about 50 per cent lower than those of Robinson. The technique used by Robinson was based on the transient conduction solution for radiant heating of an opaque solid. Kashiwagi's technique is based on steady state measurements. Unfortunately, he has not measured α for carpet A-4. However, an extrapolation from his findings would suggest

$$\alpha = 1.8 \times 10^{-3} \text{ cm}^2/\text{sec}$$

B.3 Results for a Thermally Thin Pile

Examining the parameter γt up to the time of ignition, it is found that

$$(\gamma t)_{max} = 0.22$$

Since this parameter is small it is justifiable to approximate equation (B-3) as

$$T - T_\infty \simeq \frac{q_1}{m''c} \cdot \frac{t^2}{2} \qquad \text{(B-7)}$$

Then

$$T = 30 + 3.96 \times 10^{-3} \; t^2 \qquad (^{\circ}\text{C}) \quad \text{with t in sec.}$$

B.4 Results for a Thermally Thin Carpet

Here equation (B-7) also applies. The specific heat of the pile fibers will be used for the total specific heat of the carpet. The specific heat of the carpet may be about 10 per cent lower than the pile value.

$$T = 30 + 1.78 \times 10^{-3} \; t^2 \qquad (^{\circ}\text{C}) \; .$$

B.5 Results for a Thermally Thick Carpet

Here equation (B-6) will be used. This is justified since $\beta = 0.352$ at 200 seconds. Hence convective cooling is unimportant compared with conductive heat transfer into the solid. Also the carpet acts like an infinite solid up to at least 100 seconds.

$$T = 30 + 0.113\, t^{3/2} \quad (^{\circ}C) \, .$$

For the lower α value

$$T = 30 + 80 \times 10^{-3}\, t^{3/2} \quad (^{\circ}C) \, .$$

APPENDIX C. ANALYSIS OF A LINE SOURCE PLUME IN A CROSSWIND

The interaction of the burner and carpet flame plume with the entrance air flow establishes the temperature and velocity downstream. It has been seen that the resulting temperature distribution is significant for determining conditions for flameover. In particular, the temperature of the gases at the ceiling of the model corridor establish the level of radiant preheating ahead of the carpet flame front. In the following analysis a one-dimensional model will be used to determine the variables influencing ceiling gas temperature. A turbulent line-source plume will be considered for simplicity. This means that the energy released in combustion is treated as emanating from a line-source. A turbulent entrainment model considered by Escudier [26] will be used here.

Consider that energy is being released at a rate $\dot{E}$ over width W_F in a crossflow of velocity V_∞. A schematic is shown in figure C-1. A control volume is selected for the

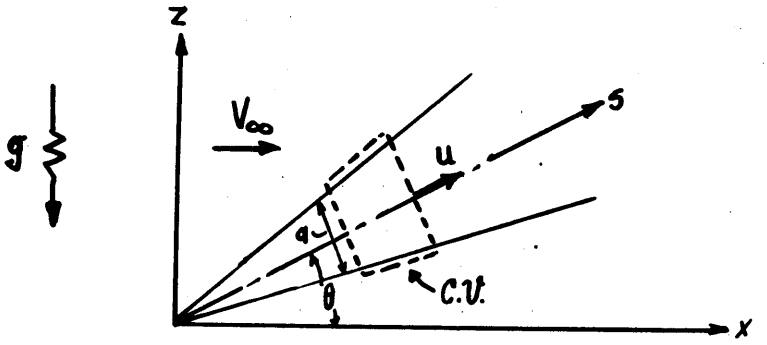

Figure C-1. Plume Coordinate System

plume and the conservation equations are written.

Conservation of Mass

$$\frac{d}{ds}(\rho A u) = \rho_\infty P v_{ent} \qquad \text{(C-1)}$$

where

$$A = aW_F$$

$$P = 2(a+W_F) \cong 2W_F$$

and

$$v_{ent} = \alpha(u - V_\infty \cos\theta) + \beta(V_\infty \sin\theta) \qquad \text{(C-2)}$$

The entrainment velocity v_{ent} is based on the relative tangential velocity and the normal velocity to the plume. The parameter α and β are non-dimensional entrainment constants.

Conservation of Z momentum

$$\frac{d}{ds}\left(\rho A u^2 \sin\theta\right) = (\rho_\infty - \rho) g A \quad . \tag{C-3}$$

Conservation of X momentum

$$\frac{d}{ds}\left(\rho A u^2 \cos\theta\right) = V_\infty \frac{d}{ds}(\rho u A) \quad . \tag{C-4}$$

Conservation of Energy

$$\frac{d}{ds}\left[\rho c_p A u (T - T_\infty)\right] = 0 \quad . \tag{C-5}$$

Equation of State

$$\rho T = \rho_\infty T_\infty \quad . \tag{C-6}$$

All properties except in the buoyancy term, will be taken as constant and evaluated at T_∞. Also the plume width W_F will be assumed constant. This is equivalent to assuming two dimensional planar flow. The unknowns are a, u, T, ρ, and θ.

Equation (C-5) is integrated from s = 0 to yield

$$\rho_\infty c_p A u (T - T_\infty) = \dot{E} \tag{C-7}$$

where $\dot{E}$ is the rate of energy released at s = 0.

Equation (C-4) is integrated from s=0 and the condition $q = 0$ at $s = 0$ is used to yield

$$\rho_\infty A u^2 \cos\theta = V_\infty \rho_\infty u A$$

or

$$u = \frac{V_\infty}{\cos\theta} . \qquad \text{(C-8)}$$

Equation (C-3) is integrated from s=0 to yield

$$\rho_\infty A u^2 \sin\theta = \int_0^s (\rho_\infty - \rho) g A \, ds .$$

By using the equation of state (C-6), the uniform property assumption, equation (C-7), and equation (C-8), this can be written as

$$\rho_\infty A \left(\frac{V_\infty}{\cos\theta}\right)^2 \sin\theta = \frac{g \dot{E}}{T_\infty c_p V_\infty} \int_0^s \cos\theta \, ds$$

Assuming θ is independent of s, representing a mean plume angle, then

$$\frac{\sin\theta}{(\cos\theta)^2} = \frac{g \dot{E} s \cos\theta}{A \rho_\infty c_p T_\infty V_\infty^3} . \qquad \text{(C-9)}$$

Equation (C-2) is substituted into (C-1) and integrated treating θ as a constant to yield

$$q = 2 \cos\theta \sin\theta (\alpha \tan\theta + \beta) s . \qquad \text{(C-10)}$$

Substituting this result into (C-9) yields

$$\alpha \tan^3\theta + \beta \tan^2\theta = \frac{g \dot{E}}{2 \rho_\infty c_p T_\infty W_F V_\infty^3} . \qquad \text{(C-11)}$$

from which θ can be determined. To obtain an explicit solution, limiting values can be found. For θ large, corresponding to low wind speed,

$$\tan\theta = \left(\frac{g\dot{E}}{2\alpha\rho_\infty c_p T_\infty W_F V_\infty^3}\right)^{1/3} \tag{C-12a}$$

For θ small, corresponding to high wind speed,

$$\tan\theta = \left(\frac{g\dot{E}}{2\beta\rho_\infty c_p T_\infty W_F V_\infty^3}\right)^{1/2} \tag{C-12b}$$

The Froude number can be defined as

$$Fr \equiv \frac{\rho_\infty c_p T_\infty W_F V_\infty^3}{g\dot{E}} \tag{C-13}$$

It follows from equations (C-7), (C-8), and (C-10) that

$$T - T_\infty = \frac{\dot{E}}{2\rho_\infty c_p W_F V_\infty z(\alpha\tan\theta + \beta)} . \tag{C-14}$$

For small θ , or equivalently for Fr large,

$$T - T_\infty = \frac{\dot{E}}{2\beta\rho_\infty c_p W_F V_\infty z} \tag{C-15a}$$

For large θ , or equivalently for Fr small,

$$T - T_\infty = \left(\frac{T_\infty^{1/2}\dot{E}}{2\alpha g^{1/2}\rho_\infty c_p W_F}\right)^{2/3} \cdot \frac{1}{z} \tag{C-15b}$$

This corresponds to the line plume solution (no crosswind) given by Thomas [31].

If β' is defined as $(\alpha \tan + \beta)$ then for large Fr, β' approaches β ; and for small Fr, β' approaches $[(\alpha^2/2Fr)^{1/2} + \beta]$. This trend is observed in figure C-2. The data were obtained from ceiling temperature data after long time during blank runs in the model corridor facility. A flame width of 8 inches was used and data at x = 1 and 2 feet were used.

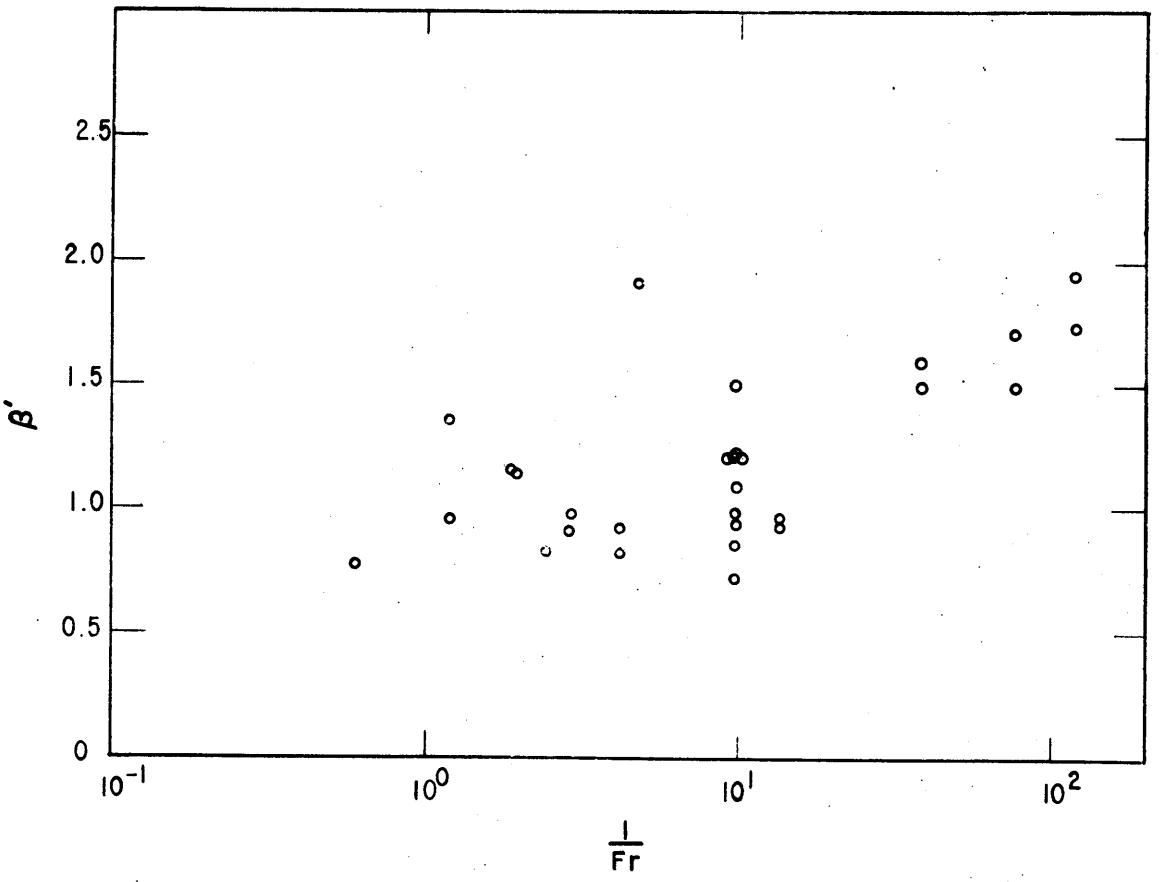

C-2. Plume measured results for β' vs. Fr.

REFERENCES

1. "Carpet and Rugs (Pill Test) Standard for the Surface Flammability of Carpets and Rugs", DOC FF 1-70, Federal Register, Vol. 35, No. 74, April 16, 1970, p. 6211.

2. "Standard Method of Test for Burning Characteristics of Building Materials", ASTM E84-68, American Society for Testing and Materials, Philadelphia, Pennsylvania (1968).

3. "Standard Method of Test for Flame-Propagation Classification of Flooring and Floor-Covering Materials", Subject 992, Underwriters' Laboratories, Inc., February 1971.

4. "Surface Flammability of Materials Using a Radiant Heat Source", ASTM E162-67, American Society for Testing and Materials, Philadelphia, Pennsylvania (1968).

5. Memorandum from Mr. Z. Zabawsky to ASTM Subcommittee IV Task Group on Floor Covering, "Armstrong Cork Company Flooring Radiant Panel", May 17, 1971.

6. W. Denyes and J. W. Raines, "A Model Corridor for the Study of the Flammability of Floor Coverings", NBSIR 73-200, May 1973.

7. A. C. Rhodes and P. B. Smith, "Experiments with Model Mine Fires", The Use of Models in Fire Research, ed. W. G. Berl, National Academy of Sciences-National Research Council, pp. 235-55 (Washington, D. C. 1961).

8. A. F. Roberts and G. Clough, "The Propagation of Fires in Passages lined with Flammable Materials", Combustion and Flame, Vol. 11, No. 5, October 1967, pp. 365-76.

9. A. F. Roberts, "Fires in Ducts under Forced Ventilation Conditions", Fire Technology, February 1970, p. 13.

10. J. de Ris, "Duct Fires", Combustion and Science Technology, Vol. 2, 1970, pp. 239-58.

11. P. H. Thomas, "The Movement of Smoke in Horizontal Passages Against an Air Flow", Fire Research Note 723/1968, Fire Research Station, Borehamwood, Herts, England.

12. J. H. McGuire, "The Spread of Fire in Corridors", Fire Technology, Vol. 4, No. 2, 1968.

13. G. Christensen, U. Lohse, and K. Malmstedt, "Full Scale Fire Tests-The Spread of Fire from a Chamber to a Corridor", The Danish National Institute of Building Research, S.B.I. Report No. 59, Copenhagen, 1967.

14. W. J. Christen and T. E. Waterman, "Characteristics of Full-Scale Fires in Various Occupances", Fire Technology, August 1971, p. 205.

15. F. Fung, M. Suchomel, and P. Oglesby, "The NBS Program on Corridor Fires", Fire Journal, May 1973, p. 41.

16. R. Siegel and J. R. Howell, Thermal Radiation Heat Transfer, Vol. 3, NASA SP-164, 1971, p. 336.

17. J. G. Knudsen and D. L. Katz, Fluid Dynamics and Heat Transfer, McGraw-Hill Book Co., Inc., New York, 1958, p. 232.

18. W. J. Parker and M. E. Long, "Development of a Heat Release Rate Calorimeter at NBS", ASTM STP 502, Ignition, Heat Release, and Noncombustibility of Materials, ASTM, 1972, pp. 135-151.

19. W. J. Parker, Personal Communications, National Bureau of Standards, 1972.

20. T. Kashiwagi, Personal Communications, National Bureau of Standards, 1972.

21. D. B. Spalding, "A Standard Formulation of the Steady Convective Mass Transfer Problem", Int. J. Heat Mass Transfer, Vol. 1, 1960, pp. 192-207.

22. W. J. Parker, "Flame Spread Model for Cellulosic Materials", 1969 Meeting Central States Section, The Combustion Institute, Univ. of Minnesota, March 1969.

23. S. S. Kutatedadze and V. M. Borishanskii, A Concise Encyclopedia of Heat Transfer, Pergamon Press, New York, 1966, pp. 469-71.

24. J. N. de Ris, "The Spread of a Laminar Diffusion Flame", Twelfth Symposium (International) on Combustion, The Combustion Institute, 1969, p. 241.

25. R. J. McCarter, Personal Communications, National Bureau of Standards, 1972.

26. M. P. Escudier, "Aerodynamics of a Burning Turbulent Gas Jet in a Crossflow", Combustion Science and Technology, Vol. 4, 1972, pp. 293-301.

27. T. Kasuda, Personal Communications, National Bureau of Standards, 1972.

28. J. Baker, Personal Communications, Urban and Environmental Systems, Honeywell, Inc., Minneapolis, Minn. 1972.

29. H. S. Carslaw and J. C. Jaeger, Conduction of Heat in Solids, Oxford, 1959.

30. G. Robinson, Personal Communications, National Bureau of Standards, 1972.

31. P. H. Thomas, "The Size of Flames from Natural Fires", Ninth Symposium (Inter.) on Combustion, Academic Press, New York, 1963, p. 844.

32. C. Huggett, "Carpet Flammability and the NBS Corridor Fire Program", Standardization News, Vol. 1, No. 5, May 1973.

FORM NBS-114A (1-71)

U.S. DEPT. OF COMM. BIBLIOGRAPHIC DATA SHEET	1. PUBLICATION OR REPORT NO. NBSIR 73-199	2. Gov't Accession No.	3. Recipient's Accession No.

4. TITLE AND SUBTITLE

Experimental and Analytical Studies of Floor Covering Flammability with a Model Corridor

5. Publication Date

6. Performing Organization Code

7. AUTHOR(S)

Wells Denyes and James Quintiere

8. Performing Organization NBSIR 73-199

9. PERFORMING ORGANIZATION NAME AND ADDRESS

NATIONAL BUREAU OF STANDARDS
DEPARTMENT OF COMMERCE
WASHINGTON, D.C. 20234

10. Project/Task/Work Unit No. 490 0572

11. Contract/Grant No.

12. Sponsoring Organization Name and Address

Man-Made Fiber Producers Association, Inc.
1150 Seventeenth St. N.W., Washington, D.C. 20036 and
National Bureau of Standards
Washington, D.C. 20234

13. Type of Report & Period Covered: Final

14. Sponsoring Agency Code

15. SUPPLEMENTARY NOTES

16. ABSTRACT (A 200-word or less factual summary of most significant information. If document includes a significant bibliography or literature survey, mention it here.)

An experimental model corridor facility was designed, constructed, and instrumented. The facility examines flame spread over floor covering materials in a small scale corridor under a forced air flow condition. A gas burner flame serves as the ignition source.

A study was made of the factors influencing flame spread in the model corridor. These factors included energy release rate of the ignition source, air velocity, and model corridor geometry. Twenty-six carpet materials and 5 other floor covering materials were studied in the model corridor, and 369 flame spread runs were conducted.

It was found that flame spread behavior in the model corridor generally involves either a rapidly accelerating flame front which propagates the full 8 foot length of the test section ("flameover"), or involves a decelerating flame front which results in extinction a short distance from the ignition source. Radiant heating of the floor material due to hot products of combustion heating the ceiling is a significant factor in causing flameover. Carpet assembly was found to affect flame spread more significantly than pile fiber type.

The data have been analyzed to determine quantitatively the effects of the factors influencing flame spread. Scaling relationships have been presented to attempt to extrapolate the model corridor results to full scale corridor fires.

Finally a procedure has been suggested for using the facility in a floor covering flammability test method. The procedure is based on determining the minimum energy input rate to cause flameover.

17. KEY WORDS (Alphabetical order, separated by semicolons)

Flame spread; floor covering materials; model corridor; scaling laws; test method

18. AVAILABILITY STATEMENT

[X] UNLIMITED.

[ ] FOR OFFICIAL DISTRIBUTION. DO NOT RELEASE TO NTIS.

19. SECURITY CLASS (THIS REPORT): UNCLASSIFIED

21. NO. OF PAGES

20. SECURITY CLASS (THIS PAGE): UNCLASSIFIED

22. Price